Investigation of a simplified open boundary condition for coastal and shelf sea hydrodynamic models

by

Patrick Eminet Shabangu

Thesis presented in partial fulfilment of the requirements for the degree of Master of Science in Applied Mathematics in the Faculty of Science at Stellenbosch University

Department of Mathematical Sciences,
Applied Mathematics Division,
Stellenbosch University,
Private Bag X1, Matieland 7602, South Africa.

Supervisors:

Prof. G.J.F. Smit

Dr. G.P.J. Diedericks

Mr. R. C. Van Ballegooyen

March 2015

Stellenbosch University https://scholar.sun.ac.za

Declaration

By submitting this thesis electronically, I declare that the entirety of the work contained therein is my own, original work, that I am the sole author thereof (save to the extent explicitly otherwise stated), that reproduction and publication thereof by Stellenbosch University will not infringe any third party rights and that I have not previously in its entirety or in part submitted it for obtaining any qualification.

Signature: .....
Patrick Eminet Shabangu

Date: 24 February 2015 .....

Copyright © 2015 Stellenbosch University
All rights reserved.

Stellenbosch University https://scholar.sun.ac.za

Abstract

In general, coastal and shelf hydrodynamic modelling is undertaken with limited area numerical models such as Delft3D or Mike 21. To conduct successful numerical simulations these programmes require appropriate boundary conditions. Various options exist to obtain boundary conditions such as Neumann conditions, specifying water levels, specifying velocities and combination of these, amongst others. In this study one specific method is investigated, namely the specification of water levels on all the open boundaries using a "reduced physics" approach. This method may be more appropriate than Neumann conditions when the domain is fairly large and is also of particular interest as it allows measured data to be incorporated in the boundary conditions, although the latter was not considered in this study.

The boundary conditions of interest are determined by separating the cross-shore and alongshore components of the momentum equations. To justify the separation, the equations of motion are firstly non-dimensionalised to determine the relative importance of various terms and then scaled to determine under which conditions the cross-shore and alongshore components can be solved independently.

The efficacy of a computer program, *Tilt*, to calculate the open boundary conditions have been investigated for a number of idealised cases. Based on an understanding of the underlying physics and scaling assumptions, situations where these open boundary conditions underperformed have been analysed and reasons given for their underperformance. When applied to "real-life" situations it is likely that one or more of the scaling assumptions will be violated. Comment is provided on the likely errors in model simulations should this occur.

The main conclusions are that the "reduced physics" approach used in *Tilt* restricts fairly significantly the range of flow that can be simulated. Should the scaling assumptions underlying *Tilt* be satisfied, *Tilt* performs adequately for limited area model simulations of coastal and shelf regions, however there remain some concerns:

- The no flux condition at the coast and clamped water level offshore

Stellenbosch University https://scholar.sun.ac.za

restrict flow cross-shore and enforce alongshore flow. As a result, open boundary conditions determined from *Tilt* only satisfy the alongshore motion of a barotropic fluid when tested with winds that deflect flows towards the coast due to Coriolis effects. Where the winds deflect flow in an offshore direction significant errors in flow conditions may occur at the offshore boundary. This is probably caused by the very long time taken for the coastal boundary to signal its presence.

- Where the scaling assumptions underpinning *Tilt* are violated significant errors may be introduced at the model open boundaries. The likelihood of their formulation and magnitude depends on the extent to which these scaling assumptions are violated. Pragmatic solutions to some of these situations are offered.

Stellenbosch University https://scholar.sun.ac.za

Opsomming

Oor die algemeen word kus en kontinentale bank hidrodinamiese modellering met beperkte area numeriese modelle soos Delft3D of Mike 21 gedoen. Om suksesvolle simulasies te doen, benodig hierdie programme geskikte randwaardes. Daar bestaan verskeie opsies om randwaardes te verkry soon byvoorbeeld Neuman kondisies, spesifisering van watervlakke, spesifisering van snelheid en kombinasies van hierdie. In hierdie studie word een spesifieke metode ondersoek, naamlik om watervlakke op al die oop rande te spesifiseer deur 'n "gereduseerde fisika" benadering te gebruik. Hierdie metode is meer van toepassing as Neuman randwaardes wanneer die modelleringsgebied redelik groot is en ook van spesifieke belang aangesien dit die inkorporering van gemete data in die randwaardes moontlik maak, alhoewel laasgenoemde nie in hierdie studie ondersoek is nie.

Die randwaardes wat van belang is, word bepaal vanaf die momentumvergelykings wat in komponente loodreg op die kus en parallel aan die kus geskei word. Om die skeiding te regverdig, word die bewegingsvergelykings eerstens nie-dimensionaliseer om die relatiewe belangrikheid van terme te bepaal en daarna word die vergelykings geskaal om te bepaal onder watter kondisies mag die komponente loodreg op die kus en parallel aan die kus onafhanklik opgelos word.

Die doeltreffendheid van 'n bestaande rekenaarprogram, *Tilt*, wat gebruik word om die randwaardes te bepaal, word getoets vir 'n aantal ge-idialiseerde toetsgevalle. Gebasseer op die verstaan van die onderliggende fisika en aannames in die skaling, is situasies waar die randwaardes onderpresteer analiseer en redes vir die onderprestering word gegee. Tydens toepassings in werklike situasies is dit heel moontlik dat daar nie voldoen sal word aan al die aannames wat in die skaling gebruik is nie. Kommentaar word oor die moontlike foute wat in die simulasies kan voorkom gelewer indien daar nie aan die aannames voldoen word nie.

Die belangrikste gevolgtrekkings is dat die "gereduseerde fisika" benadering in *Tilt*, *Tilt* die bereik van die skaal van die vloei wat gesimuleer kan word tot 'n redelike mate beperk. Indien voldoen word aan die aannames in die

Stellenbosch University https://scholar.sun.ac.za

skaling wat onderliggend is aan *Tilt*, dan presteer *Tilt* goed vir beperkte area model simulasies van die kus en kontinentale bank gebiede. Daar is egter wel kommer:

- Die geen-vloed kondisie teen die kus en geklampde watervlakke aflandig, beperk die vloei dwars op die kus en dwing vloei parallel aan die kus af. Gevolglik bevredig die oop randwaardes vanaf *Tilt* vloei tot parallel aan die kus van barotropiese vloei wanneer die simulasies getoets is met winde wat vloei na die kus toe deflekteer as gelog van die Coriolis krag. Waar die wind vloei in 'n aflandige rigting deflekteer, kan redelike groot foute voorkom langs die aflandige rand. Dit is waarskynlik omdat dit 'n lang tyd neem vir die rand langs die kus om sy invloed te laat geld.

- Waar nie aan die aannames in die skaling wat onderliggend is aan *Tilt* voldoen word nie, kan beduidende foute in die oop rande van die model gebied voorkom. Die voorkoms van die foute hang af van die mate waarin daar nie aan die aannames voldoen word nie. Praktiese oplossings vir sommige van hierdie situasies word verskaf.

Stellenbosch University https://scholar.sun.ac.za

Acknowledgements

I would like to acknowledge:

- God, who gave me the strength and love.
- my supervisors, Prof. G.J.F. Smit, Dr. G.P.J. Diedericks and Mr. R. C. Van Ballegooyen, in their own special way for their guidance, inspiration, support, continuous motivation and encouragement when was most needed.
- my mother for moral support and the whole family for their understanding.
- the CSIR, for their funding of this study.
- the CSIR NRE Coastal Systems group, for their concern and words of encouragement.

Stellenbosch University https://scholar.sun.ac.za

Contents

Stellenbosch University https://scholar.sun.ac.za

Stellenbosch University https://scholar.sun.ac.za

Stellenbosch University https://scholar.sun.ac.za

List of Figures

Stellenbosch University https://scholar.sun.ac.za

Stellenbosch University https://scholar.sun.ac.za

List of Tables

Stellenbosch University https://scholar.sun.ac.za

Nomenclature

Standard symbols

A	Area	$[\mathrm{m}^2]$
c	Speed of sound in seawater	$[\mathrm{m/s}]$
c_v	Specific heat capacity at constant volume	$[\mathrm{J/(kg\ ^\circ C)}]$
c_p	Specific heat capacity at constant pressure	$[\mathrm{J/(kg\ ^\circ C)}]$
C	Wave speed	$[\mathrm{m/s}]$
C_0	Shallow water wave speed	$[\mathrm{m/s}]$
f	Coriolis parameter	$[\mathrm{s}^{-1}]$
f_0	Coriolis parameter at a reference latitude	$[\mathrm{s}^{-1}]$
$F_\eta(t)$	Water level imposed at the model open boundary	$[\mathrm{m}]$
$F_u(t)$	Velocity imposed at the model open boundary	$[\mathrm{m/s}]$
g	Gravitational acceleration constant	$[\mathrm{m/s}^2]$
G	Earth gravitational constant	$[\mathrm{Nm}^{\ 2}/\mathrm{kg}^2]$
h	Still water depth	$[\mathrm{m}]$
H	Total water depth	$[\mathrm{m}]$
H_z	Water depth scale	$[\mathrm{m}]$
k	Wave number	$[\mathrm{m}^{-1}]$
K	Constant of integration	$[\,]$
$L(X,Y)$	Horizontal length scale	$[\mathrm{m}]$
m	Mass	$[\mathrm{kg}]$
M	Mass of the Earth	$[\mathrm{kg}]$
N	Brunt-Väisälä frequency	$[\mathrm{Hz}]$
p, $F_p(x,z)$	Pressure	$[\mathrm{Pa}]$
p_a	Atmospheric pressure	$[\mathrm{Pa}]$
$F_p^0, F_p^1, \ldots$	Pressure: zeroth and first order solution	$[\mathrm{Pa}]$
P_*	Pressure scale	$[\mathrm{Pa}]$
q	Fluid discharge	$[\mathrm{m}^2\mathrm{s}^{-1}]$
R	Radius of the earth magnitude	$[\mathrm{m}]$
S	Salinity	$[\mathrm{psu}]$

Stellenbosch University https://scholar.sun.ac.za

t	Time	[s]
t_τ	Time scale	[s]
t_p	Peak wave period	[s]
T	Temperature	[°C]
V_{vo}	Control volume	[m^3]
X	Cross-shore length scale	[m]
X_h	Cross-shore scale of variations in bottom topography scale	[m]
Y	Alongshore length scale	[m]
Y_h	Alongshore scale of variations in bottom topography scale	[m]

Vectors and Tensors

$\boldsymbol{a}$	Acceleration	[m/s^2]
$\mathbf{F}$	Force	[N]
$\hat{\mathbf{F}}$	Force per unit volume	[N/m^3]
$\mathbf{g}$	Gravitational acceleration	[m/s^2]
$\boldsymbol{n}(\boldsymbol{i},\boldsymbol{j},\boldsymbol{k})$	Unit vector	[ ]
$\mathbf{R}$	Position from the center of the earth (radius)	[m]
$\mathbf{v}(u,v,w)$	Flow velocity	[m/s]
$\overline{\mathbf{v}}(\overline{u},\overline{v},\overline{w})$	Time averaged flow velocity	[m/s]
$\widehat{\mathbf{v}}(\widehat{u},\widehat{v},\widehat{w})$	Depth averaged flow velocity	[m/s]
$\mathbf{V}(\mathrm{V}(U,V),W)$	Velocity scale	[m/s]
$\boldsymbol{x}(x,y,z)$	Position vector	[m]
$\mathbf{X}$	Position vector	[m]
$\underline{\underline{\sigma}}$	Total shear stress tensor	[Pa]
$\underline{\underline{\tau}}$	Viscous stress tensor	[Pa]
$\underline{\underline{1}}$	Unit dyad	[ ]
$\boldsymbol{\chi}$	Position vector	[m]
$\boldsymbol{\Omega}$	Earth's rotation rate	[rad/s]

Greek symbols

α	Relaxation time	[s]
α_0	Constant for relaxation time	[s]
β_T	Isothermal compressibility	[m^2/N]
β_0	Latitudinal gradient in coriolis parameter (f)	[ ]
δ	Thin Ekman layer	[m]
ϵ	Divergence parameter	[ ]

Stellenbosch University https://scholar.sun.ac.za

ϵ_{Bu}	Burger number expansion parameter	[ ]
ζ	Small parameter	$[10^{-1}]$
η	Sea level elevation	[m]
η_a	Sea level elevation due to changes in atmospheric pressure	[m]
λ	Wavelength	[m]
μ	Molecular viscosity	$[m^2/s]$
ν	Kinematic viscosity	$[m^2/s]$
ν_t	Eddy viscosity	$[m^2/s]$
ρ	Fluid density	$[kg/m^3]$
$\widehat{\rho}$	Depth averaged fluid density	$[kg/m^3]$
ρ_0	Reference fluid density	$[kg/m^3]$
τ	Shear stress	[Pa]
ϕ	Latitude	[°]
ϕ_0	Specific latitude	[°]
ω	Wave frequency	[Hz]
Ω	Constant for Earth's rotation rate	[rad/s]

Special symbols

$\parallel$	Parallel	[ ]
$\perp$	Perpendicular	[ ]
$\widehat{\ }$	Depth averaging	[ ]
$\overline{v}$	Time averaging	[ ]
$\vert$	Evaluated at	[ ]
*	Non-dimensional	[ ]
∇	Del operator	[ ]
$Ro = \frac{\mathrm{V}}{fL}$	Rossby number	[ ]
$Ro' = \frac{1}{ft_\tau}$	Temporal Rossby number	[ ]
$Re = \frac{\mathrm{V}L}{\nu}$	Reynolds number	[ ]
$Ri = \frac{gH_z}{\mathrm{V}^2}$	Richardson number	[ ]
$Fr = \frac{\mathrm{V}}{\sqrt{gH_z}}$	Froude number	[ ]
$Bu = \frac{N^2H_z^2}{f^2L^2}$	Burger number	[ ]
$E_k = \frac{\nu_t}{fL^2}$	Ekman number	[ ]

Subscripts

b	Bottom
B	Boundary

Stellenbosch University https://scholar.sun.ac.za

e	Entropy
i	Inertial frame
r	Rotating frame
w	Wind
x	x component
y	y component
z	z component
P/O	Position P relative to position O
Q/O	Position Q relative to position O
P/Q	Position P relative to position Q
pr	Primary
se	Secondary
vo	Volume
Cor	Coriolis
pre	Pressure
gra	Gravity
vis	Viscous
$crit$	Critical

Stellenbosch University https://scholar.sun.ac.za

Chapter 1

Introduction

1.1 Background to the study

The field of oceanography is devoted to studying dynamic and physical phenomena, from deep oceans to shallow coastal areas and estuaries (Pond & Pickard, 1978; Bowden, 1983). The physical features of coastal and shelf seas and their dynamical processes are the focus of this study. For this study, coastal and shelf seas refer to that area of the ocean that extends from the continental shelf edge to the coast.

Many human activities take place in coastal and shelf seas. These include shipping, mineral exploitation, fishing, extraction of renewable energy as well as sailing and swimming (Bowden, 1983; Pond & Pickard, 1978). All of these require an understanding of the behaviour and dynamics of coastal and shelf seas. This understanding can be achieved either through observations, which only describe the present state, or through predictions of the future state. Direct observation through data collection focuses on a quantitative description of the ocean and its movements, whereas physical laws may be used to predict fluid flow through algebraic relations or analytical expressions that suggest what kind of motions are likely to occur and the forces that may be causing the motion.

The ocean is a complex system to understand fully. The usual approach taken in ocean modelling is to investigate the behaviour of the ocean with *mathematical models* and *computer models*. Generally, the state of the ocean may be described by continuous distributions of several parameters such as temperature, salinity, flow velocity and water levels. In the field of descriptive physical oceanography, data is collected in the ocean and characteristics of the ocean inferred from these data. In dynamic oceanography, mathematical models are developed to predict the behaviour of the ocean and the changes expected in the observational data. Ocean flow is governed by a system of partial differ-

Stellenbosch University https://scholar.sun.ac.za

ential equations (PDEs) characterising the changes of ocean dynamics. The models range from simple models (e.g. linearized, inviscid, one-dimensional flow, etc.) to complex and highly realistic models (Herzfeld *et al.*, 2011). An increase in model complexity typically requires that the relevant equations of motion be solved numerically on computers. This allows highly realistic simulations of physical process in the ocean, particularly where (Computational Fluid Dynamics (CFD)) codes are utilized. Examples of physical processes that can be simulated in this manner are changes in water column stratification, beach erosion, upwelling events, etc. Such computer models therefore are key to gaining a better understanding of the ocean.

The various types of ocean models are however not free from errors. An important requirement is for the system of equations which describe the ocean to be mathematically closed and well-posed. If this is achieved, the system will ensure unique solutions and stability, with the prescribed initial information. However, this is not sufficient to ensure accuracy of the solution with respect to the physical processes occurring in the ocean (Blayo & Debreu, 2004). In addition to the above, critical to ensuring that mathematical or computational models produce sensible and acceptable results is the imposition of appropriate boundary conditions at the open boundaries of the model. A particular challenge is to specify boundary conditions that are consistent with the model solution in the interior of the model domain.

Previous authors (e.g. Roed & Cooper (1987)) have discussed the importance of open boundary conditions in determining the interior solution. Generally acceptable types of open boundary conditions suitable for modelling coastal and shelf seas have been summarized by a number of authors (e.g. Herzfeld *et al.* (2011), Palma & Matano (1998)) and categorized (e.g. Palma & Matano (1998)) into, radiation conditions (e.g. Sommerfeld (1949); Orlanski (1976); Chapman (1985)), characteristic methods (e.g. Roed & Cooper (1987)) and relaxation schemes (Martinsen & Engedahl, 1987). Different types of open boundary conditions have been implemented (e.g. Herzfeld *et al.* (2011); Martinsen & Engedahl (1987); Palma & Matano (1998, 2001)), tested (e.g. Tang & Grimshaw (1996); Martinsen & Engedahl (1987)) and compared to each other (e.g. Chapman (1985)). In particular, Herzfeld *et al.* (2011) have discussed issues confronting modellers when dealing with open boundary conditions in limited area models and proposed how one can solve them.

Stellenbosch University https://scholar.sun.ac.za

1.2 Modelling techniques and assumptions relevant to the study

Modelling of coastal and shelf currents is difficult due to the complexity introduced by the many driving forces operating in this region associated with wind, tides, waves and the Coriolis effect. A situation that is particularly difficult to simulate is the inclusion of wind forcing that results in the development of cross-shore (i.e. perpendicular to the coast) water level gradients. For the boundary conditions to be consistent with the water levels in the interior domain of the model, appropriate water levels need to be imposed at the model boundaries. Specifically, there needs to be agreement between the model solution and the information imposed on the lateral boundaries, in this case the wind setup. However, if these water levels are not correctly specified at the open boundaries this can give rise to discontinuities that propagate through the model for the duration of the model simulation period.

Existing computer models (e.g. Delft3D, MIKE 21, etc.) used to investigate shallow water coastal regions, typically are based on the shallow water equations and/or shallow water wave equations. Similar equations are also applicable in estuaries, river channels, etc., (Leendertse *et al.*, 1973; Leendertse & Liu, 1975). These equations are also encountered in atmospheric modelling (Gill, 1982).

Delft3D is an open source computer model Deltares (2015) comprising a set of software modules (i.e. Delft3D-FLOW, Delft3D-WAVE, etc.) used to model a range of coastal engineering and environmental problems. These modules can be used independently or in various combinations with one another (Deltares, 2011) to solve problems of ocean dynamics, sediment dynamics and water quality. This study will use only the Delft3D-FLOW module to evaluate the efficacy of selected boundary conditions when modelling coastal and shelf flows.

Many coastal area models include a land boundary, cross-shore lateral boundaries and an offshore boundary. Various methods are used to model these lateral boundaries. For a given model it is assumed that the information generated inside the model will propagate out of the model in the form of waves. In which case, the waves approaching the lateral boundaries typically are assumed to have variable phase speeds (Orlanski, 1976) that typically are considered to be non-dispersive (Chapman, 1985).

Herzfeld *et al.* (2011) investigated various types of boundary conditions, the most elementary being where open boundary conditions were chosen through trial and error. This approach is considered by Bennett & McIntosh (1982) to constitute an *ad hoc* approach as, being valid only for specific model cases, it

Stellenbosch University https://scholar.sun.ac.za

is neither robust nor universally valid. A more robust approach is to prescribe the lateral boundaries by imposing predicted water level setup or current velocity along the lateral boundaries. This is achieved by utilizing predicted water levels or current velocities from large-scale models, from measured data or obtained by solving a set of "reduced physics" shallow water equations along the cross-shore boundaries, i.e. the use of simplified two-dimensional (2D) shallow water equations on the open boundaries which is the focus of the study.

Roelvink & Walstra (2004) proposed to investigate a small scale domain with wind blowing at an angle to an alongshore uniform sloping beach, and suggested the following approach: Allow the model in its interior to determine the correct solution to impose at the open boundaries. This is obtained by imposing a zero alongshore water level gradient (a so-called Neumann boundary condition) instead of a fixed water level or velocity. A limitation of this approach is that it does not allow one to specify information at the boundary that will influence flows in the interior model domain. For this reason an alternative approach is followed in this study, i.e. the prediction of water level setup along the open boundaries by solving a system of one dimensional hydrodynamic equations based on "reduced physics" along the open boundaries of the model. Should measured current data exist, then boundary conditions may be specified so that these measured currents can be recovered at the location they were measured within the interior of the model domain.

The Council for Scientific and Industrial Research (CSIR) has developed a computer code to calculate water levels to specify at the lateral boundaries for a model forced by wind and large-scale currents. This code is referred to as *Tilt* since the cross-shore tilt in water levels is calculated. The *Tilt* code was developed for situations where the model domain typically is much larger than that used by Roelvink & Walstra (2004).

1.3 Objective

As noted above, the role of boundaries for coastal and shelf seas is to enclose the model area. Numerically, a solution to a coastal and shelf seas model will depend on the information imposed on the boundaries of a model as well as the forcing imposed in the interior of the model domain. However, the solution at the open boundaries is unknown, whereas Delft3D-FLOW can be used to determine the solution in the interior model domain. A solution to the open boundaries can only be assumed, extrapolated or predicted (Roed & Cooper, 1987), because there exist no general open boundary condition that one can impose at the open boundaries that consistently will be in agreement with interior solution. For coastal models, it is particularly difficult to simulate a situation when synoptic-scale wind forcing is included.

Stellenbosch University https://scholar.sun.ac.za

The CSIR, in an attempt to find a boundary condition that resolves many of the above issues for limited area coastal and shelf models, has developed the *Tilt* code that is used both for undertaking research and commercial work. The *Tilt* code computes open boundary condition water levels that are both consistent with the solution in the interior of the model domain and provide the requisite open boundary forcing in the absence of a larger-scale model within which to nest the limited area model. Its main draw back is that due to the scaling arguments used in developing the boundary conditions, there is a significant limitation on the range of situations for which it is applicable.

The primary objectives of the study include:

- To determine the scaling assumptions required to allow appropriate time series to be specified at the model open boundaries using a "reduced physics" approach, i.e. the necessary scaling assumptions that allow 2D shallow water equations to be solved at the open boundaries and to be decoupled into cross-shore and alongshore equations to be solved separately.
- To investigate and understand when it is appropriate to use *Tilt*, i.e. what are the temporal and spatial restrictions on the scales of motion that may be considered when *Tilt* boundary conditions are used in a limited area model?
- To understand the implications of applying *Tilt* boundary conditions (e.g. errors that may be introduced at the model open boundaries) when there is not full compliance with the required scale restrictions.

To be able to provide a clear exposition of the scaling arguments used to derive the equations underlying *Tilt*, it has been necessary to show all of the scaling arguments required to move from the generalized Navier-Stokes equations, through the shallow water equations, to ultimately the "reduced physics" equations used in *Tilt*. The scaling arguments used to derive the shallow water equations from the Navier-Stokes equations are clearly described, as are the additional scaling assumptions used to show the conditions under which the synoptic-scale coastal and shelf flow responses may be considered to be barotopic. Of particular relevance are the further scaling assumptions that allow the "reduced physics" approach used in developing Tilt, i.e. the scaling assumptions that allow the decoupling of the 2D shallow water equations into the separate cross-shore and alongshore equations used in *Tilt*.

It is expected that the open boundary conditions produced using *Tilt* will produce acceptable flow simulations, only for situations where there is substantial compliance with the above scaling assumptions.

Stellenbosch University https://scholar.sun.ac.za

This study will commence with the presentation of the Navier-Stokes equations. For the purpose of describing ocean dynamics, it is necessary to include rotational effects (Coriolis forcing) in these Navier-Stokes equations. To achieve this, the equations are expressed in terms of coordinates with the axes fixed to a rotating frame of reference. Under the shallow water assumption, shallow water equations then are derived from the Navier-Stokes equations with rotation. Taking into account the effects of density, the shallow water equations can be separated into a baroclinic mode (with density stratification) and a barotropic mode (without density stratification). In this study, the focus is on situations where the barotropic shallow water equations adequately describe the motion of the ocean. For the purpose of investigating water level setup, the barotropic shallow water equations are separated into cross-shore and alongshore unidirectional equations. In literature, these equations may be associated with the Saint-Venant equations (a one-dimensional version of shallow water equations) (Aldrighetti, 2007).

1.4 Outline of the thesis

The derivation of the governing equations for continuity and momentum are presented in Chapter 2. This is followed by the derivation of the shallow water equations for coastal modelling in Chapter 3, where the shallow water equations are derived from the Navier-Stokes equations by imposing a number of scaling assumptions relevant to coastal and shelf flows. Chapter 4 contains an overview of open boundary conditions and presents the open boundary imposed through the Delft3D-FLOW interface which controls the time series information specified at the open boundary and also the relaxation time scales used when imposing these open boundary conditions on the flows in the model interior. Chapter 5 presents the derivation of spatially decoupled alongshore and cross-shore equations from linearized shallow water equations that describe water level setup in coastal areas. Here associated boundary conditions are discussed based on reduced physics described by linearized shallow water equations and their local solutions. In Chapter 6, the model simulations used to evaluate open boundary conditions are presented. Chapter 7 contains the findings and conclusion of the study as well as recommendations for further investigation.

Stellenbosch University https://scholar.sun.ac.za

Chapter 2

Governing Equations

2.1 Introduction

In this chapter a number of concepts are discussed based on two important principles, namely mass conservation and momentum conservation. The latter is derived from Newton's second law of motion. In dynamic oceanography these laws are presented with the aim of establishing the mathematical models necessary to study, describe and predict oceanographic phenomena and physical processes. Therefore, the governing equations of fluid flow comprise the continuity equation for conservation of mass and the momentum equation for conservation of momentum. In the case of sea water, additional equations are required due to the dynamic significance of thermodynamic variables such as salinity and temperature.

2.2 Mass conservation (continuity) equation

Consider a control volume V_{vo}, fixed in space, through which a fluid can move. The mass of the fluid in the control volume is defined as

$$m = \rho V_{vo}, \tag{2.2.1}$$

which can also be expressed as mass per unit volume (density):

$$\rho = \frac{m}{V_{vo}}. \tag{2.2.2}$$

The density is often used to describe the state of a fluid and may be given by a non-linear function of thermodynamic variables. In the case of sea water the equation of state for density may be expressed as a function of these variables:

$$\rho \quad = \quad \rho(S, T, p), \tag{2.2.3}$$

where S is the salinity, T is the temperature and p is the pressure (Pond & Pickard, 1978). These three thermodynamic variables are normally measured.

Stellenbosch University https://scholar.sun.ac.za

Salinity is a variable that measures the amount of dissolved salt in sea water and one of the main properties that distinguishes sea water from pure water. The fundamental aspect of equation (2.2.3) is the quantitative manner in which changes of density are affected by the changes of the thermodynamic variables.

From the continuum point of view, there will be influx into, a change in mass and the efflux out of the control volume. This is called mass conservation, and is expressed as

$$\frac{\partial \rho}{\partial t} + \nabla \cdot (\rho \mathbf{v}) = 0, \tag{2.2.4}$$

where $\mathbf{v}$ is the velocity of the fluid, t is the time and $\nabla = (\frac{\partial}{\partial x}, \frac{\partial}{\partial y}, \frac{\partial}{\partial z})$ denote the spatial derivatives. To emphasize the effects of local change of density in a continuum, equation (2.2.4) is often expressed in terms of advection effects and in terms of the velocity divergence, yielding

$$\frac{\partial \rho}{\partial t} + \mathbf{v} \cdot \nabla \rho + \rho \nabla \cdot \mathbf{v} = 0. \tag{2.2.5}$$

As noted in equation (A.1.1) in Appendix A, the first and the second terms in this equation constitute the material derivative. Therefore, equation (2.2.5) can be expressed as

$$\frac{D\rho}{Dt} + \rho \nabla \cdot \mathbf{v} = 0. \tag{2.2.6}$$

Following from equation (2.2.3), the differential of the density may be expressed as

$$d\rho = \left(\frac{\partial \rho}{\partial S}\right)_{T,p} dS + \left(\frac{\partial \rho}{\partial T}\right)_{p,S} dT + \left(\frac{\partial \rho}{\partial p}\right)_{T,S} dp, \tag{2.2.7}$$

where the subscripts denote the particular variables that are held constant. Taking the material derivative of equation (2.2.7) leads to

$$\frac{D\rho}{Dt} = \left(\frac{\partial \rho}{\partial S}\right)_{T,p} \frac{DS}{Dt} + \left(\frac{\partial \rho}{\partial T}\right)_{p,S} \frac{DT}{Dt} + \left(\frac{\partial \rho}{\partial p}\right)_{T,S} \frac{Dp}{Dt}. \tag{2.2.8}$$

The continuity equation (2.2.6) is usually simplified to

$$\nabla \cdot \mathbf{v} = 0, \tag{2.2.9}$$

by assuming that

$$\frac{D\rho}{Dt} \approx 0. \tag{2.2.10}$$

Stellenbosch University https://scholar.sun.ac.za

For this to be true the fluid is assumed to be both incompressible and non-diffusive (Batchelor, 1967). In the remainder of this section the assumptions are discussed in more detail to investigate under which conditions the continuity equation may be expressed as equation (2.2.9).

LeBlond & Mysak (1978) state that

$$\left(\frac{\partial \rho}{\partial p}\right)_e = 0, \tag{2.2.11}$$

implies incompressibility, where e is the entropy per unit mass that is held constant. The isothermal compressibility β_T is defined as (Batchelor, 1967)

$$\beta_T = \frac{1}{\rho}\left(\frac{\partial \rho}{\partial p}\right)_T = 0. \tag{2.2.12}$$

Incompressibility alone is not sufficient to neglect the material derivative in equation (2.2.6).

Assumption 2.2.1 *The fluid is incompressible.*

According to LeBlond & Mysak (1978)

$$\left(\frac{\partial \rho}{\partial p}\right)_e = \frac{1}{c^2}, \tag{2.2.13}$$

where c is the speed of sound. For use in equation (2.2.8) it is required that the temperature be held constant. Moran & Shapiro (2006) have shown that

$$\left(\frac{\partial \rho}{\partial p}\right)_T = \frac{c_p}{c_v}\frac{1}{c^2}, \tag{2.2.14}$$

where c_v and c_p are the specific heat capacities at constant volume and pressure, respectively. By comparing equations (2.2.11) to (2.2.14), it is evident that a specific flow may be considered incompressible if the speed of sound is considered to be infinite in the fluid.

The assumption of incompressibility only implies that the last term on the right hand side of equation (2.2.8) may be neglected, but the density may still vary with temperature and salinity $\rho(S, T)$.

Assumption 2.2.2 *The ocean is non-diffusive.*

The material derivative of the salinity and temperature in equation (2.2.8) can be related to the diffusion of temperature and salinity through two balance laws, namely the energy balance equation (Pedlosky, 1987) and the conservation of dissolved solids (Philips, 1980). The assumption that the thermal

Stellenbosch University https://scholar.sun.ac.za

diffusivity and molecular diffusivity is negligible, implies that the first two terms on the right hand side of equation (2.2.8) also may be neglected.

Under assumptions 2.2.1 and 2.2.2 above

$$\frac{D\rho}{Dt} \approx 0, \tag{2.2.15}$$

and the continuity equation may be simplified to

$$\nabla \cdot \mathbf{v} = 0. \tag{2.2.16}$$

Given that molecular diffusion is small and considered negligible, the fluid elements may have different values of density. Should this density variability be significant, the ocean then is considered to comprise a baroclinic fluid. However, if the density differences of the fluid elements are very small compared to the overall density of the fluid (i.e. the magnitude of the relative differences in density is small), the fluid can be considered to have a uniform density. Such a fluid with a uniform density is called a barotropic fluid.

2.3 Momentum conservation (momentum) equation

The derivation of the momentum conservation equation begins with an application of Newton's second law of motion. Newton's second law of motion may be stated mathematically as,

$$\mathbf{F} = m\mathbf{a}, \tag{2.3.1}$$

and when rearranged to give

$$\mathbf{a} = \frac{\mathbf{F}}{m}, \tag{2.3.2}$$

implies that the acceleration $\mathbf{a}$ of an object of mass m is caused by the resultant force $\mathbf{F}$ and the acceleration has the same direction as the resultant force. In fluids the acceleration is a function of a velocity field and time $\mathbf{a} = \mathbf{a}(\mathbf{v}, t)$, so that when equation (A.1.1) in Appendix A is applied, the acceleration of a fluid element may be written as

$$\mathbf{a} = \frac{D\mathbf{v}}{Dt}.$$

According to equation (2.2.1) the mass is related to density and equation (2.3.1) may be written as

$$\rho\frac{D\mathbf{v}}{Dt} = \hat{\mathbf{F}}, \tag{2.3.3}$$

Stellenbosch University https://scholar.sun.ac.za

where

$$\hat{\mathbf{F}} = \frac{\mathbf{F}}{V_{vo}},$$

is the resultant force per unit volume ($\mathrm{N/m^3}$). The resultant force $\hat{\mathbf{F}}$ in equation (2.3.3) may comprise of primary forces $\hat{\mathbf{F}}_{pr}$ and secondary forces $\hat{\mathbf{F}}_{se}$. In the context of oceanography, primary forces (e.g. gravitation, pressure differences and viscous forces) cause the motion, whereas secondary forces (e.g. Coriolis force) arise as a response to the flow (Pond & Pickard, 1978). However, secondary forces are generally accelerations and result from the acceleration term expressed in a non-inertial (rotating) frame of reference (introduced later in the chapter). Equation (2.3.3), when expressed in terms these forces, reads

$$\rho \frac{D\mathbf{v}}{Dt} = \hat{\mathbf{F}}_{pr} + \hat{\mathbf{F}}_{se}. \tag{2.3.4}$$

The primary and secondary forces will be defined shortly.

Primary forces $\hat{\mathbf{F}}_{pr}$

The forces acting on a control volume V_{vo} are:

- *Force due to gravity*

  An object of mass m, will have a weight of $|\mathbf{F}_{gra}| = mg$ where g is the value of the acceleration due to gravity. Moreover, the weight per unit volume, would then be $|\hat{\mathbf{F}}_{gra}| = (m/V_{vo})g = \rho g$. Generally, this force due to gravity may be written as

  $$\begin{aligned} \hat{\mathbf{F}}_{gra} &= \rho g \boldsymbol{n} \\ &= -\rho \mathbf{g}. \end{aligned} \tag{2.3.5}$$

  where $\mathbf{g} = g\boldsymbol{n}$, $\boldsymbol{n}$ is a unit vector and in the z-direction is $-\mathbf{k}$. Hence, $\mathbf{g}$ is formal defined by equation (B.1.13) in Appendix B.

- *Force due to pressure*

  Generally, pressure p is a stress, a force $\mathbf{F}$ per unit area A, i.e.:

  $$p = \frac{\mathbf{F}}{A}, \tag{2.3.6}$$

  and its direction is normal to the surface (parallel to $\boldsymbol{n}$). Therefore, pressure always acts inward, then

  $$\mathbf{F}_{pre} = -pA. \tag{2.3.7}$$

Stellenbosch University https://scholar.sun.ac.za

Of interest here is pressure exerted by the fluid surrounding a control volume V_{vo}. The net force per unit volume is given as

$$\mathbf{F}_{pre} = -\nabla p V_{vo}, \tag{2.3.8}$$

or

$$\hat{\mathbf{F}}_{pre} = -\nabla p, \tag{2.3.9}$$

over the surface bounding the volume.

- *Force due to viscous stress*

  A viscous stress arises by fluid motion. The resistance of a fluid to flow is viscosity, the ratio of shear stress to shear strain rate. Generally, the viscous stress is a tangential forcing to the surface (perpendicular to $\boldsymbol{n}$) that is proportional to the viscosity. In an equation form:

$$\boldsymbol{n} \cdot \underline{\underline{\tau}} = \frac{\mathbf{F}}{A}, \tag{2.3.10}$$

  or

$$\mathbf{F}_{vis} = \boldsymbol{n} \cdot \underline{\underline{\tau}} A, \tag{2.3.11}$$

  where $\underline{\underline{\tau}}$ denotes the viscous stress tensor. Usually, viscous forces are expressed as the divergence of the viscous stress.

$$\mathbf{F}_{vis} = \nabla \cdot \underline{\underline{\tau}} V_{vo}, \tag{2.3.12}$$

  or

$$\hat{\mathbf{F}}_{vis} = \nabla \cdot \underline{\underline{\tau}}, \tag{2.3.13}$$

  Note, $\underline{\underline{\tau}}$ is an array of 9 components, defined shortly.

Equations (2.3.9) and (2.3.13) combined constitute the divergence of stress or total stress (pressure and viscous stress), i.e.:

$$\nabla \cdot \underline{\underline{\sigma}} = \nabla \cdot \left(-p \underline{\underline{1}} + \underline{\underline{\tau}} \right), \tag{2.3.14}$$

where $\underline{\underline{1}}$ is the unit dyad. The total stress tensor $\underline{\underline{\sigma}}$ is

$$\underline{\underline{\sigma}} = -p \underline{\underline{1}} + \underline{\underline{\tau}} \tag{2.3.15}$$

$$= \begin{bmatrix} -p + \tau_{xx} & \tau_{xy} & \tau_{xz} \\ \tau_{yx} & -p + \tau_{yy} & \tau_{yz} \\ \tau_{zx} & \tau_{zy} & -p + \tau_{zz} \end{bmatrix}, \tag{2.3.16}$$

where p is the thermodynamic pressure. Hence, τ_{xz} for example, is the force per unit area in the x-direction on the surface whose outward unit normal is in the z-direction.

Stellenbosch University https://scholar.sun.ac.za

Secondary forces $\hat{\mathbf{F}}_{se}$

In the context of oceanography, the most common secondary forces, amongst others, is the Coriolis force and the centrifugal force. Secondary force, result from the acceleration term when expressed in a non-inertial (rotating) frame of reference (given in Appendix B and later in the chapter).

- *Force due to Coriolis effects*

  Based on Appendix B, the force due to Coriolis effects can be written as

$$\hat{\mathbf{F}}_{Cor} = -\rho\left(2\boldsymbol{\Omega}\times\mathbf{v}\right). \tag{2.3.17}$$

Of interest here is the presentation of Navier-Stokes equations.

2.3.1 Momentum equation expressed in inertial (non-rotating) frame of reference

The primary forces (i.e. equations (2.3.5), (2.3.9) and (2.3.13)) substituted into equation (2.3.4) yields the general momentum equation:

$$\rho\frac{D\mathbf{v}}{Dt} = \nabla\cdot\underline{\underline{\sigma}} - \rho\mathbf{g} + \hat{\mathbf{F}}_{se}, \tag{2.3.18}$$

If $\hat{\mathbf{F}}_{se} = \mathbf{0}$, equation (2.3.18) becomes the Cauchy equation of motion

$$\begin{aligned}\rho\frac{D\mathbf{v}}{Dt} &= \nabla\cdot\underline{\underline{\sigma}} - \rho\mathbf{g}\\ &= -\nabla p + \nabla\cdot\underline{\underline{\tau}} - \rho\mathbf{g}.\end{aligned} \tag{2.3.19}$$

Usually, sea water is assumed to behave as a Newtonian fluid. This implies that the constitutive equations that describe ocean dynamics assume all the necessary conditions for a Newtonian fluid. In this study such conditions are made without emphasizing that there are conditions for a Newtonian fluid.

Assumption 2.3.1 *A linear relationship exists between stress and shear strain rate.*

This means that,

$$\underline{\underline{\tau}}(\mathbf{v}) \propto \nabla\mathbf{v}. \tag{2.3.20}$$

In the ocean the viscosity (or viscosity tensor) may vary with salinity and temperature (Gill, 1982; Pond & Pickard, 1978).

Stellenbosch University https://scholar.sun.ac.za

By comparing equations (A.4.7) to (A.4.9), it follows that equation (2.3.20) may be expressed as equation (A.4.10):

$$\nabla \cdot \underline{\underline{\tau}} = \mu \nabla^2 \mathbf{v}, \tag{2.3.21}$$

where μ is a constant molecular viscosity. Substituting equation (2.3.21) into equation (2.3.19) yields the Navier-Stokes equation for incompressible flow, namely

$$\rho \frac{D\mathbf{v}}{Dt} = -\nabla p + \mu \nabla^2 \mathbf{v} - \rho \mathbf{g}. \tag{2.3.22}$$

For the sake of generality, equation (2.3.22) may be written as

$$\rho \frac{D\mathbf{v}}{Dt} = -\nabla p + \mu \nabla^2 \mathbf{v} - \rho \mathbf{g} + \hat{\mathbf{F}}_{se}, \tag{2.3.23}$$

to account for other forces not mentioned in this equation. This represents the final equation expressed in inertial (non-rotating) frame of reference. In the next section, Newton's second law in a non-inertial (rotating) frame of reference (i.e. momentum equation expressed in non-inertial (rotating) frame of reference) is presented.

2.3.2 Momentum equation expressed in non-inertial (rotating) frame of reference

So far, the description of fluid flow is constrained to fluid flow without rotation. However, sea water is situated on the earth's surface, which is in itself rotating. The aim of this section is to transform equation (2.3.3) to a non-inertial (rotating) frame of reference. Equation (2.3.3) may be written as

$$\rho \left(\frac{D\mathbf{v}}{Dt} \right)_i = \hat{\mathbf{F}}, \tag{2.3.24}$$

where the subscript i is used to emphasize that the equation is only applicable in inertial (non-rotating) frame of reference. As noted above, the resultant force has been defined in equation (2.3.23) as

$$\hat{\mathbf{F}} = -\nabla p + \mu \nabla^2 \mathbf{v} - \rho \mathbf{g} + \hat{\mathbf{F}}_{se}, \tag{2.3.25}$$

which remains the same in both an inertial (non-rotating) and non-inertial (rotating) frame of reference.

Following from Appendix B (particularly equation (B.1.12)) the acceleration term may be expressed in a non-inertial (rotating) frame of reference as

$$\left(\frac{D\mathbf{v}}{Dt} \right)_i = \left(\frac{D\mathbf{v}}{Dt} \right)_r + 2\boldsymbol{\Omega} \times \mathbf{v} + \boldsymbol{\Omega} \times (\boldsymbol{\Omega} \times \mathbf{R}), \tag{2.3.26}$$

Stellenbosch University https://scholar.sun.ac.za

where the subscript r represents non-inertial (rotating) frame of reference and distinguish a similar term to that in inertial i frame of reference. The first term on the right hand side of equation (2.3.26) represents the acceleration of the fluid element in non-inertial (rotating) frame of reference, the second term is the Coriolis acceleration, and the last term is the centrifugal acceleration, where $\mathbf{v}$ is the velocity of the fluid element in coordinates fixed to the earth, $\boldsymbol{\Omega}$ is the angular velocity and $\mathbf{R} = \mathbf{X}|_{Q/O}$ (given in Appendix B) is the position from the center of the earth.

Equations (2.3.25) and (2.3.26) when substituted into equation (2.3.24), yield

$$\rho\left(\frac{D\mathbf{v}}{Dt} + 2\boldsymbol{\Omega}\times\mathbf{v} + \boldsymbol{\Omega}\times(\boldsymbol{\Omega}\times\mathbf{R})\right) = -\nabla p + \mu\nabla^2\mathbf{v} - \rho\mathbf{g}, \tag{2.3.27}$$

given that equation (2.3.17) is noted to be replacing $\hat{\mathbf{F}}_{se}$ in equation (2.3.25). The terms $\boldsymbol{\Omega}\times(\boldsymbol{\Omega}\times\mathbf{R})$ and $\mathbf{g}$ can be combined to give

$$\mathbf{g}_i = \mathbf{g} + \boldsymbol{\Omega}\times(\boldsymbol{\Omega}\times\mathbf{R}), \tag{2.3.28}$$

which when rearranged yields the following equation (equation (B.1.13) in Appendix B)

$$\mathbf{g} = \mathbf{g}_i - \boldsymbol{\Omega}\times(\boldsymbol{\Omega}\times\mathbf{R}). \tag{2.3.29}$$

Equation (2.3.29) is the acceleration due to gravity as seen in a non-inertial (rotating) frame of reference, where $\mathbf{g}_i$ represents the acceleration due to gravity as seen in an inertial (non-rotating) frame of reference. By definition, the acceleration due to gravity is directed along the negative z-axis and can be defined as follows (equation (B.1.9) in Appendix B)

$$\mathbf{g}_i = -\frac{GM}{|\mathbf{R}|^3}\mathbf{R}, \tag{2.3.30}$$

where M represents the mass of the earth and G represents the earth gravitational constant. Note that $\mathbf{g}_i = \mathbf{g}$ only in an inertial (non-rotating) frame of reference as previous defined in Section 2.3.1, where the centrifugal acceleration is not present $\boldsymbol{\Omega}\times(\boldsymbol{\Omega}\times\mathbf{R}) = \mathbf{0}$. Therefore, equation (2.3.27) can be expressed as

$$\rho\left(\frac{D\mathbf{v}}{Dt} + 2\boldsymbol{\Omega}\times\mathbf{v}\right) = -\nabla p + \mu\nabla^2\mathbf{v} - \rho\mathbf{g}. \tag{2.3.31}$$

Equation (2.3.31) is the Navier-Stokes equations in a non-inertial (rotating) frame of reference.

In summary, the equations of mass conservation and momentum conservation

Stellenbosch University https://scholar.sun.ac.za

have been presented in this chapter. From mass conservation equation the continuity equation and density variations equation are formulated. From momentum conservation a number of equations are presented based on Newton's second law of motion. Table 2.1 contains a summary of the equations presented in this chapter, culminating at the Navier-Stokes equations expressed in a non-inertial (rotating) frame of reference.

Stellenbosch University https://scholar.sun.ac.za

Table 2.1: Summary of equations presented in Chapter 2.

Equation	Designation	Eqn. no.
$\frac{D\rho}{Dt} \approx 0$	Density equation	(2.2.15)
$\nabla \cdot \mathbf{v} = 0$	Continuity equation	(2.2.16)
Inertial frame of reference		
$\rho\frac{D\mathbf{v}}{Dt} = \nabla \cdot \underline{\underline{\sigma}} - \rho\mathbf{g} + \hat{\mathbf{F}}_{se}$	General momentum equation	(2.3.18)
$\rho\frac{D\mathbf{v}}{Dt} = -\nabla p + \nabla \cdot \underline{\underline{\tau}} - \rho\mathbf{g}$	Cauchy equation	(2.3.19)
$\rho\frac{D\mathbf{v}}{Dt} = -\nabla p + \mu\nabla^2\mathbf{v} - \rho\mathbf{g}$	Navier-Stokes equations	(2.3.22)
$\rho\frac{D\mathbf{v}}{Dt} = -\nabla p + \mu\nabla^2\mathbf{v} - \rho\mathbf{g} + \hat{\mathbf{F}}_{se}$	General momentum equation	(2.3.23)
Non-inertial frame of reference		
$\rho\left(\frac{D\mathbf{v}}{Dt} + 2\boldsymbol{\Omega} \times \mathbf{v}\right) = -\nabla p + \mu\nabla^2\mathbf{v} - \rho\mathbf{g}$	Navier-Stokes equations in non-inertial frame of reference	(2.3.31)

Stellenbosch University https://scholar.sun.ac.za

Chapter 3

Shallow water equations

3.1 Introduction

The shallow water equations comprise a simplified version of the Navier-Stokes equations for a situation where the scales of the vertical motion are significantly smaller than the scales of horizontal motion, i.e. the type of flow that one would expect in shallow water. The necessary scaling arguments required to move from the generalized Navier-Stokes equations to the shallow water equations are presented below.

The Navier-Stokes equations in a non-inertial (rotating) frame of reference may be written in a generalized form in terms of spherical coordinates. The transformation from spherical coordinates to a rectilinear reference framework as expressed in Cartesian coordinates is described in LeBlond & Mysak (1978) and Kee *et al.* (2003). For modelling purposes of a specific region, it is necessary to introduce a Cartesian metric centered at some reference latitude and longitude that locally approximates the spherical metric on the earth surface. This transformation from spherical to Cartesian coordinates is achieved by assuming a tangential plane attached to the earth surface ($z = 0$) and at reference latitude ($\phi = \phi_0$) and longitude, i.e. the β-plane. A Taylor series expansion is used to simplify the spherical coordinate into Cartesian coordinate equations, under the assumption that the plane is of limited horizontal extent ($\ll 10^6$ m) compared to the radius of the earth (LeBlond & Mysak, 1978). Under various scaling assumptions these culminate to the equations written in Cartesian coordinate, as sphericity and curvature effects are neglected (presented in Section 3.3).

Stellenbosch University https://scholar.sun.ac.za

3.2 The fundamentals

3.2.1 Basic fluid flow model

The governing equations for incompressible, Newtonian fluid flow have been formulated in Chapter 2. The basic fluid flow model constitutes, the continuity equation (2.2.16), the density equation (2.2.15) linked to the continuity equation and the momentum equation (2.3.31) (LeBlond & Mysak, 1978), i.e.:

$$\left.\begin{aligned} \frac{D\rho}{Dt} &= 0 \\ \nabla \cdot \mathbf{v} &= 0 \\ \frac{D\mathbf{v}}{Dt} + 2\boldsymbol{\Omega} \times \mathbf{v} &= -\frac{1}{\rho}\nabla p + \nu\nabla^2\mathbf{v} - \mathbf{g} \end{aligned}\right\} \tag{3.2.1}$$

where $\nu = \mu/\rho$ represents the kinematic viscosity.

The set of equations (3.2.1) is valid in a non-inertial frame of reference fixed on earth and are applicable to large-scale motions of a stratified fluid on a rotating earth. The application of the set of equations (3.2.1) to large scale oceanic motion, may however lead to a problem if turbulence eddies are being introduced. In which case, the use of molecular or kinematic viscosity for the transfer of momentum caused by turbulence may be regarded as inconsistent. In the next section the relationship between kinematic viscosity and eddy viscosity is discussed, in the context of modelling turbulence effects in large scale oceanic motions.

3.2.2 Large scale oceanic equations of motion

For most engineering or computational fluid dynamics purposes mean flow is commonly investigated. The usual procedure followed to isolate the desired phenomenon is to decompose all the state variables into contributions from averaged variables and perturbations about these averaged variables. When the governing equations are expressed in terms of these decomposed variables, averaging may then be used to simplify the equations as is shown in Appendix C.1. This leads to the addition of turbulent Reynolds stresses which represent scales of motion that are not resolved in the averaged equations. This necessitates the modelling of turbulent Reynolds stresses linked to eddy viscosity and the modelling may become complex. Eddy viscosity characterize turbulent effects in large-scale motion. The turbulent transfer of momentum by small-scale vortices (or eddies) in the motion giving rise to transport and dissipation of energy characterized by an internal fluid friction. The simplest model to

Stellenbosch University https://scholar.sun.ac.za

represent turbulent chaotic behaviour assumes that the eddy viscosity has a similar form to that used to model molecular or kinematic viscosity. Consequently, the viscous term in the momentum equations in the set of equations of (3.2.1) is expressed as (LeBlond & Mysak, 1978; Pond & Pickard, 1978)

$$\nu\nabla^2\mathbf{v} \approx \nabla\cdot(\nu_t\nabla\mathbf{v}) \quad \text{or} \quad \nu\nabla^2\mathbf{v} \approx \nu_t\nabla^2\mathbf{v} \tag{3.2.2}$$

where ν_t represents eddy viscosity that is assumed to be slowly varying or a constant.

The time averaging of the continuity and the momentum equations to achieve the above result is described in Appendix C.1, where Reynolds stresses have been introduced to the momentum equations. As noted above, the Reynolds stresses are simplified and expressed in terms of eddy viscosity which replaces molecular viscosity in the equations. The Navier-Stokes equations, when time-averaged, as given in Appendix C.1 (equation (C.1.18)) become the Reynolds averaged Navier-Stokes equations (RANS),

$$\frac{D\overline{\rho}}{Dt} = 0, \tag{3.2.3}$$

$$\nabla\cdot\overline{\mathbf{v}} = 0, \tag{3.2.4}$$

$$\frac{\partial\overline{\mathbf{v}}}{\partial t} + \nabla\cdot\overline{(\mathbf{vv})} + 2\boldsymbol{\Omega}\times\overline{\mathbf{v}} = -\frac{1}{\overline{\rho}}\nabla\overline{p} + \nu_t\nabla^2\overline{\mathbf{v}} - \mathbf{g}. \tag{3.2.5}$$

Note that these equations describe time-averaged variables (indicated by an overbar or time averaging symbol). For the remainder of this study, this overbar has been omitted without changing the meaning of the variable.

3.3 Equations valid for a plane attached to a surface of a rotating earth

Under the assumption of the β-plane the shallow water equations of motion (3.2.3) to (3.2.5) can be written in Cartesian coordinates as follows

$$\frac{\partial\rho}{\partial t} + u\frac{\partial\rho}{\partial x} + v\frac{\partial\rho}{\partial y} + w\frac{\partial\rho}{\partial z} = 0, \tag{3.3.1}$$

$$\frac{\partial u}{\partial x} + \frac{\partial v}{\partial y} + \frac{\partial w}{\partial z} = 0, \tag{3.3.2}$$

for the density equation (3.2.3) and the continuity equation (3.2.4), respectively. Following from the approach used in Appendix B,the components of

Stellenbosch University https://scholar.sun.ac.za

the momentum equation (3.2.5) may be written as follows, in the x-direction

$$\frac{\partial u}{\partial t}+\frac{\partial (uu)}{\partial x}+\frac{\partial (uv)}{\partial y}+\frac{\partial (uw)}{\partial z}-2\Omega \sin\phi v+2\Omega \cos\phi w=-\frac{1}{\rho}\frac{\partial p}{\partial x}+ \nu_t\left(\frac{\partial^2 u}{\partial x^2}+\frac{\partial^2 u}{\partial y^2}+\frac{\partial^2 u}{\partial z^2}\right), \tag{3.3.3}$$

in the y-direction

$$\frac{\partial v}{\partial t}+\frac{\partial (vu)}{\partial x}+\frac{\partial (vv)}{\partial y}+\frac{\partial (vw)}{\partial z}+2\Omega \sin\phi u=-\frac{1}{\rho}\frac{\partial p}{\partial y}+ \nu_t\left(\frac{\partial^2 v}{\partial x^2}+\frac{\partial^2 v}{\partial y^2}+\frac{\partial^2 v}{\partial z^2}\right), \tag{3.3.4}$$

in the z-direction

$$\frac{\partial w}{\partial t}+\frac{\partial (wu)}{\partial x}+\frac{\partial (wv)}{\partial y}+\frac{\partial (ww)}{\partial z}-2\Omega \cos\phi u-\frac{(u^2+v^2)}{R}=-\frac{1}{\rho}\frac{\partial p}{\partial z}+ \nu_t\left(\frac{\partial^2 w}{\partial x^2}+\frac{\partial^2 w}{\partial y^2}+\frac{\partial^2 w}{\partial z^2}\right)-g, \tag{3.3.5}$$

where $R\approx 6.37\times 10^3$ km is the radius of the earth. In equation (3.3.5), the term $-\frac{(u^2+v^2)}{R}$ represents sphericity effects (LeBlond & Mysak, 1978).

Implicit in moving from spherical coordinates using the β-plane approximation to Cartesian coordinates are a number of scaling assumptions. Following Dellar (2010), the β-plane approximation exploits the fact that typical scales of motion X, Y and H_z are small compared with R. LeBlond & Mysak (1978) used assumptions around the following ratios of length scales ((L/R) and (H_z/L) where $L(X,Y)$ is the horizontal length scale and H_z is the water depth scale) to arrive at the equations (3.3.1) to (3.3.5). Below the scaling assumptions used to move from spherical to Cartesian coordinates (Equations (3.3.1) to (3.3.5)) are discussed in detail below.

Assumption 3.3.1 *(limited area) The horizontal length scale is much smaller than the radius of the earth and the curvature of the earth can be neglected.*

Under assumption 3.3.1 it follows that

$$\frac{L}{R}\ll 1, \tag{3.3.6}$$

which implies that modelling is restricted to an area of limited horizontal extent, i.e $L\ll O(10^6$ m).

Stellenbosch University https://scholar.sun.ac.za

Assumption 3.3.2 *(shallow water approximation) The scale of the vertical motion is significantly smaller than the scale of horizontal motion.*

This implies that, sea water moving over the surface of the rotating earth may be assumed to comprise a thin layer of fluid Vallis (2006), i.e.:

$$\frac{H_z}{R} \ll 1, \tag{3.3.7}$$

where H_z is the water depth scale. By transforming from spherical to β-plane equations, the value of z may be different. However, by the condition in equation (3.3.7) the radial distortion caused when moving from one value of z to another through transformation can be neglected (LeBlond & Mysak, 1978).

In addition to Assumption 3.3.2 two further scaling assumptions are required to allow the use of Taylor series expansion in moving from spherical to Cartesian coordinates using the β-plane approximation. These assumptions are as follows:

Assumption 3.3.3 *The horizontal scale of the motion is assumed to be appreciably smaller than the earth's radius.*

This implies that

$$\left(\frac{L}{R}\right)^2 \ll 1, \tag{3.3.8}$$

since $R \approx O(10^6 \text{ m})$ and $L \ll O(10^6 \text{ m})$. The condition place a rather stringent restriction on the scales of motions that can be considered using the β-plane equations. A more stringent approximation is

Assumption 3.3.4 *The motion is limited to the horizontal scale at the latitude ϕ_0, for non-high latitudes or non-polar seas.*

This implies that

$$\left(\frac{L}{R}\right) \tan\phi_0 \ll 1 \quad \text{or} \quad L \ll R\cot\phi_0, \tag{3.3.9}$$

where $R\cot\phi_0$ is the radius of the local small circle at the latitude ϕ_0.

At $\phi_0 = 45°$ the condition (3.3.9) is similar to condition (3.3.6). Upon approaching the poles $\tan\phi_0$ becomes very large, meaning the above condition can not be met. This implies that the β-plane equations are not valid upon approaching the poles and thus are valid for only low- to mid-latitudes. According to Dellar (2010), the derivation in LeBlond & Mysak (1978) neglects terms of $O((L/R)\tan\phi_0)$ while retaining terms of $O((L/R)\cos\phi_0)$ results in

Stellenbosch University https://scholar.sun.ac.za

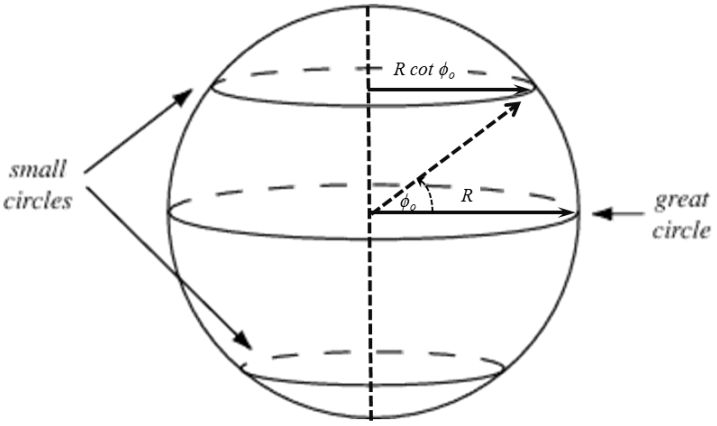

Figure 3.1: Great circle and small circle.

the same conclusions.to consider motions in mid- or low-latitudes.

Using the nomenclature $f = 2\Omega \sin\phi$ to represent the local vertical component of $2\boldsymbol{\Omega}$ and $\tilde{f} = 2\Omega\cos\phi$ to represent the local horizontal component of $2\boldsymbol{\Omega}$, the equations of motion or the β-plane equations (equations (3.3.1) to (3.3.5)) may be written as follows:

$$\frac{\partial \rho}{\partial t} + u\frac{\partial \rho}{\partial x} + v\frac{\partial \rho}{\partial y} + w\frac{\partial \rho}{\partial z} = 0, \tag{3.3.10}$$

$$\frac{\partial u}{\partial x} + \frac{\partial v}{\partial y} + \frac{\partial w}{\partial z} = 0, \tag{3.3.11}$$

for the density equation (3.3.1) and the continuity equation (3.3.2), respectively, rewritten here for clarity. The components of the momentum equations (3.3.3) to (3.3.5) may be written as

$$\frac{\partial u}{\partial t} + \frac{\partial (uu)}{\partial x} + \frac{\partial (uv)}{\partial y} + \frac{\partial (uw)}{\partial z} - fv + \tilde{f}w = -\frac{1}{\rho}\frac{\partial p}{\partial x} + \nu_t\left(\frac{\partial^2 u}{\partial x^2} + \frac{\partial^2 u}{\partial y^2} + \frac{\partial^2 u}{\partial z^2}\right), \tag{3.3.12}$$

$$\frac{\partial v}{\partial t} + \frac{\partial (vu)}{\partial x} + \frac{\partial (vv)}{\partial y} + \frac{\partial (vw)}{\partial z} + fu = -\frac{1}{\rho}\frac{\partial p}{\partial y} + \nu_t\left(\frac{\partial^2 v}{\partial x^2} + \frac{\partial^2 v}{\partial y^2} + \frac{\partial^2 v}{\partial z^2}\right), \tag{3.3.13}$$

Stellenbosch University https://scholar.sun.ac.za

$$\frac{\partial w}{\partial t}+\frac{\partial (wu)}{\partial x}+\frac{\partial (wv)}{\partial y}+\frac{\partial (ww)}{\partial z}-\tilde{f}u-\frac{(u^2+v^2)}{R}=-\frac{1}{\rho}\frac{\partial p}{\partial z}+$$
$$\nu_t\left(\frac{\partial^2 w}{\partial x^2}+\frac{\partial^2 w}{\partial y^2}+\frac{\partial^2 w}{\partial z^2}\right)-g. \tag{3.3.14}$$

The local vertical component of $2\boldsymbol{\Omega}$, i.e. the Coriolis parameter $f = 2\Omega\sin\phi$, may be expressed in terms of a reference latitude ϕ_0. This can be achieved if $f = 2\Omega\sin\phi$ is expanded by a Taylor series about $\phi = \phi_0$, in which case the Coriolis parameter f_0 and the parameter β_0 are introduced at latitude ϕ_0. For the latitude $\phi = \phi_0$ the Coriolis parameter may be approximated by a linear approximation

$$f = f_0 + \beta_0 y, \tag{3.3.15}$$

where y represents the variation in latitude, f_0 is the local Coriolis parameter and the parameter β_0 the local variation in the Coriolis parameter at the reference latitude ϕ_0. The reference value of f is given by

$$f_0 = 2\Omega\sin\phi_0. \tag{3.3.16}$$

The variations of the Coriolis parameter with latitude is given as the latitudinal gradient (Gill, 1982; LeBlond & Mysak, 1978; Pedlosky, 1987; Pond & Pickard, 1978; Bowden, 1983)

$$\beta_0 = \frac{\partial f}{\partial y} = \frac{2\Omega}{R}\cos\phi_0. \tag{3.3.17}$$

Equations (3.3.10) to (3.3.14) may be further simplified in a manner that allows curvature and sphericity effects, i.e. $\tilde{f}$ and $-\frac{(u^2+v^2)}{R}$ to be neglected. To do this requires further scaling assumptions as follows.

Assumption 3.3.5 *The scales of motion are such that*

$$\left(\frac{H_z}{L}\right)\cot\phi_0 \ll 1. \tag{3.3.18}$$

This condition allows one to assume that $|\tilde{f}w/fv| \ll 1$ in equation (3.3.12) and $|\tilde{f}u/(\frac{1}{\rho}\frac{\partial p}{\partial z})| \ll 1$ in equation (3.3.14), where the pressure scale is assumed to be $P_* = \rho f \mathrm{V} L$ based on the assumption that the motions under consideration are quasi-geostrophic. Consequently, the terms $\tilde{f}w$ in equation (3.3.12) and $\tilde{f}u$ in equation (3.3.14) may be neglected. According to LeBlond & Mysak (1978), this condition (3.3.19) will be met beyond $\pm 1^\circ$ of latitude from the equator. This implies that should $\tilde{f}$ be neglected, the equations are only valid

Stellenbosch University https://scholar.sun.ac.za

for modelling of non-equatorial motions.

According to Dellar (2010), a combination of equations (3.3.10) to (3.3.14) with f given by equation (3.3.15) and $\tilde{f} \approx 0$, is the traditional approximation widely used in theorectical studies of the wind-driven ocean flows, e.g. Gill (1982) and Pedlosky (1987). Under this approximation, the terms $\tilde{f}w$ and $-\tilde{f}u$ are neglected in equations (3.3.12) and (3.3.14), respectively. Dellar (2010) is of the opinion that the traditional approximation cannot be derived as a rational approximation.

Assumption 3.3.6 *The scales of motion are such that*

$$\left(\frac{\mathrm{V}}{fL}\right)\left(\frac{\mathrm{H}}{R}\right) \ll 1. \tag{3.3.19}$$

This allows one to neglect the term $-\frac{(u^2+v^2)}{R}$ when compared to the dominant terms in equation (3.3.14), i.e. the pressure term $\frac{1}{\rho}\frac{\partial p}{\partial z}$ and gravity g.

Under Assumptions (3.3.5) and (3.3.6), the sphericity and curvature terms in equations (3.3.10) to (3.3.14) can be neglected resulting in the following β-plane equations:

$$\frac{\partial \rho}{\partial t} + u\frac{\partial \rho}{\partial x} + v\frac{\partial \rho}{\partial y} + w\frac{\partial \rho}{\partial z} = 0, \tag{3.3.20}$$

$$\frac{\partial u}{\partial x} + \frac{\partial v}{\partial y} + \frac{\partial w}{\partial z} = 0, \tag{3.3.21}$$

for the density equation (3.3.10) and the continuity equation (3.3.11), respectively, rewritten here for clarity. The components of the momentum equations (3.3.12) to (3.3.14) may be written as

$$\frac{\partial u}{\partial t} + \frac{\partial (uu)}{\partial x} + \frac{\partial (uv)}{\partial y} + \frac{\partial (uw)}{\partial z} - fv = -\frac{1}{\rho}\frac{\partial p}{\partial x} + \nu_t\left(\frac{\partial^2 u}{\partial x^2} + \frac{\partial^2 u}{\partial y^2} + \frac{\partial^2 u}{\partial z^2}\right), \tag{3.3.22}$$

$$\frac{\partial v}{\partial t} + \frac{\partial (vu)}{\partial x} + \frac{\partial (vv)}{\partial y} + \frac{\partial (vw)}{\partial z} + fu = -\frac{1}{\rho}\frac{\partial p}{\partial y} + \nu_t\left(\frac{\partial^2 v}{\partial x^2} + \frac{\partial^2 v}{\partial y^2} + \frac{\partial^2 v}{\partial z^2}\right), \tag{3.3.23}$$

Stellenbosch University https://scholar.sun.ac.za

$$\frac{\partial w}{\partial t} + \frac{\partial (wu)}{\partial x} + \frac{\partial (wv)}{\partial y} + \frac{\partial (ww)}{\partial z} = -\frac{1}{\rho}\frac{\partial p}{\partial z} + \nu_t \left(\frac{\partial^2 w}{\partial x^2} + \frac{\partial^2 w}{\partial y^2} + \frac{\partial^2 w}{\partial z^2} \right) - g. \tag{3.3.24}$$

The equations applicable for the various scales of motion are as follows:

(i) for very large-scales, i.e. $L/R \sim O(1)$, where $L \approx R \approx 10^6$ m, the original equations (3.2.1) written in spherical coordinates need to be used. As noted above, in this case it is important to replace the molecular or kinematic viscosity with eddy viscosity.

(ii) for intermediate scales, i.e. $L/R \sim O(10^{-1})$, where $10^5 < L < 10^6$ m, the β-plane equations (3.3.10) to (3.3.14) are applicable. In which case, the domain of limited horizontal extent include curvature and sphericity effects.

(iii) for smaller-scale motions, i.e. $L/R \sim O(10^{-2})$, where $L < 10^5$ m, the f-plane equations (3.3.20) to (3.3.24) can be used. In which case, the curvature and sphericity effects are neglected as the domain is that of limited horizontal extent.

3.4 The 3D shallow water equations

As noted above in the condition (3.3.7), in shallow water the aspect ratio (of vertical scales to horizontal scales of motions) is relatively small. This means that the flow can be characterized as predominantly horizontal, under the condition (3.3.7). It is at this stage that equations (3.3.20) to (3.3.24) can be simplified to represent the shallow water equations. The hydrostatic assumption is the key to shallow water assumptions and the shallow water equations (Pedlosky, 1987). In the place of the condition (3.3.7), a commonly used and more restrictive approximation is

$$\frac{H_z}{L} \ll 1, \tag{3.4.1}$$

which states that:

Assumption 3.4.1 *(alternative shallow water approximation) The scale water depth is much smaller than the horizontal length scale.*

The condition in equation (3.4.1) is necessary to allow the hydrostatic assumption to be made.

Stellenbosch University https://scholar.sun.ac.za

3.4.1 Equations for hydrostatic sea water

Based on Assumption 3.4.1 above, the hydrostatic assumption can be made (Gill, 1982; LeBlond & Mysak, 1978; Pond & Pickard, 1978) where it is assumed that the gravity force is balanced by the pressure gradient (Landau & Lifshitz, 1959) and it is assumed that the vertical acceleration and the vertical shear stress terms are negligible in equation (3.3.24) as shown by Pedlosky (1987) and Dingemans (1997a), i.e.:

$$\frac{\partial p}{\partial z} = -\rho g. \tag{3.4.2}$$

Based on the above discussion, equations (3.3.20) to (3.3.24) may be simplified to represent the 3D shallow water equations, expressed as

$$\frac{\partial \rho}{\partial t} + u\frac{\partial \rho}{\partial x} + v\frac{\partial \rho}{\partial y} + w\frac{\partial \rho}{\partial z} = 0, \tag{3.4.3}$$

$$\frac{\partial u}{\partial x} + \frac{\partial v}{\partial y} + \frac{\partial w}{\partial z} = 0, \tag{3.4.4}$$

for the density equation (3.3.20) and the continuity equation (3.3.21), respectively, rewritten here for clarity. The momentum equation (3.3.22) in the x-direction,

$$\frac{\partial u}{\partial t} + \frac{\partial (uu)}{\partial x} + \frac{\partial (uv)}{\partial y} + \frac{\partial (uw)}{\partial z} - fv = -\frac{1}{\rho}\frac{\partial p}{\partial x} + \nu_t \left(\frac{\partial^2 u}{\partial x^2} + \frac{\partial^2 u}{\partial y^2} + \frac{\partial^2 u}{\partial z^2} \right), \tag{3.4.5}$$

the momentum equation (3.3.23) in the y-direction,

$$\frac{\partial v}{\partial t} + \frac{\partial (vu)}{\partial x} + \frac{\partial (vv)}{\partial y} + \frac{\partial (vw)}{\partial z} + fu = -\frac{1}{\rho}\frac{\partial p}{\partial y} + \nu_t \left(\frac{\partial^2 v}{\partial x^2} + \frac{\partial^2 v}{\partial y^2} + \frac{\partial^2 v}{\partial z^2} \right), \tag{3.4.6}$$

and in the z-direction, the momentum equation (3.3.24) is replaced by equation (3.4.2), rewritten here for clarity

$$\frac{\partial p}{\partial z} = -\rho g. \tag{3.4.7}$$

Basically, the fluid has a density structure given as $\rho = \rho(z)$ (Landau & Lifshitz, 1959), i.e:

$$\rho = -\frac{1}{g}\frac{\partial p}{\partial z}. \tag{3.4.8}$$

Stellenbosch University https://scholar.sun.ac.za

The latter equation is further explored to distinguish between baroclinic and barotropic sea water, i.e. sea water of non-uniform and constant density, respectively.

3.4.2 Equations for a Boussinesq fluid

The Boussinesq approximation for density changes, proposed by Boussinesq in 1903 (Gill, 1982; LeBlond & Mysak, 1978; Pedlosky, 1987; Pond & Pickard, 1978) is as described below.

Assumption 3.4.2 *(Boussinesq approximation) The effects of density differences are small enough so that these density differences may be neglected, except for determining buoyancy where even small density changes are important.*

This implies that in the vertical momentum equation density differences only appear in the terms multiplied by gravity g. The essence of the Buossinesq approximation is that the differences in inertia due to small changes in density are negligible but gravity is sufficiently strong for such small density differences to result in significant changes in buoyancy. Consequently, according to Pond & Pickard (1978), the Boussinesq approximation leads to:

(i) The retention of a variable density in the vertical momentum equations, i.e. the weight of the fluid.

(ii) Buoyancy effects may be evident in the vertical direction, with neglible effects in the horizontal direction.

The necessary condition underlying the Assumption 3.4.2 is that small pertubations to stratified sea water initially at rest, only produce very smaller corrections to the inertia, Coriolis accelerations and the viscous stresses in equations (3.4.5), (3.4.6) and (3.4.7).

Gill (1982), LeBlond & Mysak (1978) and Pond & Pickard (1978) state that

$$\mathbf{v}(u, v, w) = \mathbf{0}, \rho = \rho_0, p = p_0, \tag{3.4.9}$$

characterize sea water initially at rest, where ρ_0 and p_0 represent the reference density and pressure, respectively. Equation (3.4.9) implies that for a fluid at rest equation (3.4.7) simplifies to

$$\frac{\partial p_0}{\partial z} = -\rho_0 g, \tag{3.4.10}$$

and that equations (3.4.3) and (3.4.4) remain unchanged, i.e. hydrostatic sea water (Landau & Lifshitz, 1959; Batchelor, 1967).

Stellenbosch University https://scholar.sun.ac.za

To understand assumption 3.4.2, equations (3.4.7) and (3.4.10) are combined to give

$$\begin{aligned}\frac{\partial(p+p_0)}{\partial z} &= -g(\rho+\rho_0)\\ &= -\rho_0\left(1+\frac{\rho}{\rho_0}\right)g. \end{aligned} \tag{3.4.11}$$

This equation characterizes a displacement of any fluid element, that per definition has density of ρ_0 at its original equilibrium position. The term $-g\frac{\rho}{\rho_0}$ in equation (3.4.11) represents the buoyancy force, responsible to restore to its equilibrium position any fluid element that has been displaced from its original equilibrium position. In the case of a stratified incompressible fluid $\frac{\rho}{\rho_0} \ll 1$ (i.e. $O(10^{-3})$) (Gill, 1982; Pond & Pickard, 1978; Philips, 1980; LeBlond & Mysak, 1978). This is basically the original observation proposed by Boussinesq in 1903.

LeBlond & Mysak (1978) states that the Brunt-Väisälä frequency, defined by

$$N^2(z) = -\frac{g}{\rho_0}\frac{\partial\rho}{\partial z}, \tag{3.4.12}$$

is an important quantity when characterizing changes due to effects of density. Equation (3.4.12) physically describes the natural frequency of oscillations for the displaced fluid elements. In particular, when equation (3.4.12) is written as

$$\frac{\partial\rho}{\partial z} = -\frac{\rho_0 N^2}{g}, \tag{3.4.13}$$

it represents a natural response of density in the fluid to a change from equilibrium ρ_0.

Under the hydrostatic assumption and the Boussinesq approximation, the β-plane equations (3.4.3) to (3.4.7) simplify to the 3D shallow water equations:

$$\frac{\partial\rho}{\partial t} + u\frac{\partial\rho}{\partial x} + v\frac{\partial\rho}{\partial y} + w\frac{\partial\rho}{\partial z} = 0, \tag{3.4.14}$$

$$\frac{\partial u}{\partial x} + \frac{\partial v}{\partial y} + \frac{\partial w}{\partial z} = 0, \tag{3.4.15}$$

for the density equation (3.4.3) and the continuity equation (3.4.4), respectively, rewritten here for clarity. By the Boussinesq approximation the density

Stellenbosch University https://scholar.sun.ac.za

is set to $\rho = \rho_0$, as under this approximation changes due to density are assumed to occur in the z-direction. The momentum equation (3.4.5) in the x-direction may be written as

$$\frac{\partial u}{\partial t} + \frac{\partial (uu)}{\partial x} + \frac{\partial (uv)}{\partial y} + \frac{\partial (uw)}{\partial z} - fv = -\frac{1}{\rho_0}\frac{\partial p}{\partial x} + \nu_t \left(\frac{\partial^2 u}{\partial x^2} + \frac{\partial^2 u}{\partial y^2} + \frac{\partial^2 u}{\partial z^2} \right), \tag{3.4.16}$$

the momentum equation (3.4.6) in the y-direction,

$$\frac{\partial v}{\partial t} + \frac{\partial (vu)}{\partial x} + \frac{\partial (vv)}{\partial y} + \frac{\partial (vw)}{\partial z} + fu = -\frac{1}{\rho_0}\frac{\partial p}{\partial y} + \nu_t \left(\frac{\partial^2 v}{\partial x^2} + \frac{\partial^2 v}{\partial y^2} + \frac{\partial^2 v}{\partial z^2} \right), \tag{3.4.17}$$

and the momentum equation (3.4.7) in the z-direction,

$$\frac{\partial p}{\partial z} = -\rho g. \tag{3.4.18}$$

The above equations are not the only representation of the shallow water equations used to solve flows in the marine environment. For example Aldrighetti (2007) presents the shallow water equations for a version of Saint-Venant equations and in literature various 3D models for marine and estuarine dynamics are presented.

3.5 Pressure gradients in baroclinic and barotropic fluid

The hydrostatic equation (3.4.2) may be expressed as a hydrostatic pressure distribution, after integration of equation (3.4.2) i.e.:

$$p = p_a - g \int_{-h}^{\eta} \rho\,(S,T)\, dz, \tag{3.5.1}$$

where p_a represents the atmospheric pressure at the sea surface that is, usually, neglected $p_a = 0$, S is the salinity and T is the temperature.

The horizontal pressure gradients in equations (3.4.16) and (3.4.17) are determined below, for a baroclinic fluid and for a barotropic fluid.

Stellenbosch University https://scholar.sun.ac.za

3.5.1 The pressure gradients in baroclinic fluid

For a fluid of non-uniform density $N^2 \neq 0$ (LeBlond & Mysak, 1978; Gill, 1982), the differences between fluid elements are characterize by varying temperature and salinity, both of which vary in space and time. After calculating derivatives of pressure in equation (3.5.1), i.e. in the x-direction:

$$\frac{\partial p}{\partial x} = \frac{\partial p_a}{\partial x} - g\frac{\partial}{\partial x}\int_{-h}^{\eta} \rho dz. \tag{3.5.2}$$

Note that $\frac{\partial p_a}{\partial x}$ can be set to zero as $p_a = 0$ is constant at zero and the second term on the right hand side of equation (3.5.2) may be expanded using Leibniz's theorem (A.2.1). Therefore from equation (3.5.2) it follows that

$$\begin{aligned}\frac{\partial p}{\partial x} &= -g\frac{\partial}{\partial x}\int_{-h}^{\eta} \rho dz \\ &= -g\left(\int_{-h}^{\eta} \frac{\partial \rho}{\partial x}dz + \rho|_{\eta}\frac{\partial \eta}{\partial x} - \rho|_{-h}\frac{\partial h}{\partial x}\right) \\ &= -g\int_{-h}^{\eta} \frac{\partial \rho}{\partial x}dz - g\rho|_{\eta}\frac{\partial \eta}{\partial x},\end{aligned} \tag{3.5.3}$$

where $-\rho|_{-h}\frac{\partial h}{\partial x} = 0$ assuming that the bottom sloping topography is set to zero. Similarly, in the y-direction the derivative of pressure in equation (3.5.1) yields

$$\frac{\partial p}{\partial y} = -g\int_{-h}^{\eta} \frac{\partial \rho}{\partial y}dz - g\rho|_{\eta}\frac{\partial \eta}{\partial y}. \tag{3.5.4}$$

This means that pressure changes in stratified or baroclinic sea water is characterized by both changes in water levels and the density structure of the water column.

3.5.2 The pressure gradients in barotropic fluid

In a barotropic fluid $N^2 = 0$ (LeBlond & Mysak, 1978; Gill, 1982). In equations (3.5.3) and (3.5.4), the respective terms $\frac{\partial \rho}{\partial x}$ and $\frac{\partial \rho}{\partial y}$ are negligible, since $\rho(z)$ is characterized by a change in the vertical direction. The necessary condition to simplify equations (3.5.3) and (3.5.4) is that density, ρ, is constant and has the same value in depth as at the surface. Then the horizontal pressure gradients, equations (3.5.3) and (3.5.4) respectively, simplifies to

$$\frac{\partial p}{\partial x} = -g\rho\frac{\partial \eta}{\partial x}, \tag{3.5.5}$$

$$\frac{\partial p}{\partial y} = -g\rho\frac{\partial \eta}{\partial y}. \tag{3.5.6}$$

Stellenbosch University https://scholar.sun.ac.za

This implies that the gradients of water level elevation of barotropic pressure gradients for non-stratified sea water are proportional only to the change in pressure. Therefore, changes in density are not a driving force in a fluid of uniform density.

3.6 Summary

This chapter has presented the derivation of the shallow water equations of motion applicable for flows in coastal and shelf regions from the more comprehensive Navier-Stokes equations relevant for CFD. The various assumptions necessary to do so have been discussed as well as any implications for the validity of the shallow water equations for modelling flows in coastal and shelf regions. For the purpose of numerical simulations using the Delft3D-FLOW suite, the hydrodynamic equations derived above (i.e. equations (3.4.14) to (3.4.18)) can be transformed to represent orthorgonal curvilinear equations used in Delft3D-FLOW.

The shallow water equations are of course incomplete without boundary conditions. Stelling (1983) presents how one can solve the shallow water equations, using finite difference method, including how to numerically approximate the solutions near the boundaries.

Stellenbosch University https://scholar.sun.ac.za

Chapter 4

Boundary Conditions

4.1 Introduction

The shallow water equations described in Chapter 3, needs to be solved within a model domain while at the same time satisfying the specified boundary and initial conditions. Boundary conditions may be generally categorised into closed and open boundary conditions (OBCs). Closed boundaries are physical boundaries and relate to an actual existing boundary, e.g. the land or coastal boundary. Open boundaries are artificial boundaries, essentially introduced to restrict the size of the model domain. In the context of CFD, boundary conditions may be prescribed just outside the physical boundaries, e.g. the structure of a staggered grid includes ghost nodes for the said purpose. This chapter comprises a general introduction to boundary conditions applicable to numerical models of the ocean.

4.2 Background to boundary conditions

The specification of boundary conditions is not necessary dependent on the equations being modelled, but rather on the nature of the model domain or the boundaries. It is important that boundary conditions are correctly specified and their role to the model is understood.

Open boundaries are required in computer codes to limit computations only to a restricted model domain. In which case, the boundaries represent virtual barriers of communication of information into and out of the model domain. The main requirement is for the boundaries to allow phenomena generated inside the model domain to leave the domain and to allow information from the exterior environment to pass through the boundaries and into the model interior without undergoing deterioration (Orlanski, 1976; Blayo & Debreu, 2004). Specifically it is the lack of knowledge of the dynamical behaviour of the environment in the region outside the model domain, that is the limiting

Stellenbosch University https://scholar.sun.ac.za

factor.

Boundary conditions cannot be easily generalized, consequently there are many boundary conditions developed in literature, mostly designed for specific problems. In Chapter 5, OBCs that are based on linearized equations of motion are investigated. Such OBCs are provided in terms of a local solution based on "reduced physics" (Oddo & Pinardi, 2007). In this study, OBCs generally are formulated in terms of the velocity perpendicular ($u_\perp$) and the velocity parallel ($u_\parallel$) to the open boundaries, as well as water levels (η).

4.3 Boundary conditions for coastal and shelf seas

Many coastal area models have a land boundary, cross-shore lateral boundaries and an offshore boundary. These are the closed and the open boundaries which enclose the computational domain. Note that the problem being studied is of general application. For illustration purposes consider Figure 4.1, in which the computational or model domain is chosen on the East coast of South Africa and the boundaries are defined as discussed below. The land boundary constitutes a closed boundary and is the only physical boundary for many coastal and shelf models. Open boundaries on the other hand do not constitute physical boundaries but are boundaries of the limited area model that are subject to forcing from the surrounding open ocean. The particular open boundaries discussed for the coastal and shelf models under consideration here are the two cross-shore boundaries (i.e. OB1 and OB2 in the x-direction in Figure 4.1) and an offshore boundary (OB3, along the y-direction in Figure 4.1).

Delft3D-FLOW is the numerical model used in this study. To produce results the model needs boundary conditions to be specified by the user. In mathematical models and computer models, open boundaries have always been difficult to handle. Herzfeld *et al.* (2011) discuss numerous common issues confronting modellers, including issues surrounding configuration of active and passive boundaries, evaluation of model skill and boundary error when modelling limited areas. In particular, boundary conditions which are transparent and compatible with the model solution are difficult to determine.

Generally, the boundaries are subject to effects due to perpendicular $u_\perp$ and/or parallel $u_\parallel$ flow velocities and the water level η in the model interior, as well as the water levels $F_\eta(t)$ and flow velocities $F_u(t)$ imposed at boundaries. The question is, should external data be specified at the open boundary, what is the required consistency between these data and the solution to the open boundary problem (Blayo & Debreu, 2004)? In the case of measured external data,

Stellenbosch University https://scholar.sun.ac.za

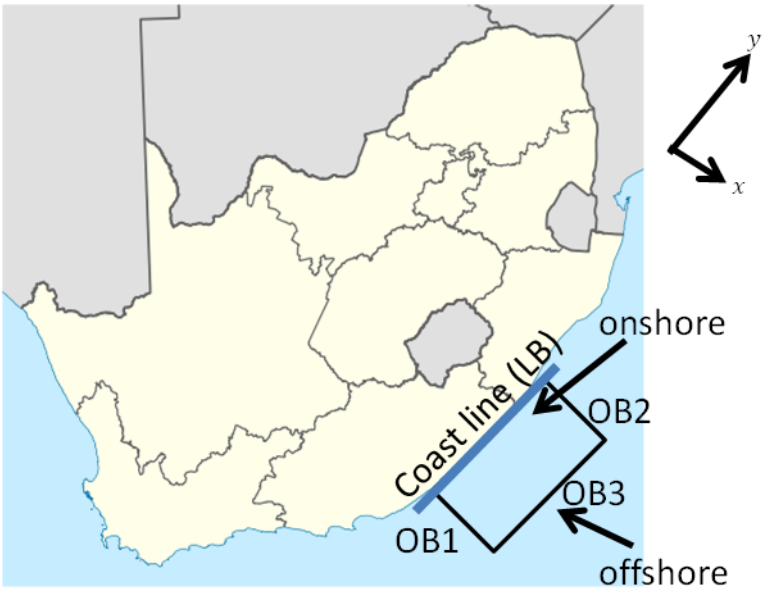

Figure 4.1: A limited area on the East coast of South Africa, enclosed by boundaries.

e.g. water levels and currents the boundary conditions may be implemented as discussed below.

4.3.1 The closed boundary, coastal boundary conditions

The land or coastal boundary comprises a water-land boundary. Stelling (1983) states that

$$u_{\perp} = 0, \tag{4.3.1}$$

$$(1-\alpha)u_{\parallel} + \alpha\frac{\partial}{\partial n}u_{\parallel} = 0, \tag{4.3.2}$$

may be used to describe boundary condition at the coast. These describe a perfect slip boundary conditon if $\alpha = 1$, and a no-slip boundary condition if $\alpha = 0$. It is commonly assumed that at the coastal boundary the flow velocities are zero perpendicular to the boundary, i.e. $\mathbf{v} \cdot \boldsymbol{n} = 0$, where $\boldsymbol{n}$ is a normal vector.

4.3.2 The open boundaries, boundary conditions

Generally, open boundaries are characterized by artificial water-water open boundaries. For the purpose of this study, open boundary conditions that characterize water level and velocity boundary condition are considered and

Stellenbosch University https://scholar.sun.ac.za

discussed below. Based on Stelling (1983) the simplest open boundary conditions usually applied to practical flow problems in nature are given by:

(i) The velocity boundary conditions,

$$u_{\perp} = F_u(t), \tag{4.3.3}$$

$$u_{\parallel} = 0, \tag{4.3.4}$$

$$\frac{\partial}{\partial n} u_{\parallel} = 0 \quad \text{if} \quad \nu_t \neq 0. \tag{4.3.5}$$

(ii) The water level boundary conditions,

$$\eta = F_\eta(t), \tag{4.3.6}$$

$$u_{\parallel} = 0, \tag{4.3.7}$$

$$\frac{\partial}{\partial n} u_{\parallel} = 0 \quad \text{if} \quad \nu_t \neq 0, \tag{4.3.8}$$

where $F_u(t)$ and $F_\eta(t)$, respectively, represent the water level and velocity time series imposed at the open boundaries. These sets of boundary conditions can be applied together at the same time or separately. According to Stelling (1983), the boundary conditions (4.3.4) and (4.3.7) only apply to inflow conditions. The well-posedness problem concerning these boundary conditions is treated by Verboom *et al.* (1981, 1982) as described in Stelling (1983). Furthermore, Stelling (1983) describes in detail how these boundary conditions should be treated, also how to fix arising problems.

Offshore open boundaries

The boundary situated far from the coast at a distance X is the offshore boundary, usually defined at $x \to \infty$ where the water depth is much larger than at the coast. Possible boundary conditions at the offshore boundary include:

(i) A boundary condition where the water level is clamped to zero and that allows no changes over time, i.e. $\eta = 0$.

(ii) A boundary condition where the pressure gradient tends to zero at the distance far from the coast (X, at the offshore boundary), i.e. $\frac{\partial p}{\partial x} \to 0$ or $\frac{\partial \eta}{\partial x} \to 0$ as $x \to \infty$. Under this boundary condition the pressure p or water level η can assume any value. For example one can assume $\eta = 0$

Stellenbosch University https://scholar.sun.ac.za

for no change in water levels or $\eta = -p_a$ where there is an inverse barometer response to fluctuation in the atmospheric pressure, i.e. atmospheric pressure effects are not neglected in equation (3.5.1).

(iii) A boundary condition based on characteristic variables or Riemann invariants Blayo & Debreu (2004). According to Stelling (1983), Riemann invariants are quantities that are not measured in nature. When Riemann invariants boundary conditions are used, a stabilizing effect is often experienced (Stelling, 1983). Moreover, Stelling (1983) presents Riemann invariants boundary conditions that may be used to replace equations (4.3.3) to (4.3.8).

Cross-shore open boundaries

For the purpose of this study, the cross-shore open boundaries are required to be transparent and allow the model solution to pass through without any deterioration, which is important when modelling the nearly alongshore motion. For illustration purposes in this study coastal trapped waves (see Appendix A.5.3) are referred to, without ruling out that other phenomena are as prevalent in coastal and shelf seas. Note that $F_u(t)$ and $F_\eta(t)$ in equations (4.3.3) and (4.3.6) comprise unkown forcing and/or dynamics on the cross-shore open boundaries. In literature these are determined through extrapolation, modelling or assumed values.

For the purpose of this study a modified version of the Sommerfeld radiation condition proposed by Blumberg & Khanta (1985) is considered, i.e.:

$$\frac{\partial \eta}{\partial t} \pm C_0 \frac{\partial \eta}{\partial n} = -\frac{(\eta - F_\eta(t))}{\alpha}. \tag{4.3.9}$$

where

- η is the sea level elevation (water level),
- $F_\eta(t)$ is the imposed water level at the open boundary,
- C_0 is the wave phase speed,
- n is the coordinate normal to the open boundary,
- $C_0 \frac{\partial \eta}{\partial n}$ represents the boundary normal component of the wave phase speed vector,
- α is the relaxation time scale within which the water level elevation is restored to the imposed water level $F_\eta(t)$ at the open boundary.

Stellenbosch University https://scholar.sun.ac.za

The solutions determined from equation (4.3.9) are sensitive to the choice of radiation condition, its numerical implementation and to the relaxation time scale (Herzfeld *et al.*, 2011).

The right hand side of equation (4.3.9) represents damping which tends to force the water level to the imposed water level at the open boundary. Note that the transient response in water level, i.e. $\eta - F_\eta(t)$ on the open boundaries would only be known if forcing or dynamics on the open boundaries are known. In the next chapter, reduced hydrodynamic equations are described based on the model dynamics. This allows water levels at the boundaries to be predicted based on simplified dynamic equations.

The relaxation time scale α in equation (4.3.9) determines the behaviour of the solution inside the model domain. Particularly how quickly the solution in the interior model domain response to the imposed boundary conditions. The conditions which satisfy the open boundaries under controlled relaxation time scales are discussed below.

Case 1: $\alpha \to 0$

If the relaxation time becomes very small, the term on the right hand side becomes relatively large compared to the Sommerfeld condition on the left hand side of equation (4.3.9). Consequently,

$$\eta = F_\eta(t), \tag{4.3.10}$$

is the clamped water level. In this case, the open boundaries act as barriers which do not allow radiation of waves out of the model domain, however information from the outside environment does influence the solution in the interior model domain. The boundary condition (equation (4.3.10)) does not readily allow transients from the interior model domain to pass out through the boundaries and consequently lead to the accumulation of numerical errors in the vicinity of the open boundaries, particularly for rapidly changing boundary time series.

The trivial case of the boundary condition (equation (4.3.10)) being

$$\eta = F_\eta(t) = 0, \tag{4.3.11}$$

do not allow both radiation of waves out of the interior model domain and influence of the outside environment into the interior model domain. This retains transients inside the model domain generated by local forcing.

According to Blumberg & Khanta (1985), the clamped OBC may be useful

Stellenbosch University https://scholar.sun.ac.za

when one is interested in the final steady state solution attained due to impulsively applied forcing or due to a change in forcing. Alternatively, this means that the clamped OBC may not be appropriate when one is interested in the resulting transient response solution as the OBC can introduce unwanted transients into the interior model domain (associated with imposed mismatches in water levels and/or currents at the open boundaries).

Case 2: $\alpha \to \infty$

If the relaxation time tends to infinity, $\alpha \to \infty$, equation (4.3.9) reduces to the Sommerfeld radiation condition (4.3.12). The boundaries are transparent to travelling waves, in particular those that exit in a normal direction to the boundaries. The information prescribed on the open boundaries is rendered redundant. In which case, the determination of open boundary conditions is solely depend on the determination of the phase speed of the waves exiting the model interior domain.

The Sommerfeld radiation condition, is given by a one-dimensional wave equation written as

$$\frac{\partial \eta}{\partial t} \pm C_0 \frac{\partial \eta}{\partial n} = 0. \tag{4.3.12}$$

The role of equation (4.3.12) is solely depend and on C_0, which may be determined via methods discussed in Herzfeld *et al.* (2011). In idealized test cases the solution to equation (4.3.12) can be decomposed into outgoing and incoming waves where the phase speed of the outgoing wave is represented by positive C_0 and incoming wave phase speed is represented by negative C_0. The information for outgoing wave phase speed is available within the computation domain, and no additional information or condition is required. The solutions determined from equation (4.3.12) are very sensitive to how C_0 is estimated (Van Ballegooyen, 1995). Contrary, in the case of incoming waves, the information about the external enviroment may not be available and will need to be specified.

Case 2.1: $\alpha \to \infty$ and $C_0 \frac{\partial \eta}{\partial n} \ll \frac{\partial \eta}{\partial t}$ or $C_0 \to 0$

Under these conditions the changes in water level at the boundaries are very slow resulting in the following condition

$$\frac{\partial \eta}{\partial t} = 0, \tag{4.3.13}$$

being applicable at the open boundary.

Stellenbosch University https://scholar.sun.ac.za

Case 2.2: $\alpha \to \infty$ and $\frac{\partial \eta}{\partial t} \ll C_0 \frac{\partial \eta}{\partial n}$ and $C_0 \to \infty$

These conditions lead to a Neumann boundary condition being applicable at the open boundaries. The Neumann boundary condition may be expressed as a normal derivative set to zero, i.e.:

$$C_0 \frac{\partial \eta}{\partial n} = 0. \tag{4.3.14}$$

This boundary condition allows continuity at the boundaries and allows no information from the external environment, as the values near the boundary on the interior domain will always be the same as that at the boundary. The Neumann boundary condition is useful for obtaining a simulation where the solution in the interior model domain is entirely dependent on the local forcing rather than forcing imposed at the model boundaries.

Case 3: $\alpha \to \alpha_{crit}$

If α is assigned to a reasonable value (say $\alpha = \alpha_{crit}$) the model becomes less sensitive on the information prescribed on the open boundaries. However, depending on the α_{crit} specified, this may lead to a problem of under-relaxation or over-relaxation at the boundaries. Under these conditions the open boundary condition is given by

$$\frac{\partial \eta}{\partial t} \pm C_0 \frac{\partial \eta}{\partial n} = -\frac{(\eta - F_\eta(t))}{\alpha_{crit}}. \tag{4.3.15}$$

Experience has shown that a good estimate of α_{crit} ranges from 10^2 to 10^3 when Delft3D-FLOW is used.

Table 4.1 contains a summary of some open boundary conditions from literature. Many of these boundary conditions are developed from the radiation conditions originally suggested by Sommerfeld (1949) (e.g. Palma & Matano (2001, 1998); Herzfeld *et al.* (2011)).

In summary, general boundary conditions for a limited computational domain have been presented. Appropriate coastal and offshore boundary conditions have been presented for use in limited computational coastal and shelf models. A modified version of the Sommerfeld radiation condition has been selected for further investigation as an appropriate cross-shore open boundary condition for use in limited area modelling where boundary information is not available from measured data or large-scale model results.

Stellenbosch University https://scholar.sun.ac.za

Table 4.1: Summary of the OBCs from literature as in Palma & Matano (2001, 1998); Herzfeld *et al.* (2011).

Open Boundary Conditions	Analytic form	References
Gravity wave implicit, GWI	$\frac{\partial \eta}{\partial t} \pm C_0 \frac{\partial \eta}{\partial n} = 0$ where $C_0 = \sqrt{gh}$	Chapman (1985)
Flather radiation, FLA	$U = \pm \left(\frac{C_0}{h} \right) \eta$	
Flather radiation and Roed local solution, FRO	$U - U_0(t) = \pm \frac{C_0}{h} [\eta - F_\eta(t)]$	Flather (1976), Palma and Matano (1998)
Martisen and Roed local solution, MRO	$\eta = \alpha F_\eta(t) + (1 + \alpha)\eta$	Martisen and Engedahl (1987)
Blumberg and Khanta implicit, BKI	$\frac{\partial \eta}{\partial t} \pm C_0 \frac{\partial \eta}{\partial n} = -\frac{(\eta - F_\eta(t))}{\alpha}$	Blumberg and Khanta (1985), Kourafalou *et al.* (1996)
Orlanski Radiation, ORI or ORE; Somerfeld explicit, SOE; Sommerfeld radiation explicit second order, SRE; Modified Orlanski implicit, MOI	$\frac{\partial \eta}{\partial t} \pm C \frac{\partial \eta}{\partial n} = 0$ where $C = \pm \frac{\partial \eta / \partial t}{\partial \eta / \partial x}$	Chapman (1985), Orlanski (1976), Miller & Thorpe (1981), Tang and Grimshaw (1996), Camerlengo & O'Brien (1980)
Hedstrom O'Brien characteristic, HOC	$\frac{\partial (UH)}{\partial t} = \pm 0.5 C_0 \frac{\partial (UH \pm C_0 \eta)}{\partial n} + F_n$	Roed and Cooper (1987), Palma and Matano (1998)
Flow relaxation scheme, FRS	$\eta = (1 - \alpha)\eta$ where $\alpha = 1 - \tanh[\pm 0.5(x - x_B)]$	Martisen and Engedahl (1987), Engedahl (1995)

Stellenbosch University https://scholar.sun.ac.za

Chapter 5

Simplified hydrodynamic boundary equations

The problem of wind driven flow in coastal and shelf seas requires open boundary conditions that take into account realistic density stratification, bottom topography and bottom friction. Understanding these processes is key to answering the question asked by Clarke & Brink (1985): i.e. under what conditions is the response barotropic? How do currents change over distance from the coast and what is their magnitude for a given wind stress, bottom topography, density stratification and bottom friction? In coastal and shelf seas these dynamics are best explained in terms of coastal trapped wave theory (Brink, 1991). In this study similar questions are considered as general to be asked, although this study focus on the development of open boundary conditions assuming a barotropic response at the boundaries.

In this chapter, simplified hydrodynamic boundary equations are developed, through linearization. According to Blumberg & Khanta (1985), this is necessary to be able to describe at the open boundary equations with reduced physics (Oddo & Pinardi, 2007). Simple equations that represent minimum variables, realistic stratification and friction, will be presented. To achieve these, the approach taken will be that used by Clarke & Brink (1985) and Brink (1991) to derive relevant "reduced physics" open boundary conditions based on linearised shallow water equations of motion.

5.1 Linearized 3D shallow water equations

The governing equations for modelling coastal and shelf currents, the 3D shallow water equations (3.4.14) to (3.4.18) below are as described in Chapter 3, i.e.:

$$\frac{\partial \rho}{\partial t} + u\frac{\partial \rho}{\partial x} + v\frac{\partial \rho}{\partial y} + w\frac{\partial \rho}{\partial z} = 0, \tag{5.1.1}$$

Stellenbosch University https://scholar.sun.ac.za

$$\frac{\partial u}{\partial x} + \frac{\partial v}{\partial y} + \frac{\partial w}{\partial z} = 0, \tag{5.1.2}$$

for the density equation (3.4.14) and the continuity equation (3.4.15), respectively. The momentum equation (3.4.16) in the x-direction,

$$\frac{\partial u}{\partial t} + \frac{\partial (uu)}{\partial x} + \frac{\partial (uv)}{\partial y} + \frac{\partial (uw)}{\partial z} - fv = -\frac{1}{\rho_0}\frac{\partial p}{\partial x} + \nu_t \left(\frac{\partial^2 u}{\partial x^2} + \frac{\partial^2 u}{\partial y^2} + \frac{\partial^2 u}{\partial z^2} \right), \tag{5.1.3}$$

the momentum equation (3.4.17) in the y-direction,

$$\frac{\partial v}{\partial t} + \frac{\partial (vu)}{\partial x} + \frac{\partial (vv)}{\partial y} + \frac{\partial (vw)}{\partial z} + fu = -\frac{1}{\rho_0}\frac{\partial p}{\partial y} + \nu_t \left(\frac{\partial^2 v}{\partial x^2} + \frac{\partial^2 v}{\partial y^2} + \frac{\partial^2 v}{\partial z^2} \right), \tag{5.1.4}$$

and the momentum equation (3.4.18) in the z-direction,

$$\frac{\partial p}{\partial z} = -\rho g. \tag{5.1.5}$$

Under the condition that the Rossby number Ro is assumed to be small, i.e.:

$$Ro = \frac{\mathrm{V}}{f\mathrm{L}} \tag{5.1.6}$$

the above equations may be linearized. This leads to the removal of nonlinear terms (LeBlond & Mysak, 1978). The ratio of the horizontal turbulence to vertical turbulence terms $|\frac{\partial^2 v}{\partial x^2}/\frac{\partial^2 v}{\partial z^2}| \approx (H/L)^2$ and $|\frac{\partial^2 v}{\partial y^2}/\frac{\partial^2 v}{\partial z^2}| \approx (H/L)^2$. Given that $H/L \ll 1$ (condition (3.4.1)) the horizontal turbulence terms are neglected and only the vertical turbulent terms are retained.

The linearized 3D shallow water equations therefore may be written as

$$\frac{\partial \rho}{\partial t} + w\frac{\partial \rho}{\partial z} = 0, \tag{5.1.7}$$

$$\frac{\partial u}{\partial x} + \frac{\partial v}{\partial y} + \frac{\partial w}{\partial z} = 0, \tag{5.1.8}$$

Stellenbosch University https://scholar.sun.ac.za

for the density equation (5.1.1) and the continuity equation (5.1.2), respectively. The momentum equation (5.1.3) in the x-direction,

$$\frac{\partial u}{\partial t} - fv = -\frac{1}{\rho_0}\frac{\partial p}{\partial x} + \nu_t \frac{\partial^2 u}{\partial z^2}, \tag{5.1.9}$$

the momentum equation (5.1.4) in the y-direction,

$$\frac{\partial v}{\partial t} + fu = -\frac{1}{\rho_0}\frac{\partial p}{\partial y} + \nu_t \frac{\partial^2 v}{\partial z^2}, \tag{5.1.10}$$

and the momentum equation (5.1.5) in the z-direction,

$$\frac{\partial p}{\partial z} = -\rho g, \tag{5.1.11}$$

where the vertical turbulent terms $\nu_t \frac{\partial^2 u}{\partial z^2}$ and $\nu_t \frac{\partial^2 v}{\partial z^2}$ are retained allowing the inclusion of wind and bottom shear stresses.

5.2 Scaling of linearized 3D shallow water equations

Generally, currents flow are mainly driven by wind, earth's rotation and density differences in ocean water. In this study scaling is presented to indicate and emphasize on the description of the dominate or main drives currents flow. A similar approach is presented by Pond & Pickard (1978) in their chapter 7 pages 47 to 54. In the next section, scaling is used in order to understand the drivers of currents flow.

Non-dimensionalization and scaling

Non-dimensionalization allows a system of equations to be expressed in terms of dimensionless quantities. The purpose for non-dimensionalizing and scaling the linearized 3D shallow water equations is to examine the magnitudes of the various terms in the equations. Firstly, the non-dimensional variables are introduced in Table 5.1 to represent the basic scales and dimensionless variables. Note that in Table 5.1, that V is the horizontal velocity scale (i.e. given by $\sqrt{U^2 + V^2}$) and L is the horizontal length scale (i.e. given by $\sqrt{X^2 + Y^2}$). These are the scales that are used in the expression $W = (H_z \mathrm{V}/\mathrm{L})$. The time scale is taken to be approximately proportional to f. Moreover, the scale for the vertical velocity W is determined from scaling the continuity equation (5.1.2) and the scale for pressure is determined from the momentum equation

Stellenbosch University https://scholar.sun.ac.za

Table 5.1: Basic scales and dimensionless variables.

Scale	Dimensionless variables	Dimensions
Length $(\mathrm{L}(X,Y);H_z)$	$x^* = \frac{x}{\mathrm{L}}, y^* = \frac{y}{\mathrm{L}}, z^* = \frac{z}{H_z}$	$L \approx 10$ m to 10^6 m, $H_z \approx 10^3$ to 10^4 m LeBlond & Mysak (1978)
Velocity $(\mathrm{V}(U,V);W)$	$u^* = \frac{u}{\mathrm{V}}, v^* = \frac{v}{\mathrm{V}}, w^* = \frac{w}{W} = \frac{w}{(H_z\mathrm{V}/\mathrm{L})}$ where $W = (H_z\mathrm{V}/\mathrm{L})$	$\mathrm{V}(U,V) \approx 0.5$ m/s, $W \approx 10^{-4}$ m/s Pond & Pickard (1978); Gill (1982)
Time t	$t^* = \frac{t}{(1/f)}$	inertial time scale Pedlosky (1987)
Density ρ	$\rho^* = \frac{\rho}{(\rho_0 f\mathrm{VL}/gH_z)}$	density scale as in (LeBlond & Mysak, 1978), where $\rho_0 \approx 1.2 \times 10^{-3}$ kg m^{-3}
Pressure p	$p^* = \frac{p}{\mathrm{P}_*}$ where $\mathrm{P}_* = \rho_0 f\mathrm{V}\ \mathrm{L}$	$\mathrm{P}_* \approx \lvert\mathrm{P}_*\rvert$ Pa
Viscosity ν_t	$\nu_t^* = \frac{\nu_t}{\mathrm{A}}$	$\mathrm{A} \approx 10^{-5}$ m^{2}s^{-1} to 10^{-6} m^{2}s^{-1} Gill (1982)

Stellenbosch University https://scholar.sun.ac.za

(5.1.5) in the z-direction. These are discussed shortly. The scaled continuity equation (5.1.2) is given by

$$\frac{\partial u^*}{\partial x^*}\left[\frac{\mathrm{V}}{\mathrm{L}}\right] + \frac{\partial v^*}{\partial y^*}\left[\frac{\mathrm{V}}{\mathrm{L}}\right] + \frac{\partial w^*}{\partial z^*}\left[\frac{W}{H_z}\right] = 0,$$

$$\left(\frac{\partial u^*}{\partial x^*} + \frac{\partial v^*}{\partial y^*}\right)\left[\frac{\mathrm{V}}{\mathrm{L}}\right] + \frac{\partial w^*}{\partial z^*}\left[\frac{W}{H_z}\right] = 0, \tag{5.2.1}$$

and is mainly useful to determine the scale for the vertical velocity W where

$$\frac{W}{H_z} \approx \frac{\mathrm{V}}{\mathrm{L}} \quad \text{or} \quad W \approx \frac{\mathrm{V}H_z}{\mathrm{L}}. \tag{5.2.2}$$

For illustration purposes, the terms denoted by asterisks, e.g.

$$\frac{\partial v^*}{\partial y^*} \sim O(1), \tag{5.2.3}$$

represent terms of order 1 (Batchelor, 1967). Whereas, the terms in the square brackets, e.g.

$$\left[\frac{\mathrm{V}}{\mathrm{L}}\right] \sim \text{is either large or small}, \tag{5.2.4}$$

represents the magnitude of the relevant terms in the equations or the scales used to retain or neglect terms (Gill, 1982; Pedlosky, 1987; Pond & Pickard, 1978; LeBlond & Mysak, 1978). The scaling presented in this study, provides means to decide whether the latter is large or small, when compared with other terms. The application of these scaling factors thus allows one to simplify the equations of motions but, in the process, also restrict the range (scales) of motions that may be investigated using these simplified equations.

The momentum equation (5.1.5) in the z-direction,

$$\frac{\partial p}{\partial z} = -\rho g, \tag{5.2.5}$$

is mainly useful to determine the scale for pressure P_*. The scaling of equation (5.2.5) may be written as

$$\frac{\partial p^*}{\partial z^*}\left[\frac{\mathrm{P}_*}{H_z}\right] = -\rho^*\left[g\frac{\rho_0 f\ \mathrm{V}\ \mathrm{L}}{gH_z}\right]. \tag{5.2.6}$$

Therefore, the scale for pressure may be given as

$$\frac{\mathrm{P}_*}{H_z} \approx g\frac{\rho_0 f\ \mathrm{V}\ \mathrm{L}}{gH_z}$$

$$\mathrm{P}_* \approx \rho_0 f \mathrm{V}\ \mathrm{L}, \tag{5.2.7}$$

Stellenbosch University https://scholar.sun.ac.za

where $\mathrm{V} = (U, V)$. Under non-dimensionalization, the only modifications are to equations (5.1.7), (5.1.9) and (5.1.10), and therefore these equations linearized and scaled may be written as follows from the discussion below.

The density equation (5.1.7)

$$\frac{\partial \rho}{\partial t} + w\frac{\partial \rho}{\partial z} = 0, \tag{5.2.8}$$

where $\frac{\partial \rho}{\partial z}$ is defined by equation (3.4.13), is rewritten here for clarity, i.e.:

$$\frac{\partial \rho}{\partial z} = -\frac{\rho_0 N^2}{g}. \tag{5.2.9}$$

Therefore, equations (5.2.8) and (5.2.9) combined yield

$$\frac{\partial \rho}{\partial t} - w\frac{\rho_0 N^2}{g} = 0. \tag{5.2.10}$$

Moreover, under non-dimensionalization equation (5.2.10) becomes

$$\begin{aligned}
\frac{\partial \rho^*}{\partial t^*}\left[\frac{\left(\frac{\rho_0 f \mathrm{VL}}{g H_z}\right)}{(1/f)}\right] - w^*\left[\frac{\rho_0 N^2}{g}\frac{H_z \mathrm{V}}{\mathrm{L}}\right] &= 0, \\
\frac{\partial \rho^*}{\partial t^*}[1] - w^*\left[\frac{\rho_0 N^2}{g}\frac{H_z \mathrm{V}}{\mathrm{L}}\frac{g H_z}{\rho_0 f^2 \mathrm{VL}}\right] &= 0, \\
\frac{\partial \rho^*}{\partial t^*}[1] - w^*\left[\frac{N^2 H_z^2}{f^2 \mathrm{L}^2}\right] &= 0, \\
\frac{\partial \rho^*}{\partial t^*}[1] - w^*[Bu] &= 0,
\end{aligned} \tag{5.2.11}$$

where

$$Bu = \frac{N^2 H_z^2}{f^2 \mathrm{L}^2}, \tag{5.2.12}$$

is the Burger number, important for characterizing the stratification of ocean water.

The momentum equation (5.1.3) in the x-direction, becomes

$$\begin{aligned}
\frac{\partial u^*}{\partial t^*}\left[\frac{\mathrm{V}}{(1/f)}\right] - v^*[f\mathrm{V}] &= -\frac{\partial p^*}{\partial x^*}\left[\frac{\mathrm{P}_*}{\rho_0 \mathrm{L}}\right] + \nu_t^* \frac{\partial^2 u^*}{\partial z^{*2}}\left[\frac{\mathrm{AV}}{H_z^2}\right], \\
\frac{\partial u^*}{\partial t^*}[1] - v^*[1] &= -\frac{\partial p^*}{\partial x^*}\left[\frac{\mathrm{P}_*}{\rho_0 f V \mathrm{L}}\right] + \nu_t^* \frac{\partial^2 u^*}{\partial z^{*2}}\left[\frac{\mathrm{A}}{f H_z^2}\right],
\end{aligned} \tag{5.2.13}$$

Stellenbosch University https://scholar.sun.ac.za

and when equation (5.2.7) or the pressure scale is used, this equation becomes

$$\frac{\partial u^*}{\partial t^*}\left[1\right] - v^*[1] = -\frac{\partial p^*}{\partial x^*}\left[1\right] + \nu_t^* \frac{\partial^2 u^*}{\partial z^{*2}}\left[\frac{\mathrm{A}}{fH_z^2}\right]. \tag{5.2.14}$$

Similarly, the momentum equation (5.1.10) in the y-direction, is given by

$$\frac{\partial v^*}{\partial t^*}\left[\frac{\mathrm{V}}{(1/f)}\right] + u^*[f\mathrm{V}] = -\frac{\partial p^*}{\partial y^*}\left[\frac{\mathrm{P}_*}{\rho_0 \mathrm{L}}\right] + \nu_t^* \frac{\partial^2 v^*}{\partial z^{*2}}\left[\frac{\mathrm{AV}}{H_z^2}\right],$$

$$\frac{\partial v^*}{\partial t^*}\left[1\right] + u^*[1] = -\frac{\partial p^*}{\partial y^*}\left[1\right] + \nu_t^* \frac{\partial^2 v^*}{\partial z^{*2}}\left[\frac{\mathrm{A}}{fH_z^2}\right]. \tag{5.2.15}$$

Based on the scaling, these equations are later expressed in terms of the Burger number (i.e. equation (5.2.12)) and the Ekman number introduced below. Note that the earth's rotation or Coriolis forcing is of order one in equations (5.2.14) and (5.2.15). Thus the Coriolis forcing is a dominant forcing appropriate for driving large-scale flow, in particular currents due to large scale oceanic wind patterns.

Hence, then the horizontal non-linear terms (in particular the advection terms) would have been neglected by assuming that $Ro \ll 1$. Basically, this condition is inherent for geophysical fluids characterized by rotation. The scaling introduced in equations (5.2.14) and (5.2.15), is the Ekman number, i.e.:

$$E_k = \frac{\mathrm{A}}{fH_z^2}, \tag{5.2.16}$$

that characterizes frictional terms, in particular wind or bottom shear stress for the purpose of this study. Again, should non-dimensionalization and scaling have been based on the non-linear 3D shallow water equations (5.1.1) to (5.1.5) the horizontal Ekman number, i.e.:

$$E_h = \frac{\mathrm{A}}{fL^2}, \tag{5.2.17}$$

would have been introduced and the horizontal non-linear viscous terms neglected (i.e. justified by assuming $E_h \approx 0$).

The frictional terms are important when the Ekman number is $E_k \approx 1$. The wind blowing parallel to surface water over the ocean, tends to drag surface water along with it. Consequently, shear may develop in the z-direction and these penetrate through to the bottom ocean floor. Basically, this forcing in the horizontal direction includes both the wind shear stress $\boldsymbol{\tau}_w$ and the bottom shear stress $\boldsymbol{\tau}_b$. In component form the shear stresses are given by the wind shear stress $\boldsymbol{\tau}_w = (\tau_{xw}, \tau_{yw})$ and the bottom shear stress $\boldsymbol{\tau}_b = (\tau_{xb}, \tau_{yb})$, where

Stellenbosch University https://scholar.sun.ac.za

by definition $\tau_x = \nu_t \frac{\partial u}{\partial z}$ and $\tau_y = \nu_t \frac{\partial v}{\partial z}$ and constitute the x- and y-direction shear stresses of equations (5.1.9) and (5.1.10), respectively. Therefore, the linearized 3D shallow water equations may be rewritten as:

$$\frac{\partial \rho}{\partial t} + w\frac{\partial \rho}{\partial z} = 0, \tag{5.2.18}$$

$$\frac{\partial u}{\partial x} + \frac{\partial v}{\partial y} + \frac{\partial w}{\partial z} = 0, \tag{5.2.19}$$

for the density equation (5.1.7) and the continuity equation (5.1.8), respectively. The momentum equation (5.1.9) in the x-direction,

$$\frac{\partial u}{\partial t} - fv = -\frac{1}{\rho_0}\frac{\partial p}{\partial x} + \frac{\partial \tau_x}{\partial z}, \tag{5.2.20}$$

the momentum equation (5.1.10) in the y-direction,

$$\frac{\partial v}{\partial t} + fu = -\frac{1}{\rho_0}\frac{\partial p}{\partial y} + \frac{\partial \tau_y}{\partial z}, \tag{5.2.21}$$

and the momentum equation (5.2.5) in the z-direction,

$$\frac{\partial p}{\partial z} = -\rho g. \tag{5.2.22}$$

Hence, including scaling numbers or terms the final linearized 3D shallow water equations may be rewritten for clarity as:

$$\frac{\partial \rho^*}{\partial t^*}\left[1\right] + w^*\left[Bu\right] = 0, \tag{5.2.23}$$

$$\left(\frac{\partial u^*}{\partial x^*} + \frac{\partial v^*}{\partial y^*}\right)\left[\frac{\mathrm{V}}{\mathrm{L}}\right] + \frac{\partial w^*}{\partial z^*}\left[\frac{W}{H_z}\right] = 0, \tag{5.2.24}$$

for the density equation (5.2.18) and the continuity equation (5.2.19), respectively. The momentum equation (5.2.20) in the x-direction,

$$\frac{\partial u^*}{\partial t^*}\left[1\right] - v^*[1] = -\frac{\partial p^*}{\partial x^*}\left[1\right] + \frac{\partial \tau_x^*}{\partial z^*}\left[E_k\right], \tag{5.2.25}$$

the momentum equation (5.2.21) in the y-direction,

$$\frac{\partial v^*}{\partial t^*}\left[1\right] + u^*[1] = -\frac{\partial p^*}{\partial y^*}\left[1\right] + \frac{\partial \tau_y^*}{\partial z^*}\left[E_k\right], \tag{5.2.26}$$

Stellenbosch University https://scholar.sun.ac.za

and the momentum equation (5.2.22) in the z-direction,

$$\frac{\partial p^*}{\partial z^*}\left[\frac{\mathrm{P}_*}{H_z}\right] = -\rho^*\left[g\frac{\rho_0 f\ \mathrm{V}\ \mathrm{L}}{gH_z}\right], \tag{5.2.27}$$

where $\tau_x^* = \nu_t^* \frac{\partial u^*}{\partial z^*}$ and $\tau_y^* = \nu_t^* \frac{\partial v^*}{\partial z^*}$. In the scaled equations two important scales have been introduced, i.e. the Burger number Bu (equation (5.2.12)) to characterize stratification effects and the Ekman number E_k (equation (5.2.16)) to characterize shear stress effects.

It may be difficult to find exact solutions for the linearized 3D shallow water equations described above. For the purpose of simplifying the equations, a derived dynamic variable of preeminent importance in geophysical fluid dynamics is vorticity (Pedlosky, 1987). Usually, the linearized 3D shallow water equations are formulated into a vorticity equation.

5.3 Large-scale, low-frequency coastal and shelf motions

Based on the scaling, the drivers of currents flow, the rotation of the earth (i.e. Coriolis forcing) and the frictional shear stresses (i.e. wind and bottom shear stress) lead to an ocean response that is dependent on stratification effects. The expositions by Clarke & Brink (1985) and Brink (1991) presents numerical and analytical models for investigating coastal and shelf seas flow dynamics to discuss large-scale, low-frequency and wind-driven currents over the continental shelf. In which case, solutions were obtained by solving Ekman layers, namely the surface, interior and bottom Ekman layers.

It is at this stage that a decision tool, e.g. Table 5.2 is required to limit the problem. Previous work done by various authors shows that Gill & Schumann (1974) used the selected scales of Table 5.2 to investigate the generation of long-shelf waves by the wind. Basically, long-shelf waves are the coastal trapped waves described in Appendix A.5.3. Brink (1991) used coastal trapped waves to study wind-driven currents over the continental shelf. Clarke & Brink (1985) investigated the response of stratified frictional flow of shelf and slope waters to fluctuating, large-scale low-frequency wind forcing. (Clarke & Brink, 1985) investigated wind-induced upwelling, coastal currents and sea level changes. Van Ballegooyen (1995) applied these in the southern African coastline to study forced synoptic coastal-trapped waves. Following from these studies, in the next section coastal and shelf currents response to stratification and frictional effects, under large-scale and low-frequency is investigated. In particular, the goal is to discuss barotropic response in a fluid with and without

Stellenbosch University https://scholar.sun.ac.za

density structure.

Only some of the scales summarized in Table 5.2 are used at this stage. Clarke & Brink (1985) simplified the linearized 3D shallow water equations (5.2.18) to (5.2.22), by the low-frequency boundary layer approximation, i.e.:

$$\frac{X}{Y} \ll 1 \quad \text{and} \quad \frac{1}{ft_\tau} \ll 1. \tag{5.3.1}$$

These scales means that frequencies are small relative to the inertial frequency and that alongshore scales are large relative to cross-shelf scales (Clarke & Brink, 1985; Brink, 1991). Under condition(s) (5.3.1), the linearized 3D shallow water equations (5.2.18) to (5.2.22) are simplified into (a vorticity equation given as equation (2.4) in Clarke & Brink (1985))

$$\frac{\partial}{\partial t}\frac{\partial^2 p}{\partial x^2} + f^2\frac{\partial}{\partial z}\left(\frac{1}{N^2}\frac{\partial^2 p}{\partial z \partial t}\right) = \frac{\partial}{\partial x}\left(\frac{\partial \tau_y}{\partial z}\right). \tag{5.3.2}$$

The friction effects (wind and bottom shear stress) in this equation have been included given that $E_k \approx 1$. To understand how ocean water responds to the frictional effects, one may exclude the shear stress effects, when $E_k \approx 0$, only for the purpose of understanding the essential response. This means that

$$\frac{\partial \tau_y}{\partial z} = 0, \tag{5.3.3}$$

then the fluid describes an inviscid interior, outside of the top and bottom Ekman layers (based on Appendix D Figure D.5). Therefore, equation (5.3.2) reduces to (equations (2.5) or (6a) in Clarke & Brink (1985) and Brink (1991), respectively)

$$\frac{\partial^2 p}{\partial x^2} + f^2\frac{\partial}{\partial z}\left(\frac{1}{N^2}\frac{\partial p}{\partial z}\right) = 0, \tag{5.3.4}$$

subject to the boundary conditions at the coast, at the bottom, at the free surface and offshore (as described in Clarke & Brink (1985) and Brink (1991)).

The removal of friction effects through equation (5.3.3), implies that equation (5.3.4) only determines the motion in the inviscid interior, outside of the top and bottom Ekman layers (based on Appendix D Figure D.5). To obtain solutions inside these layers (surface and bottom Ekman layers), Clarke & Brink (1985) and Brink (1991) assumed that:

- the wind forcing is defined as

$$\tau_{yw} = \tau_{yw}^0 \mathrm{e}^{(iky + i\omega t)}, \tag{5.3.5}$$

Stellenbosch University https://scholar.sun.ac.za

Table 5.2: Basic decision criterion based on scales.

Time vs. spatial effects		
Scales	$\frac{\partial}{\partial t} \ll f$ or $\frac{1}{f t_\tau} \ll 1$	$\frac{\partial^2}{\partial t^2} \ll f^2$ or $\frac{1}{f^2 t_\tau^2} \ll 1$
$\frac{\partial}{\partial y} \ll \frac{\partial}{\partial x}$ or $\frac{X}{Y} \ll 1$	Low-frequency boundary layer (Clarke & Brink, 1985)	
$\frac{\partial^2}{\partial y^2} \ll \frac{\partial^2}{\partial x^2}$ or $\frac{X^2}{Y^2} \ll 1$		Long wave limit (Brink, 1991) Very low-frequency, allows geostrophic balance (LeBlond & Mysak, 1978)
Stratification vs. tuburlence effects		
Scales	$Bu = \frac{N^2 H_z^2}{f^2 \mathrm{L}^2} \to 0$	$Bu = \frac{N^2 H_z^2}{f^2 \mathrm{L}^2} \neq 0$
$E_k = \frac{\mathrm{A}}{f H_z^2} \approx 1$	Barotropic, under important friction effects	Baroclinic, under important friction effects
$E_k = \frac{\mathrm{A}}{f H_z^2} \neq 1$	Barotropic, under non-important friction effects	Baroclinic, under non-important friction effects

Stellenbosch University https://scholar.sun.ac.za

- pressure is defined as

$$p(x,y,z,t) = F_p(x,z)\mathrm{e}^{(iky+i\omega t)}, \tag{5.3.6}$$

Clarke & Brink (1985) also included the bottom friction $\boldsymbol{\tau}_b$ (i.e. equation (D.3.1) in Appendix D), whereas Brink (1991) omitted bottom friction effects.

Clarke & Brink (1985) formulated a barotropic response solution through a pertubation problem, in which lowest order and first order solutions were determined. Thus, follows from equation (5.3.9). Moreover, Clarke & Brink (1985) determined analytical models that describe only the barotropic response solution without any baroclinic effects. To achieve these Clarke & Brink (1985) expressed the first order solution in terms of the lowest order solution. The results of Clarke & Brink (1985) showed that, if the shelf slopes gently enough (e.g. as in equation (5.3.14)) the alongshore flow over the shelf is barotropic. Hence, Clarke & Brink (1985) showed that in the case of extremely gently sloping the shelf edge (offshore) pressure is zero and all the wind-driven changes flow occurs on the shelf.

Brink (1991) used coastal-trapped-waves theory to understand large-scale flow over the continental shelf. The result of Brink (1991) showed that wind-driven currents over the continental shelf includes barotropic and baroclinic modes as a response. In this case, according to Brink (1991) coastal-trapped-waves theory is found to be useful when investigating pressure (or sea level) and alongshore velocity, and only rarely useful for density or onshore velocity.

Equation (5.3.4) can be expressed in terms of ϵ_{Bu} when scaled using L, H_z and P_*. Therefore, equation (5.3.4) scaled reads

$$\begin{aligned}
\frac{\partial}{\partial z}\left(\frac{1}{N^2}\frac{\partial F_p^0}{\partial z}\right)\left[\frac{f^2}{N_0^2}\frac{\mathrm{P}_*}{H_z^2}\right] + \frac{\partial^2 F_p}{\partial x^2}\left[\frac{\mathrm{P}_*}{L^2}\right] &= 0 \\
\frac{\partial}{\partial z}\left(\frac{1}{N^2}\frac{\partial F_p^0}{\partial z}\right) + \frac{\partial^2 F_p}{\partial x^2}\left[\frac{f^2L^2}{N_0^2H_z^2}\right] &= 0 \\
\frac{\partial}{\partial z}\left(\frac{1}{N^2}\frac{\partial F_p}{\partial z}\right) + \epsilon_{Bu}\frac{\partial^2 F_p}{\partial x^2} &= 0,
\end{aligned} \tag{5.3.7}$$

where

$$\epsilon_{Bu} = \frac{N_0^2 H_z^2}{f^2 \mathrm{L}^2}, \tag{5.3.8}$$

where N_0 is some representative of N. Following Clarke & Brink (1985), for the purpose of developing solutions for equation (5.3.4) expressed in terms of pressure given as equation (5.3.6) a solution of the form

$$p(x,z) = F_p^0(x,z) + \epsilon_{Bu}\ F_p^1(x,z) + ..., \tag{5.3.9}$$

Stellenbosch University https://scholar.sun.ac.za

is intended, where $F_p^0, F_p^1, ...$ represents pressure, zeroth and first order solutions. Equation (5.3.7) expressed in terms of equation (5.3.9) reads

$$\frac{\partial}{\partial z}\left(\frac{1}{N^2}\frac{\partial F_p^0}{\partial z}\right) + \epsilon_{Bu}\frac{\partial^2 F_p^0}{\partial x^2} + \epsilon_{Bu}\frac{\partial}{\partial z}\left(\frac{1}{N^2}\frac{\partial F_p^1}{\partial z}\right) + \epsilon_{Bu}\epsilon_{Bu}\frac{\partial^2 F_p^1}{\partial x^2} + ... = 0. \quad (5.3.10)$$

At lowest order of ϵ_{Bu}, the problem to be solved is

$$\frac{\partial}{\partial z}\left(\frac{1}{N^2}\frac{\partial F_p^0}{\partial z}\right) = 0, \quad (5.3.11)$$

since

$$\epsilon_{Bu} = \frac{N_0^2 H_z^2}{f^2 \mathrm{L}^2} \ll 1. \quad (5.3.12)$$

At first order of ϵ_{Bu}, the problem to be solved is

$$\frac{\partial^2 F_p^0}{\partial x^2} + \frac{\partial}{\partial z}\left(\frac{1}{N^2}\frac{\partial F_p^1}{\partial z}\right) = 0. \quad (5.3.13)$$

Using the combination of equations (5.3.11) and (5.3.13), together with the appropriate boundary conditions (Clarke & Brink, 1985) obtain a solution to equation (5.3.4) indicating a response that is barotropic provided that $\epsilon_{Bu} \ll 1$ (condition (5.3.12)). Furthermore, should $\sqrt{\epsilon_{Bu}} \ll 1$, then the shelf edge pressure becomes zero and all the wind-driven changes of flow is confined to the shelf.

Based on the above, a barotropic response is possible for a range of density stratification and shelf slopes provided that condition $\epsilon_{Bu} \ll 1$ (condition (5.3.12)) is satisfied. For example all of the conditions below will results in a barotropic response:

(1.) For a gentle shelf sloping and density stratification, i.e.:

$$\frac{N_0}{f} \approx \zeta \quad \text{and} \quad \frac{H_z}{L} \approx \zeta. \quad (5.3.14)$$

(2.) For weak density stratification and very strong shelf sloping, i.e.:

$$\frac{N_0}{f} \approx \zeta^2 \quad \text{and} \quad \frac{H_z}{L} \approx 1. \quad (5.3.15)$$

(3.) For strong density stratification and weak shelf sloping, i.e.:

$$\frac{N_0}{f} \approx 1 \quad \text{and} \quad \frac{H_z}{L} \approx \zeta^2. \quad (5.3.16)$$

Note that $\frac{N_0}{f}$ represents the density stratification and $\frac{H_z}{L}$ represents the shelf sloping, and $\zeta = 10^{-1}$.

Stellenbosch University https://scholar.sun.ac.za

5.4 Barotropic response in a fluid without density structure

Under the conditions (5.3.1) and (5.3.12), the response to the 3D shallow water equations is barotropic. This means that these equations can be substituted by the 2D shallow water equations (i.e. for a fluid without density structure) when solving for flows in coastal and shelf regions. The relevant 2D shallow water equations are presented in Appendix C. These equations (written without the hat denoting the depth-averaging), i.e. the depth-averaged continuity equation (C.2.8) may be written as

$$\frac{\partial \eta}{\partial t} + \frac{\partial (uH)}{\partial x} + \frac{\partial (vH)}{\partial y} = 0, \tag{5.4.1}$$

the depth-averaged momentum equation (C.2.21) in the x-direction

$$\frac{\partial u}{\partial t} + \frac{\partial (uu)}{\partial x} + \frac{\partial (uv)}{\partial y} - fv = -g\frac{\partial \eta}{\partial x} + \frac{\tau_{xw} - \tau_{xb}}{\rho H}, \tag{5.4.2}$$

the depth-averaging momentum equation (C.2.22) in the y-direction

$$\frac{\partial v}{\partial t} + \frac{\partial (uv)}{\partial x} + \frac{\partial (vv)}{\partial y} + fu = -g\frac{\partial \eta}{\partial y} + \frac{\tau_{yw} - \tau_{yb}}{\rho H}. \tag{5.4.3}$$

The above equations are used for the remainder of this study.

In Appendix E, the possibility of decoupling the 2D shallow water equations (5.4.1) to (5.4.3) to represent the equations of "reduced physics" is investigated through scaling. In particular, the scales in condition (5.3.1), is used to decouple the 2D shallow water equations (5.4.1) to (5.4.3). As noted above, the assumption that frequencies are small relative to the inertial frequency and that alongshore scales are large relative to cross-shelf scales, allows dominant alongshore coastal and shelf dynamics. This is necessariy to describe the dynamics at the open boundaries of a limited coastal and shelf seas model.

The scales in condition (5.3.1) applied in equations (5.4.1) to (5.4.3) leads to the momentum equation (C.2.21) in the x-direction written as

$$-fv = -g\frac{\partial \eta}{\partial x}, \tag{5.4.4}$$

the momentum equation (C.2.22) in the y-direction

$$\frac{\partial v}{\partial t} + fu = -g\frac{\partial \eta}{\partial y} + \frac{\tau_{yw} - \tau_{yb}}{\rho H}, \tag{5.4.5}$$

Stellenbosch University https://scholar.sun.ac.za

and the continuity equation (C.2.8) remains unchanged

$$\frac{\partial \eta}{\partial t} + \frac{\partial (uH)}{\partial x} + \frac{\partial (vH)}{\partial y} = 0. \tag{5.4.6}$$

These equations represent separable equations and not necessarily decoupled equations. For example equation (5.4.5) has terms expressed in terms of the cross-shore velocity (fu) and alongshore velocity ($\frac{\partial v}{\partial t}$).

Following a similar approach as in Clarke & Brink (1985) described in the previous section, the above equations (5.4.4) to (5.4.6) simplify to

$$\frac{\partial \eta}{\partial t} + \frac{\partial}{\partial x}\left(-\frac{gH}{f^2}\frac{\partial^2 \eta}{\partial t \partial x} - \frac{gH}{f}\frac{\partial \eta}{\partial y} + \frac{\tau_{yw} - \tau_{yb}}{\rho f H}\right) + \frac{\partial}{\partial y}\left(\frac{gH}{f}\frac{\partial \eta}{\partial x}\right) = 0$$

$$\frac{\partial \eta}{\partial t} - \frac{gH}{f^2}\frac{\partial}{\partial x}\left(\frac{\partial^2 \eta}{\partial t \partial x}\right) + \frac{\tau_{yw} - \tau_{yb}}{\rho f H} = 0. \tag{5.4.7}$$

This is the version of equation (5.3.2) expressed in terms of water levels.

5.5 *Tilt* reduced hydrodynamic equations

To obtain the decoupled version of equations (5.4.4) to (5.4.6) it is required that the term fu is considered negligible, i.e. $fu \approx 0$. There is only clear justification for neglecting these terms at the coastal and offshore boundaries, and not necessary at the cross-shore boundaries. Under this assumption, equations (5.4.4) to (5.4.6) therefore may be written as

$$-fv = -g\frac{\partial \eta}{\partial x}, \tag{5.5.1}$$

$$\frac{\partial v}{\partial t} = -g\frac{\partial \eta}{\partial y} + \frac{\tau_{yw} - \tau_{yb}}{\rho H}, \tag{5.5.2}$$

$$\frac{\partial \eta}{\partial t} + \frac{\partial (uH)}{\partial x} + \frac{\partial (vH)}{\partial y} = 0. \tag{5.5.3}$$

The reduced hydrodynamic *Tilt* equations as developed by the CSIR are as follows:

$$-fv = -g\frac{\partial \eta}{\partial x} + \frac{\tau_{xw}}{\rho H}, \tag{5.5.4}$$

Stellenbosch University https://scholar.sun.ac.za

$$\frac{\partial v}{\partial t} = -g\frac{\partial \eta}{\partial y} + \frac{\tau_{yw} - \tau_{yb}}{\rho H}, \tag{5.5.5}$$

$$\frac{\partial \eta}{\partial t} + \frac{\partial (uH)}{\partial x} + \frac{\partial (vH)}{\partial y} = 0. \tag{5.5.6}$$

These equations include a cross-shore wind forcing in equation (5.5.4). The inclusion of this term is only valid if $\tau_{xw} \gg \tau_{yw}$. Given that typically $\tau_{xw} \approx \tau_{yw}$ or $\tau_{xw} \ll \tau_{yw}$, the inclusion of the cross-shore wind forcing in equation (5.5.4) is generally not justified.

5.5.1 Why *Tilt*

Applying Delft3D-FLOW for the Southern African conditions have been the most challenging issue, because correct open boundary conditions are difficult to determine where synoptic scale wind forcing predominates. The main issue is that, boundary conditions for models with realistic stratification, shelf and continental slope bottom topography and bottom friction, etc., is not easily found in literature. For this reason *Tilt* was developed at the CSIR to determine open boundary conditions for both research and commercial work.

The *Tilt* code produces water level boundary conditions under three options, i.e.:

Tilt option1

The first option is for currents driven by wind only and computes water level time series under the assumption that the alongshore slope is zero, i.e.:

$$\text{alongshore slope} = 0. \tag{5.5.7}$$

Tilt option2

The second option is for currents driven by wind plus a background ambient current and computes the water level time series under the assumption that

$$\text{alongshore slope} = -\text{acceleration} - \text{bottom friction}. \tag{5.5.8}$$

Tilt option3

The third option is for currents driven by measured currents plus wind and determines the open boundary conditions under the assumption that

$$\text{alongshore slope} = -\text{acceleration} + \text{wind stress} - \text{bottom friction}. \tag{5.5.9}$$

Stellenbosch University https://scholar.sun.ac.za

In summary:
From linearized 3D shallow water equations a scaling technique has been used to uderstanding the importance of the different terms. For simplicity the problem has been reduced to a barotropic unstratified fluid that is more appropriate for determining *Tilt* boundary equations. This is only valid for low frequency, large scale flows where the flow is predominantly alongshore and the shelf slopes relatively small. Should any of these assumptions around the nature of the flow be incorrect the use of *Tilt* code to determine water level boundary conditions for a baroclinic stratified fluid may not be justified.

Stellenbosch University https://scholar.sun.ac.za

Chapter 6

Simulations, Results and Analysis

6.1 Introduction

The treatment of open boundary conditions in a numerical coastal and shelf seas model is the focus in this chapter. In particular this chapter will establish an understanding of open boundary conditions and describe what it means for the simulation of flows using Delft3D-FLOW. Some of the specific issues and problems concerning open boundary conditions obtained using *Tilt* are discussed.

For the purpose of the investigation that follows, wind forcing is considered uniform and only northerly and southerly winds are tested. The aim is to test the efficacy of *Tilt* under strong persistent wind forcing on the boundaries. As a result of the scaling assumed, fully developed flow in the alongshore direction is expected to be the correct solution for strong alongshore wind-forcing. For the purpose of this study, a simulation with Neumann boundary condition cross-shore and a zero water level in the offshore is assumed to be a physically correct (reference) solution for wind-forced flow over the coastal and shelf domain. The Neumann boundary condition is a simpler and easy to use condition cross-shore, since its answer is known a prior. Thus, a flexible condition that allows continuity and no-forcing at the boundaries. The use of this boundary is motivated by its ability to allow simulations of currents flow generated by local forcing in the interior model domain, to pass through the boundaries without any disturbance. A similar result is expected should *Tilt* be used to determine the open boundary conditions.

Stellenbosch University https://scholar.sun.ac.za

6.2 The solutions to the interior of the computational domain

Generally, the solution for the model domain is known, whereas the solution to be imposed along the open boundaries of the model domain is unknown. Pond & Pickard (1978) described the balance of forces in the model interior in their Chapter 8. Following Roed & Cooper (1987), the solution to the linearized 2D shallow water equations for barotropic unstratified fluid may be either a steady state or a transient solution.

The steady state solution

For a model response in the limit $t \to \infty$, a steady state solution may be obtained based on the following observations. The inclusion of bottom friction in the model and that the uniform alongshore wind stress is a function of both time and space. Hence, the alongshore is only a function y in space. The steady state solution of the linearized barotropic shallow water equations as in Roed & Cooper (1987) is given by

$$-fv = -g\frac{\partial \eta}{\partial x} - \frac{\tau_{xb}}{H}, \tag{6.2.1}$$

$$fu = \frac{\tau_{yw}}{H} - \frac{\tau_{yb}}{H}, \tag{6.2.2}$$

$$\frac{\partial (uH)}{\partial x} = 0. \tag{6.2.3}$$

Taking in to account the role of the land boundary described in Section 4.3.1, equation (6.2.3) may be integrated, i.e.:

$$\int \frac{\partial (uH)}{\partial x} dx = 0$$

$$uH + K = 0, \tag{6.2.4}$$

where K is the constant of integration. As the integration suggests, it is not valid to assume $u = 0$ everywhere as $u = 0$ is only a valid assumption at or near the coastal land boundary or at the offshore boundary.

For the purpose of the numerical simulations presented in this study the sea surface elevation is clamped to zero at the offshore boundary, i.e. $\eta = 0$ at the offshore boundary.

Stellenbosch University https://scholar.sun.ac.za

The difference between the steady state solution (i.e. equations (6.2.1) to (6.2.3)) and *Tilt* equations (5.5.1) and (5.5.2) is the term $\frac{\partial v}{\partial t}$ at the boundaries (i.e. cross-shore). In deriving *Tilt* it is assumed that $fu \ll \frac{\partial v}{\partial t}$, resulting in the removal of the term fu from the *Tilt* equation. Consequently the effect of fu is underestimated at the cross-shore boundaries. Basically, the steady state solution in the model interior domain is characterized by a wind driven alongshore flux that is in geostrophic balance with the cross-shore water level gradient. In conclusion, there exists no major difference between the model solution and *Tilt* based on the model formulation.

The transient solution

The transient solution is characterised by spatial varying flow velocity as $t \to 0$. The alongshore flows observed are dependant on the assumption of a no flux condition at the coast and offshore. Roed & Cooper (1987) only determined a limited solution of the linearized barotropic shallow water equations given by

$$\frac{\partial u}{\partial t} - fv = -g\frac{\partial \eta}{\partial x} - \frac{\tau_{xb}}{H}, \tag{6.2.5}$$

$$\frac{\partial v}{\partial t} + fu = \frac{\tau_{yw}}{H} - \frac{\tau_{yb}}{H}, \tag{6.2.6}$$

$$\frac{\partial \eta}{\partial t} + \frac{\partial (uH)}{\partial x} = 0. \tag{6.2.7}$$

This solution is purely applicable near the coast and its application away from the coast may not be fully justified, as the no flux condition is generally only assumed at the coast and not at the offshore boundary. This means that *Tilt* may be more appropriate to predict open boundary conditions for onshore currents flow and not necessarily offshore current flow.

Geostrophic balance

For combination of a clamped offshore boundary condition and the application of Neumann boundary conditions at the offshore boundary, the characteristic flow dynamics at a very low-frequency comprises a geostrophic balance as described in Table 5.2, i.e.

$$fv = g\frac{\partial \eta}{\partial x}, \tag{6.2.8}$$

$$fu = -g\frac{\partial \eta}{\partial y}, \tag{6.2.9}$$

subject to the Neumann boundary conditions in the cross-shore boundaries

$$\frac{\partial \eta}{\partial y} = 0. \tag{6.2.10}$$

Stellenbosch University https://scholar.sun.ac.za

Since $X \ll Y$, $\frac{\partial \eta}{\partial y} = 0$ and the geostrophic balance is basically given by

$$fv = g\frac{\partial \eta}{\partial x}, \quad \text{subject to} \quad \frac{\partial \eta}{\partial y} = 0. \tag{6.2.11}$$

6.3 Simulation results

For all the simulations presented in this section, the model domain setup has $X = 15$ km cross-shore and $Y = 30$ km alongshore. The bathmetry (as in Figure 6.1) is linear over $X = 0$ to 9 km and flat over $X = 9$ to 15 km. Based on the model geometry in Figure D.5, the depth at the coast ($x = b$) is $H(b) = 1$ m. For all the simulations presented in this study the model geometry based on Figure D.5 is used, i.e. the bathmetry given by Figure 6.1. Moreover, all the simulations represents the dynamics at latitude $\phi = -30°$. For the purpose of this study, the dynamics presented in Figure 6.2 and 6.3 show consistency between the solution in the model interior and the applied boundary conditions, i.e. the model solution agrees with the information prescribed on the open boundaries.

Generally, the wind driven alongshore flux described by Figure 6.2 and 6.3 is in geostrophic balance with the cross-shore pressure gradient. In which case, the wind driven alongshore flux is determined from the cross-shore equation. For the simulations presented below only *Tilt* option 1 is used to determine the water levels to be specified on the boundaries. In which case, the use of option 1 is motivated by the fact that only idealised cases are simulated and there is no current measurements that are available.

6.3.1 Accurate alongshore currents variability due to strong signal of the coastal boundary

For wind blowing from the South over coastal and shelf seas regions, with *Tilt* boundary conditions cross-shore and clamped water level offshore produced accurate alongshore currents variabilty and water level set-up towards the coast. The response of the model to imposed *Tilt* open boundary condition tested with strong persistent wind forcing from the South for both the interior domain and the boundaries is represented by Figure 6.4. Basically, the total mass conservation is satisfied and for this case *Tilt* boundary conditions may be considered as appropriate. In this case (Figure 6.4) the *Tilt* equations together with the boundary conditions at the coast and offshore and continuity, is satisfied. For this test case, there is a water level set-up towards the coast and as a result the coast can easily signal its presence. Because of the water level rise towards the coast, it make sense to have clamped water level in the offshore boundary. In this case, the solution of the shallow water equations

Stellenbosch University https://scholar.sun.ac.za

agrees with open boundary conditions determined from *Tilt* for wind forcing from the South.

6.3.2 Requirement for flow boundary condition

Northerly wind blowing over the coastal or shelf seas is tested with *Tilt* on the cross-shore boundaries and clamped water level offshore. The model response to the imposed *Tilt* open boundary conditions tested with strong persistent wind forcing from the North for both the interior domain and the boundaries (represented by Figure 6.5) provides evidence that the necessary assumptions that allows alongshore flow are being violated. In which case, it can be concluded that this is caused by a long time required for the coast to signal its presence. This means that the no flux condition does not hold globally but only at the coast. It is evident from Figure 6.5 that near the coast most of the predicted flow velocity vectors are purely alongshore. Whereas, away from the coast non-zero cross-shore flow velocity vectors are increasingly evident. These differences in currents near the coast and further may be the source of the effects observed.

6.3.3 The role of a wall ("thin dam") offshore

Northerly wind blowing over the coastal or shelf seas for both the interior domain and the boundaries is tested with *Tilt* on the cross-shore boundaries and both clamped water level and a wall ("thin dam") offshore. The use of a thin dam or a wall in the offshore boundary enforces zero alongshore velocity at the offshore boundary and does not necessarily replace the clamped water level. The presence of the thin dam enforces mass conservation and as a result, the predicted flow motion is purely in the alongshore direction.

In Figure 6.6, it is sensible to impose both clamped water level and zero alongshore velocity at the offshore boundary. An alternative is to restrict the model forcing to an alongshore wind stress with a profile that decays offshore so as to allow zero water level and zero alongshore velocity at the offshore boundary.

In summary, in this chapter it is discussed how one can solve two dimensional shallow water equations inside the model domain. Following Roed & Cooper (1987), a steady state and transient solution for two dimensional shallow water equations solved has been presented and the differences between the model solutions and *Tilt* have been discussed. In the case of very low-frequency the solution to the model domain is in geostrophic balance LeBlond & Mysak (1978). This has been used to present simulations that satisfy total mass conservation. Delft3D-FLOW has been used for the simulations. In the model Neumann boundary conditions have been applied at the cross-shore boundaries and clamped to zero water level at the offshore boundary. Similarly,

Stellenbosch University https://scholar.sun.ac.za

Tilt boundary conditions have been applied at the cross-shore boundaries and clamped to zero water level at the offshore boundary. Tests using *Tilt* boundary conditions show that a flow boundary condition is required offshore to ensure total mass balance. A thin dam or a wall in the offshore boundary has been used to enforce zero alongshore velocity.

6.4 "Real-world" applications of *Tilt*

In practise the use of the *Tilt* "reduced physics" approach in solving wind and remotely forced coastal and shelf circulation occurs in non-idealised situations where there is not full compliance with all of the scaling assumptions used to derived the *Tilt* equations. The consequence of this is that inconsistencies between the equation in the interior model domain and those comprising *Tilt* may result in imbalances at the open boundaries and spurious flows. The greater the non-compliance with the scaling assumptions, the greater the likelihood of occurrence and magnitude of these spurious flows in the vicinity of the model open boundaries. Typical situations faced in the application of *Tilt* in real world problems are as follows:

- The temporal scales of variation in forcing both at the boundaries (e.g. winds and tides) and in the model interior (typically wind-forcing) are of such a nature that $\frac{1}{ft_\tau} \neq 1$. This violates temporal scaling assumptions ($\frac{1}{ft_\tau} \ll 1$). The consequence of this is that the terms $\frac{1}{ft_\tau}$ become significant in the model interior while such terms do not occur in *Tilt*. This leads to a transient imbalance between the equations of motions in the interior model domain and the *Tilt* equations applied at the open boundaries. Such imbalances persist for roughly the local inertial period, resulting in small-scale spurious flows or "noise" in the vicinity of the open boundaries. The pragmatic approach when applying *Tilt* under these conditions is to accept that there will be short periods when such spurious flows may prevail at the model open boundaries after the occurrence of rapid changes in (wind) forcing. Alternatively, the forcing time series may be smoothed before application, however any biases introduced in doing so will affect the full duration of the simulation. The relaxation factor alpha may be used to ameliorate some of these effects at the model open boundaries.

- The asymmetry in alongshore and cross-shore scales also may be violated. This often is due to the fact that the alongshore changes in bathymetry are of a similar scale to cross-shore changes in bathymetry. Where this occurs the flow response is expected to develop similar scales, i.e. the along-shore and cross-shore scales of the response will be of the same order. While this is unlikely to be an issue in the interior of the model domain, the violation of $\frac{X}{Y} \ll 1$ at or near the boundary will introduce

Stellenbosch University https://scholar.sun.ac.za

Table 6.1: Summary of simulations presented in Chapter 6.

Simulation	Experiment	Descriptive results
Figure 6.2	Neumann boundary conditions are used at the cross-shore boundaries and zero water level imposed at the offshore boundary. A uniform wind of 6 m/s blowing from the South is tested.	A water level set-up towards the coast and predominantly alongshore current variability is observed. Basically, the variability is driven by forcing generated from the model due to uniform wind of 6 m/s blowing from the South.
Figure 6.3	Neumann boundary conditions are used at the cross-shore bondary and zero water level imposed at the offshore boundary. A uniform wind of 6 m/s blowing from the North is tested.	The water level set-down occurs at the coast. Predominantly alongshore current variability is observed. The variability is driven by forcing generated from the model due to uniform wind of 6 m/s blowing from the North.
Figure 6.4	*Tilt* generated boundary conditions are used at the cross-shore boundaries and a zero water level imposed at the offshore boundary. A uniform wind of 6 m/s blowing from the South is tested.	A water level set-up occurs towards the coast and predominantly alongshore currents variability is observed. The variability is driven by forcing generated from the model and boundaries, due to uniform wind of 6 m/s blowing from the South.
Figure 6.5	*Tilt* generated boundary conditions are used at the cross-shore boundaries and a zero water level imposed at the offshore boundary. A uniform wind of 6 m/s blowing from the North is tested.	A water level set-down occurs at the coast. Due to the lack of balance between boundary conditions, the currents variability observed indicates some unexpected inflow from the offshore boundary. Also, the water level set-up does not match alongshore, i.e. each water level contour should not vary in an alongshore direction. This indicates a violation of total mass conservation and the water level set-up differs from that of Figure 6.3. The variability is driven by forcing generated from the model and boundaries due to uniform wind of 6 m/s blowing from the North.
Figure 6.6	*Tilt* generated boundary conditions are used at the cross-shore boundaries and a zero water level imposed at the offshore boundary. A thin dam is also included offshore to prevent cross-shore flows seen in Figure 6.5. A uniform wind of 6 m/s blowing from the North is tested.	A water level set-down occurs at the coast. A balance between boundary conditions is enforced with the inclusion of a thin dam at the offshore boundary. Based on theory, this ensure a zero alongshore velocity along the offshore boundary. As expected the result in Figure 6.6 is similar to that in Figure 6.3. The errors observed in Figure 6.5 are not present in Figure 6.6. One can assume that both water level and velocity boundary conditions are required at the offshore boundary for sinulations where wind is blowing from the North.

Stellenbosch University https://scholar.sun.ac.za

errors at the boundary. A pragmatic approach when applying *Tilt* is to smooth the model bathymetry near the cross-shore open boundaries thus minimising such errors.

- Should the water column stratification be significant AND the shelf slopes be large, it is likely that the Burger number assumption will be violated. This is likely to cause significant problems as this means that the 2D shallow water equations used in *Tilt* are no longer appropriate. It is expected that significant errors associated with the existence of stratification in the interior model domain will occur at the model boundaries, i.e. baroclinic forcing will occur in the model interior that are not present in the 2D shallow water equations used in *Tilt*. Significant errors are expected at the cross-shore boundaries, particularly at locations where the Burger number assumption is violated. Typically this will be in the vicinity of rapid changes in cross-shore bathymetry.

Stellenbosch University https://scholar.sun.ac.za

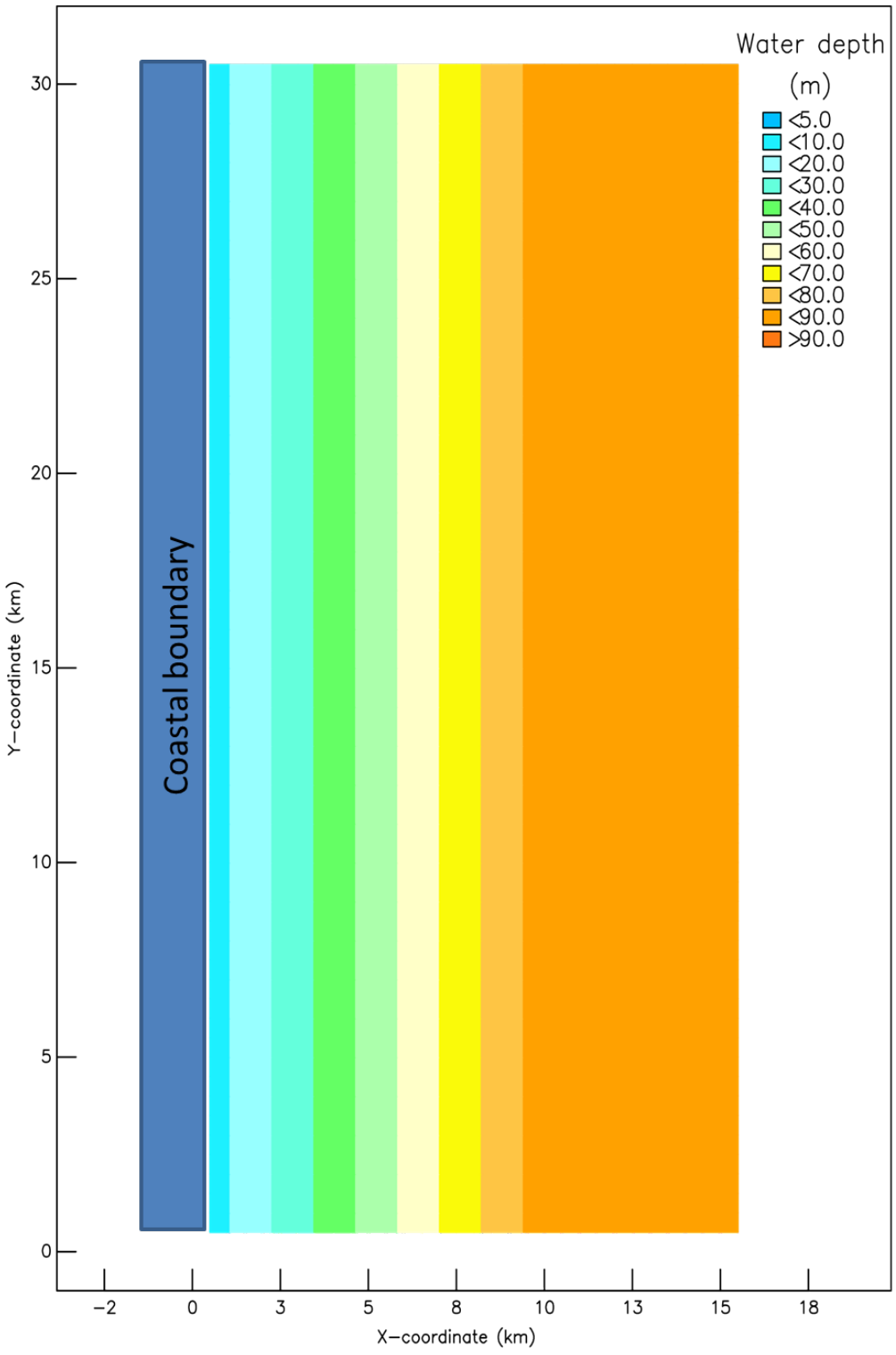

Figure 6.1: The bathmetry for all the simulations presented in this study, i.e. 1 m deep at the coast and 85 m deep offshore.

Stellenbosch University https://scholar.sun.ac.za

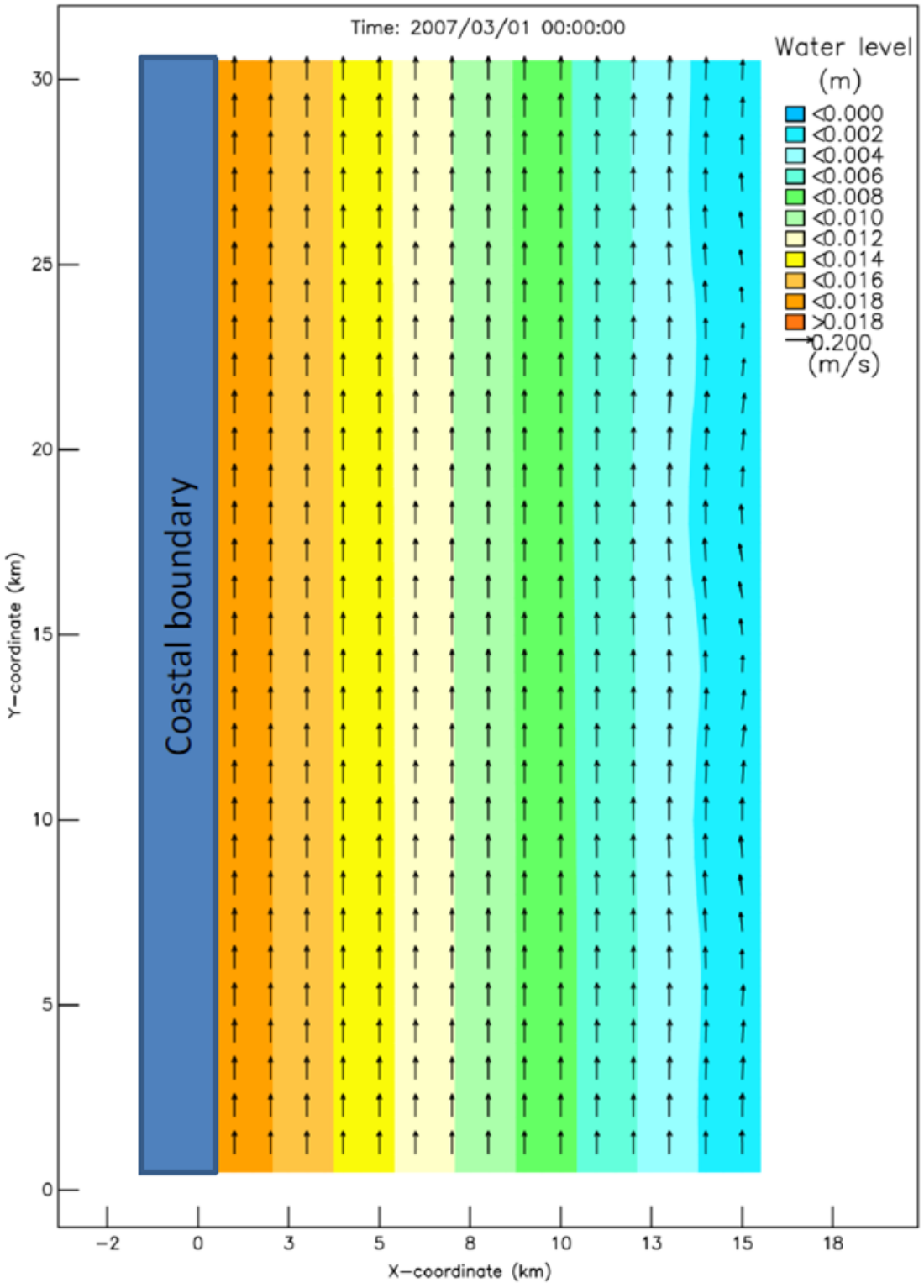

Figure 6.2: Alongshore currents variability and water level set-up driven by uniform wind of 6 m/s from the South. Neumann boundary conditions cross-shore and clamped water level offshore are tested. The flow velocity vectors and water level (in colour) are simulated.

Stellenbosch University https://scholar.sun.ac.za

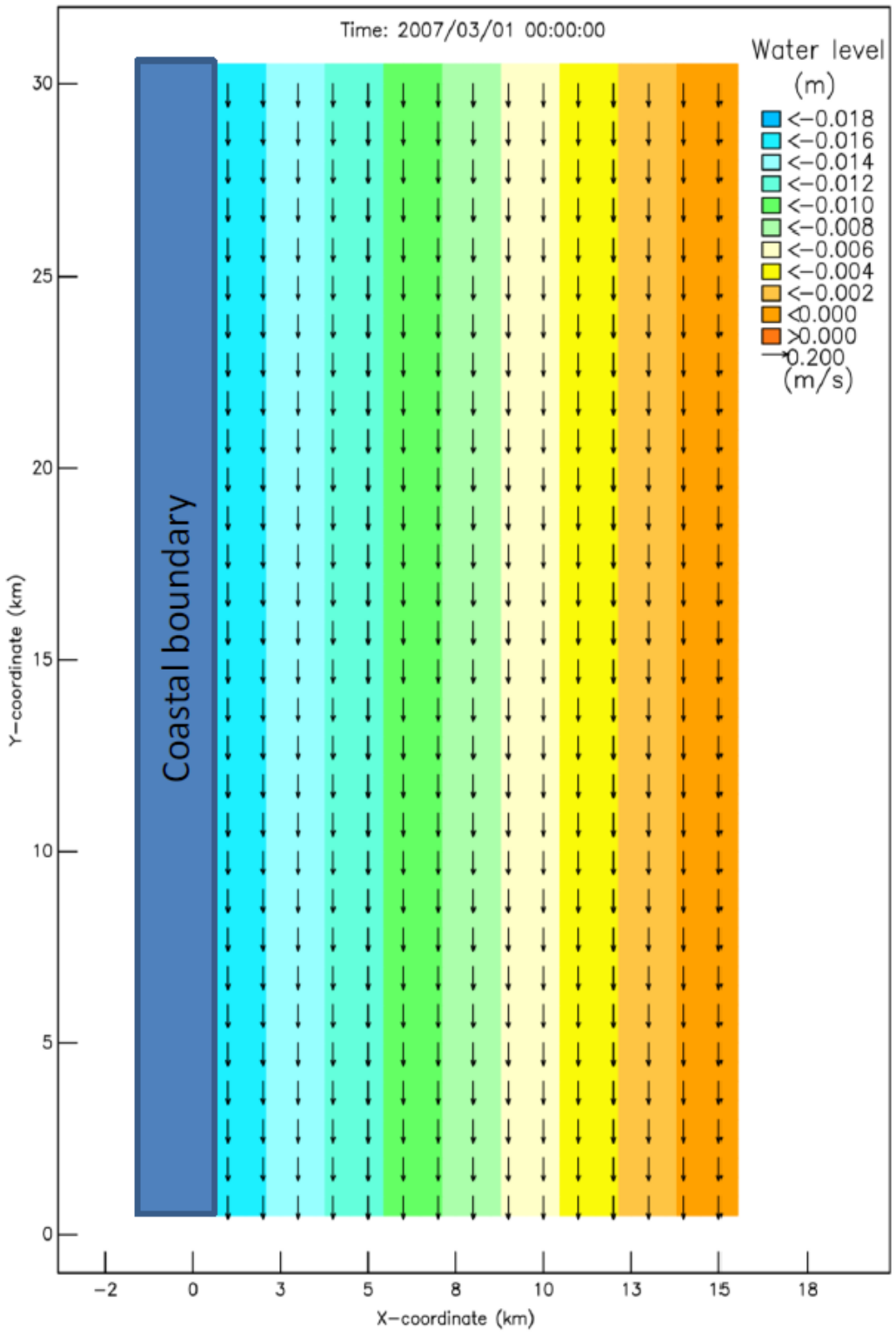

Figure 6.3: Alongshore currents variability and water level set-up driven by uniform wind of 6 m/s from the North. Neumann boundary conditions cross-shore and clamped water level offshore are tested. The flow velocity vectors and water level (in colour) are simulated.

Stellenbosch University https://scholar.sun.ac.za

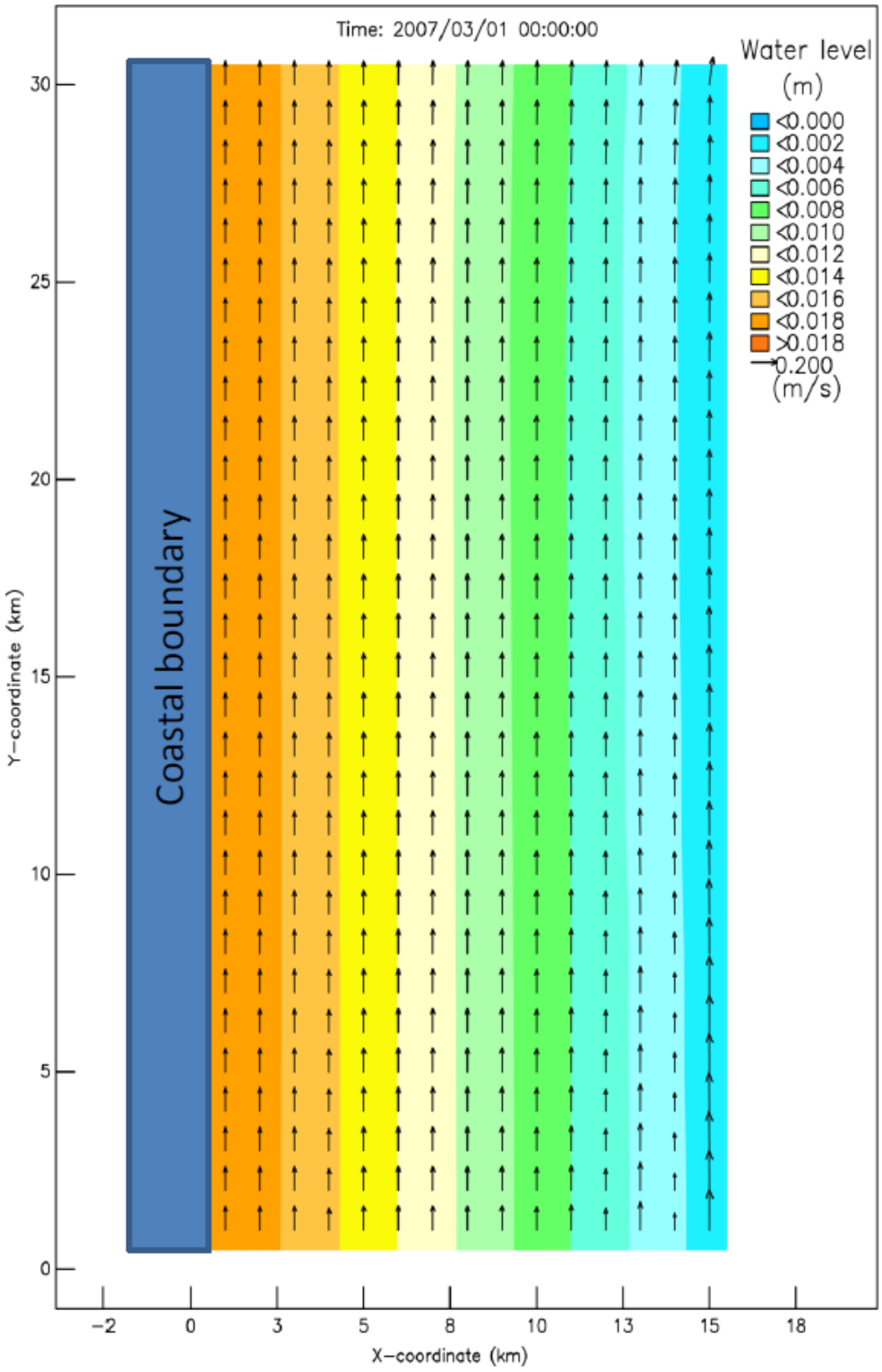

Figure 6.4: Alongshore currents variability and water level set-up driven by uniform wind of 6 m/s from the South. *Tilt* boundary conditions cross-shore and clamped water level offshore are tested. The flow velocity vectors and water level (in colour) are simulated.

Stellenbosch University https://scholar.sun.ac.za

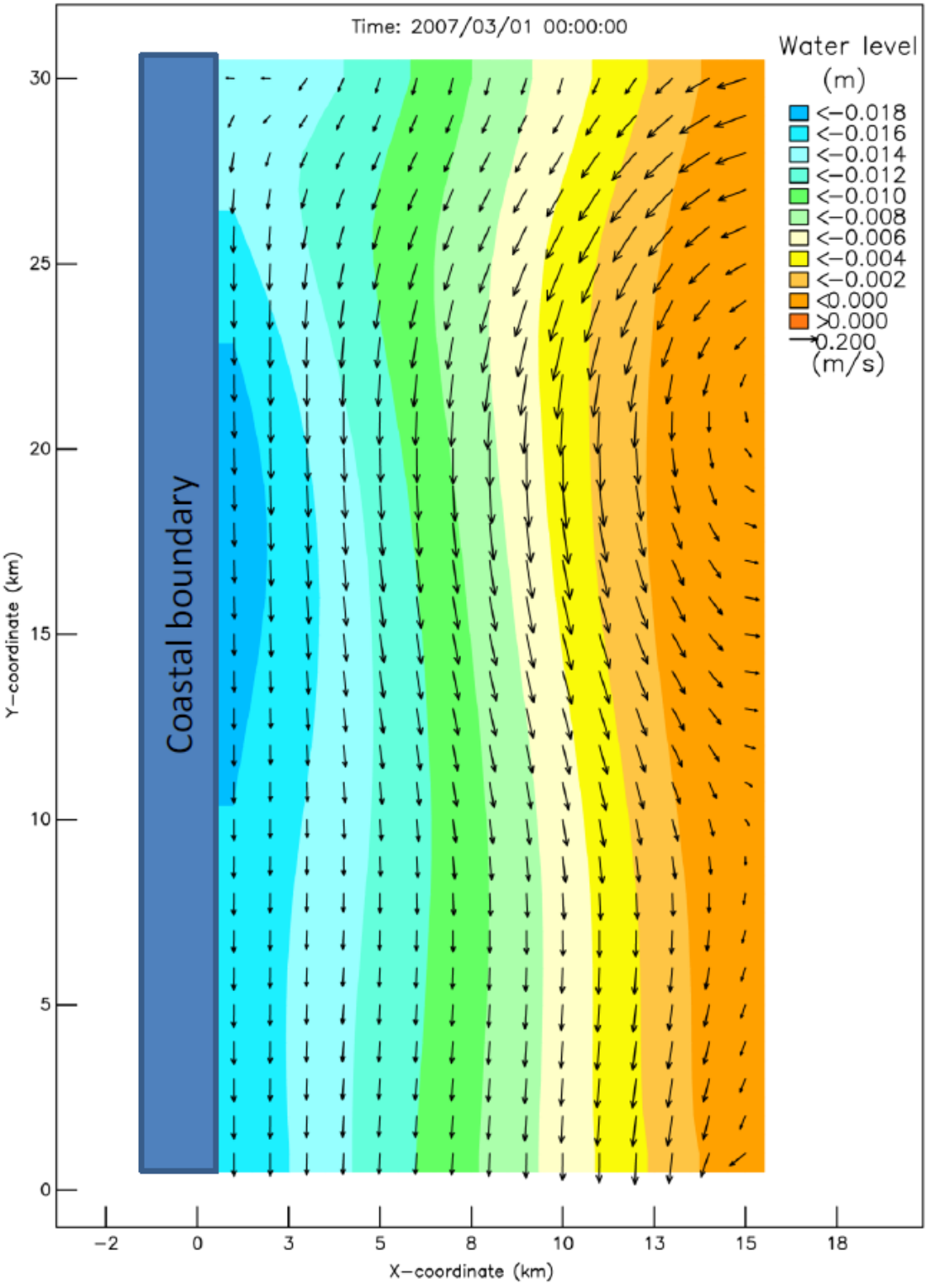

Figure 6.5: Alongshore currents variability and water level set-up driven by uniform wind of 6 m/s from the North. *Tilt* boundary conditions cross-shore and clamped water level offshore are tested. The flow velocity vectors and water level (in colour) are simulated.

Stellenbosch University https://scholar.sun.ac.za

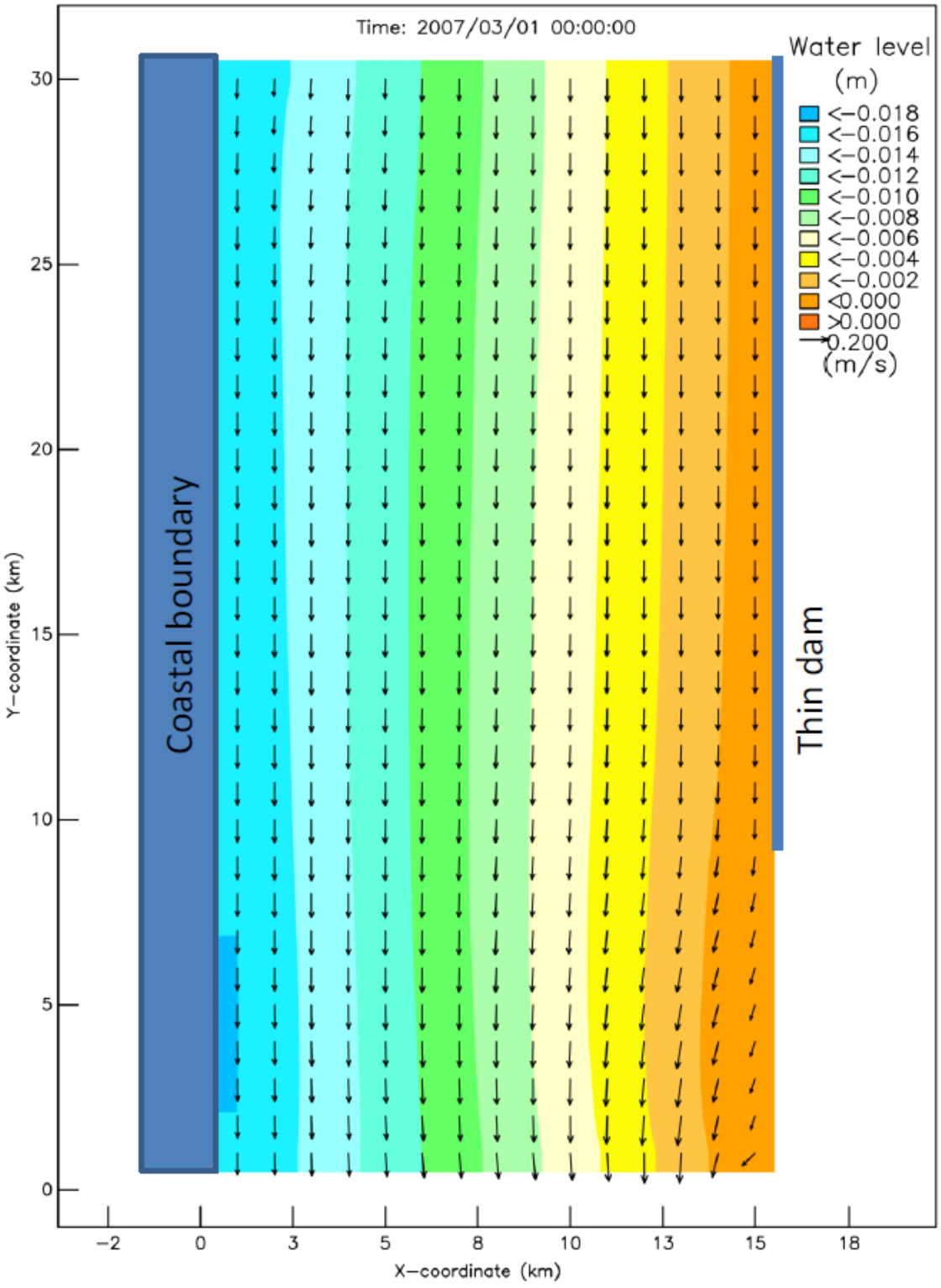

Figure 6.6: Alongshore currents variability and water level setup driven by uniform wind of 6 m/s from the North. *Tilt* boundary conditions cross-shore and clamped water level and thin dam offshore are tested. The flow velocity vectors and water level (in colour) are simulated.

Stellenbosch University https://scholar.sun.ac.za

Chapter 7

Conclusion

In this study boundary conditions applicable to coastal and shelf seas were investigated based on "reduced physics" hydrodynamic equations. The "reduced physics" hydrodynamic *Tilt* equations for determining open boundary conditions were adopted for this investigation. In this study scaling method have been used to investigate whether can *Tilt* equations be obtained by decoupling two dimensional shallow water equations. Based on literature, the theory and analysis of boundary conditions have been discussed, as the objective is to understand when can *Tilt* be used and how can it be improved. The observations based on simulations have been used to assess under which conditions the application of *Tilt* provides acceptable flows in Delft3D and its limitations.

Brief summary to the study

It is essential to coastal and shelf seas to understand cross-shore (perpendicular to the coast) and alongshore (parallel) dynamics. Navier-Stokes equations are key to understanding flow dynamics. Hence, when solved using satisfactory boundary conditions, acceptable flows may be predicted. Generally, alongshore propagation is always such that the coast is on the right (left) when the wind blows towards North (South).

An introduction to modelling of coastal and shelf seas dynamics was given in Chapters 2 and 3. Chapter 2 presented general equations of fluid mechanics with the aim to understand their physical meaning. Since coastal and shelf seas are characterized by shallow water, Navier-Stokes equations have been subjected to various assumptions to determine shallow water equations. Chapter 3 presented the derived shallow water equations, together with the necessary assumptions that characterize shallow water are presented. As a result, shallow water equations may be transformed through coordinate transformation to those developed into Delft3D-FLOW.

Stellenbosch University https://scholar.sun.ac.za

A solution to shallow water equations can be obtained, should appropriate boundary conditions be prescribed. An introduction to boundary conditions was presented in Chapter 4, generally following Stelling (1983) and a summary of commonly used boundary conditions to coastal and shelf seas models was presented. The modified version of the Sommerfeld radiation equation (4.3.9) was adopted with investigation, to understand the dynamics caused by water level imposed at the boundaries. Thus, allowing understanding of boundary conditions and its role to Delft3D, however, it provides no details to various forcing at the boundaries.

Based on shallow water equations, various assumptions were made to allow simplifications to describe reduced hydrodynamic equations at the boundaries. In Chapter 5 the simplified hydrodynamic equations were presented. In which case, characterization of various coastal or shelf seas processess were understood through scaling. Moreover, in Appendix E various scales have been investigated to determine under which scales can *Tilt* equations be obtained by decoupling two dimensional shallow water equations.

Given the necessary assumptions, models and the reduced hydrodynamic equations, various boundary conditions were tested in Chapter 6. For simulation purposes, the Delft3D-FLOW numerical model was used, subject to boundary conditions generated from *Tilt*. The above described step-by-step development characterize components of the phenomena of wind driven alongshore currents variability and water level set-up. Here the efficacy of the *Tilt* open boundary conditions have been investigated for a number of idealised cases. Based on an understanding of the underlying physics and scaling assumptions, situations where these open boundary conditions underperformed have been analysed and reasons given for their underperformance. When applied to "real-life" situations it is likely that one or more of the scaling assumptions will be violated. Comment is provided on the likely errors in model simulations should this occur.

Findings

An investigation of boundary conditions for wind driven flow in coastal and shelf seas leads to an understanding of alongshore currents variability and water level set-up for coastal and shelf seas.

A scaling approach has been undertaken in developing the *Tilt* equations. Prior to undertaking such a scaling exercise an understanding of shallow water equations was necessary. The development of shallow water equations has been described with and emphasis on all of the necessary assumptions to do so.

Stellenbosch University https://scholar.sun.ac.za

This provided the required understanding of the equations used in Delft3D-FLOW. Basically, the scaling leads to separable equations and not necessarily decoupled equations. The source of differences in all the equations obtained was the absence of the Coriolis component fu for alongshore equation in the *Tilt* equations. In order to determine *Tilt* equations, additional assumptions are required for one to neglect fu.

Based on theory, it is shown that boundary conditions determined using *Tilt* code are appropriate only for situations where there is a barotropic flow response. To understand water level set-up in a barotropic flow response, the water level set-up inside the model domain near the boundaries have been compared with that *Tilt* predicts, in which case the differences were small. The boundary offshore in *Tilt* assume a more restrictive condition of barotropic response, as the water level offshore is always clamped to zero. Furthermore, the use of *Tilt* boundary conditions to baroclinic flows cannot be justified, as *Tilt* equations are a result of 2D shallow water equations.

In the case of barotropic flows *Tilt* boundary conditions have been tested. In the cross-shore boundaries *Tilt* provides appropriate boundary conditions. Clamping of water level to zero offshore may be not enough, as flow boundary conditions are required offshore. In which case, the more restrictive condition of barotropic response offshore could be the source of the weak total mass balance observed. Particularly, when flow is tested for wind blowing from the North (e.g. Figures 6.3, 6.5 and 6.6).

The "reduced physics" approach used in *Tilt* restricts fairly significantly the range of flow that can be simulated.

Should the scaling assumptions underlying *Tilt* be satisfied, *Tilt* performs adequately for limited area model simulations of coastal and shelf regions, however there remain some concerns:

- The no flux condition at the coast and clamped water level offshore restrict flow cross-shore and enforce alongshore flow. As a result, *Tilt* open boundary conditions only satisfy the alongshore motion of a barotropic fluid when tested with winds that deflect flows towards the coast due to Coriolis effects. Where the winds deflect flow in an offshore direction siginifcant errors in flow conditions may occur at the offshore boundary. This is probably caused by the very long time taken for the coastal boundary to signal its presence.

- Where the scaling assumptions underpinning *Tilt* are violated siginifcant errors may be introduced at the model open boundaries. The likelihood of their formulation and magnitude depends on the extent to which these

Stellenbosch University https://scholar.sun.ac.za

scaling assumptions are violated. Pragmatic solutions to some of these situations are offered.

Future work

This study has indicated some of the limitations of *Tilt*, particularly where the scaling assumption underlying the development of *Tilt* have been violated. Future investigations should include:

- obtaining a better understanding of the role of the coastal and offshore boundary conditions on the interior flows of a limited area model, particularly the offshore boundary conditions in situations where the forcing at this boundary remains significant.
- undertaking of a detailed analysis of the nature of errors occurring at the open boundaries of the model when applied in situations where the scaling assumptions underlying *Tilt* are violated.
- the development of a version of *Tilt* for situations where the response is unlikely to be barotropic.
- the extension of the present version of *Tilt* to situations where there is a strong influence of offshore flows on the limited area model, i.e. when the flows due to large-scale forcing increase upon moving in an offshore direction.

Stellenbosch University https://scholar.sun.ac.za

Appendix A

Definitions

A.1 The material derivative

The material derivative is given by

$$\frac{D}{Dt} = \frac{\partial}{\partial t} + \mathbf{v} \cdot \nabla \tag{A.1.1}$$

where $\mathbf{v}$ is the velocity of the measurement point which, for the material derivative, is the same as the flow velocity (Bird *et al.*, 2007). When the velocity of the measurement point and flow velocity differ, the material derivative is referred to as the total time derivative.

A.2 Leibniz's theorem

Leibniz's theorem describes the necessary condition under which the order of differentiation and integration are interchangeable (LeBlond & Mysak, 1978; Dingemans, 1997a,b). This, may be expressed as

$$\frac{\partial}{\partial(x,y)} \int_b^a q dz = \int_b^a \frac{\partial q}{\partial(x,y)} dz + q \mid_a \frac{\partial a}{\partial(x,y)} - q \mid_b \frac{\partial b}{\partial(x,y)}, \tag{A.2.1}$$

where a and b are the limits of integration which are variable functions of (x, y), and q is an integrand, here assumed to be a continuous differentiable function.

Stellenbosch University https://scholar.sun.ac.za

A.3 Integration - theorem

Note that when the derivative is taken with respect to z, equation (A.2.1) reduces to

$$\begin{aligned}\frac{\partial}{\partial z}\int_a^b q dz &= \int_b^a \frac{\partial q}{\partial z}dz + q\mid_a \frac{\partial a}{\partial z} - q\mid_b \frac{\partial b}{\partial z} \\ &= \int_b^a \frac{\partial q}{\partial z}dz \\ &= q\mid_a - q\mid_b, \end{aligned} \tag{A.3.1}$$

where $\frac{\partial a}{\partial z} = \frac{\partial b}{\partial z} = 0$ given that a and b are not functions of z.

A.4 Viscous stress

According to Assumption 2.3.1, expressed mathematically as equation (2.3.20):

$$\underline{\underline{\tau}}(\mathbf{v}) \propto \nabla\mathbf{v}, \tag{A.4.1}$$

ocean water is assumed to be a Newtonian fluid.

The stress tensor $\underline{\underline{\tau}}$ is said to be symmetric (Batchelor, 1967; Landau & Lifshitz, 1959). Therefore, $\nabla\mathbf{v}$ is also required to be symmetric. The stress dyadic $\nabla\mathbf{v}$ decomposed into its symmetrical strain rate dyadic $\underline{\underline{D}}$ and its skew-symmetric rotation rate dyadic $\underline{\underline{W}}$ reads

$$\nabla\mathbf{v} = \underline{\underline{D}} + \underline{\underline{W}}, \tag{A.4.2}$$

The rotation rate dyadic is given by

$$\underline{\underline{W}} = \frac{1}{2}(\nabla\mathbf{v} - \widetilde{\nabla\mathbf{v}}), \tag{A.4.3}$$

where $\widetilde{\nabla\mathbf{v}}$ represents the transpose of the stress dyadic. The rotation rate dyadic, equation (A.4.3), does not cause internal shear stresses for rigid rotation, i.e. $\underline{\underline{W}} = \underline{\underline{0}}$. Therefore the stress dyadic, equation (A.4.2) becomes the symmetric strain rate dyadic

$$\nabla\mathbf{v} = \underline{\underline{D}}, \tag{A.4.4}$$

where $\underline{\underline{D}}$ is given by

$$\underline{\underline{D}} = \frac{1}{2}(\nabla\mathbf{v} + \widetilde{\nabla\mathbf{v}}). \tag{A.4.5}$$

Stellenbosch University https://scholar.sun.ac.za

Based on Newton's law of friction of rigid bodies, the relationship between the viscous stress tensor components with the flow or deformation field is entailed in the molecular viscosity coefficient μ, through the relation:

$$\underline{\underline{\tau}}(\mathbf{v}) = 2\mu\underline{\underline{D}} \tag{A.4.6}$$

$$= \mu(\nabla\mathbf{v} + \widetilde{\nabla\mathbf{v}}), \tag{A.4.7}$$

which expresses a non-negative function of space and time. Equation (A.4.7) substituted into equation (2.3.14) yields

$$\nabla \cdot \underline{\underline{\sigma}} = \nabla \cdot \left(\mu(\nabla\mathbf{v} + \widetilde{\nabla\mathbf{v}}) - p\underline{\underline{1}}\right). \tag{A.4.8}$$

which is the divergence of the total stress. Equation (A.4.8) when expanded yields

$$\nabla \cdot \underline{\underline{\sigma}} = -\nabla p + \mu\nabla^2\mathbf{v} + \mu\nabla(\nabla \cdot \mathbf{v}), \tag{A.4.9}$$

where the dyadic identity $\nabla \cdot \widetilde{\nabla\mathbf{v}} = \nabla(\nabla \cdot \mathbf{v})$ was used. This term is negligible according to the continuity equation (2.2.16). It follows that the force due to viscous stress (i.e. equation (2.3.13)) may therefore be expressed as

$$\nabla \cdot \underline{\underline{\tau}} = \mu\nabla^2\mathbf{v}. \tag{A.4.10}$$

where μ is the constant molecular viscosity.

A.5 Characterization of water waves

Various types of waves are observed in the ocean (CEM, 2002). Most of these waves are generated by wind blowing over the surface. The aim of this section is to describe different types of waves in coastal areas.

The speed at which a wave propagates may be expressed as a relationship between the phase velocity or wave celerity C to wavelength λ and the water depth H, i.e.:

$$C = \sqrt{\frac{g\lambda}{2\pi}\tanh\left(\frac{2\pi H}{\lambda}\right)}. \tag{A.5.1}$$

Different waves may have different periods t_p and travel at different speeds, e.g. longer period waves will travel faster than short period waves. In which case, based on equation (A.5.1) a general expression relating waves in motion may be written as

$$C = \frac{gt_p}{2\pi}\tanh\left(\frac{2\pi H}{\lambda}\right), \tag{A.5.2}$$

Stellenbosch University https://scholar.sun.ac.za

where $2\pi/\lambda = k$ is the wave number and $2\pi/t_p = \omega$ is the wave angular frequency.

Eqution (A.5.2) in literature has been treated in detail (CEM, 2002; Bowden, 1983; LeBlond & Mysak, 1978; Pond & Pickard, 1978; Gill, 1982). Based on the magnitude of the relative water depth H/λ and the resulting limiting values taken by $\tanh(2\pi H/\lambda)$ the water waves are classified into deep water waves, transitional water waves and shallow water waves, e.g. Table II-1-1 of the CEM (2002) Figure. 12.3 of Pond & Pickard (1978) or Figure. 3.3 of Bowden (1983).

A.5.1 Shallow water waves

In the case of shallow water waves the relative water depth H/λ varies between 0 and 1/20. This means that for small values of kH, $\tanh(kH) \approx kH$ and equation (A.5.1) may be reduced to

$$C = \sqrt{gH}, \tag{A.5.3}$$

so that the speed of a wave travelling in shallow water only depends on the water depth.

According to Kay (2008), equation (A.5.3) was developed by Joseph Lagrange (1736-1813) and verified by John Scott Russel (1808-1832). This is the celerity for shallow water waves and also hold for long waves and tidal waves (Bowden, 1983; Pond & Pickard, 1978). In numerical works, equation (A.5.3) gives details on how fast information may be transmitted by waves, from one end to another end of a flow computational domain. This is an important aspect, particularly for the open boundary conditions explored in Chapter 4.

A.5.2 Long waves

Based on the shallow water waves criterion, "long" waves may be characterized by much larger wavelengths compared to the water depth, i.e. $\lambda \gg 20H$ so that $H/\lambda \ll 1$. For long waves in shallow water (e.g. tides) the phase velocity is proportional to the square root of the water depth, i.e. characterized by $C = \omega/k = \lambda/t_p = \sqrt{gH}$.

In studies of coastal areas, estuaries, open oceans and beaches, long waves become important, since these waves are easily reflected by land (Landau & Lifshitz, 1959; Batchelor, 1967; Gill, 1982), and in numerically poorly defined boundary conditions these waves can also be reflected. This may also lead to a system which oscillates with greater amplitude at some frequencies than at others (i.e. resonance oscillations), so that even for small wind speeds (say 1 m/s) or small periodic driving forces, the system may produce strong currents.

Stellenbosch University https://scholar.sun.ac.za

A.5.3 Coastal-trapped waves

Various effects in shallow water may lead to wave trapping. Coastal-trapped waves may be characterized by alongshore motion, due to waves totally or partially reflected on the coast as they are unable to propagate back to sea.

In shallow water this phenomena may be caused by variations in bottom topography, friction and difference in water depth, i.e. in shallow water $H \to 0$ (towards the coast) and back to sea $H \to \infty$ as $k \to \infty$. According to Dingemans (1997a) based on Snell's law, it can be shown that the reflected waves cannot propagate to even deeper water. Moreover, when depth is fastly varying over the wave length, currents can cause wave trapping as the wave vector becomes nearly parallel to the bottom slope. In which case, the motion of the fluid is very nearly along the isolines of the topography (Pedlosky, 1987). These waves exist over shelf topography and even in the absence of stratification (Gill, 1982). Coastal trapped waves are apparently fundamentally barotropic in their dynamics (Pedlosky, 1987).

In literature, coastal trapped waves have broadly been discussed for various topographies (LeBlond & Mysak, 1978; Pedlosky, 1987; Gill, 1982) and the main conclusions are that bottom variations can modify the waves and yield new forms of waves. Following the work done by Van Ballegooyen (1995) coastal trapped waves have been studied for the coasts of South Africa (characterized by various topographies) and the study shows that coastal trapped waves are responsible for most of the observed variability due to currents on the shelf or coastal zones. In oceanography e.g. Pond & Pickard (1978), Bowden (1983), Gill (1982), Pedlosky (1987), wave trapping has been classified and used to distinguish between to "edge waves" in the case of gravity waves and "shelf waves" in the case of Rossby-like waves, etc.

Stellenbosch University https://scholar.sun.ac.za

Appendix B

Acceleration in a non-inertial (rotating) frame of reference

Newton's second law is only applicable to an inertial reference frame. For a reference frame fixed on the earth surface, where the earth is itself rotating, the system is said to be non-inertial. In which case, Newton's second law does not hold. Therefore, it is required that Newton's second law be expressed in terms of variables in the rotating reference frame. The aim of this appendix is to link the acceleration in the inertial reference frame to the acceleration in the non-inertial (rotating) reference frame.

Generally, the acceleration in the non-inertial (rotating) reference frame may be stated mathematically as (Batchelor, 1967; Spiegel, 1967; Pond & Pickard, 1978; Gill, 1982; Pedlosky, 1987),

$$\mathbf{a}\,|_{P/O} = \mathbf{a}\,|_{Q/O} + \frac{d\boldsymbol{\Omega}}{dt} \times \mathbf{x}\,|_{P/Q} + \boldsymbol{\Omega} \times (\boldsymbol{\Omega} \times \mathbf{x}\,|_{P/Q}) + 2\boldsymbol{\Omega} \times \mathbf{v}\,|_{P/Q} + \mathbf{a}\,|_{P/Q}\,, \qquad \text{(B.0.1)}$$

where

$$\begin{aligned}
\mathbf{a}\,|_{P/O} &= \text{acceleration of position } P \text{ relative to position } O,\\
\mathbf{a}\,|_{Q/O} &= \text{acceleration of position } Q \text{ relative to position } O,\\
\frac{d\boldsymbol{\Omega}}{dt} \times \mathbf{x}\,|_{P/Q} &= \text{linear acceleration of position } P \text{ relative to position } Q, \text{ where } d\boldsymbol{\Omega}/dt \text{ is the angular acceleration},\\
\boldsymbol{\Omega} \times (\boldsymbol{\Omega} \times \mathbf{x}\,|_{P/Q}) &= \text{centripetal acceleration of position } P \text{ relative to position } Q, \text{ where } \boldsymbol{\Omega} \text{ is the angular velocity},\\
2\boldsymbol{\Omega} \times \mathbf{v}\,|_{P/Q} &= \text{Coriolis acceleration of position } P \text{ relative to position } Q,\\
\mathbf{a}\,|_{P/Q} &= \text{acceleration of position } P \text{ relative to position } Q.
\end{aligned}$$

Stellenbosch University https://scholar.sun.ac.za

The present appendix presents the acceleration in a non-inertial (rotating) frame of reference. The aim is to present equation (B.0.1) and its simplified version under various assumptions.

B.1 The acceleration in general

Assume the earth to be a sphere with the center O, rotating about the z-axis, as shown in Figure B.1. The position of a fluid element P may be written as

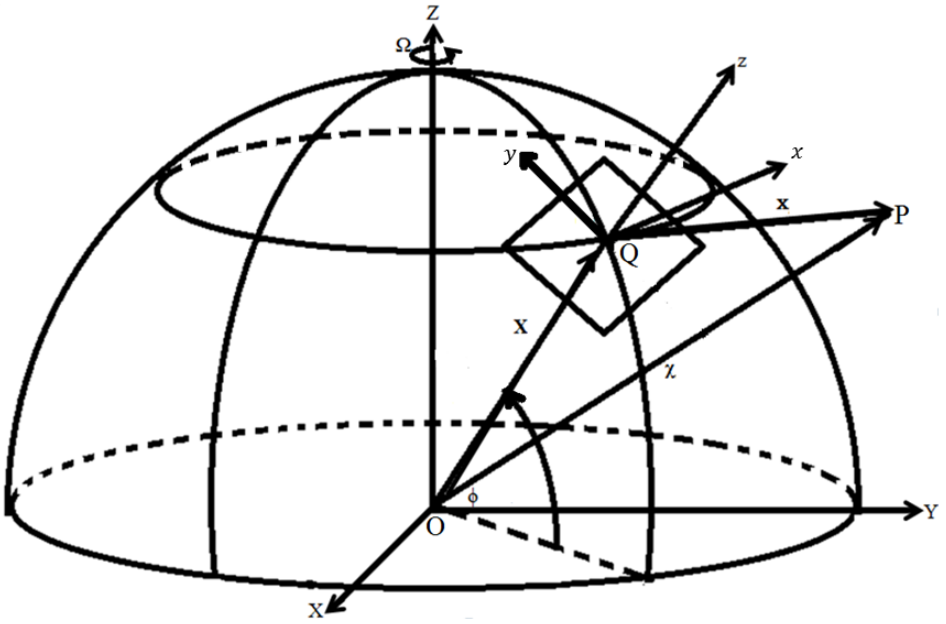

Figure B.1: General non-inertial frame of reference: Earth's hemisphere with center at O rotating about the z-axis.

$$\boldsymbol{\chi}|_{P/O} = \mathbf{X}|_{Q/O} + \mathbf{x}|_{P/Q}\,. \tag{B.1.1}$$

The rate of change of position gives the velocity. From a reference fixed to the center of the origin, according to Spiegel (1967) i.e.:

$$\left.\frac{d\boldsymbol{\chi}}{dt}\right|_{P/O} = \left.\frac{d\mathbf{X}}{dt}\right|_{Q/O} + \left[\frac{d\mathbf{x}\,|_{P/Q}}{dt} + \boldsymbol{\Omega}\times\mathbf{x}\,|_{P/Q}\right]. \tag{B.1.2}$$

In equation (B.1.2) the term $\left.\frac{d\mathbf{x}}{dt}\right|_{P/Q}$ is the velocity of point P in the rotating reference frame and $\boldsymbol{\Omega}$ is the angular velocity of the rotating system. The

Stellenbosch University https://scholar.sun.ac.za

acceleration of a moving fluid element as seen by an observer in the fixed frame is given by

$$\left.\frac{d^2\boldsymbol{\chi}}{dt^2}\right|_{P/O} = \frac{d^2\mathbf{X}\,|_{Q/O}}{dt^2} + \left[\frac{d\boldsymbol{\Omega}}{dt}\times\mathbf{x}\,|_{P/Q} + \boldsymbol{\Omega}\times(\boldsymbol{\Omega}\times\mathbf{x}\,|_{P/Q}) + 2\boldsymbol{\Omega}\times\mathbf{v}\,|_{P/Q} + \frac{d^2\mathbf{x}\,|_{P/Q}}{dt^2}\right], \tag{B.1.3}$$

which may be rewritten as

$$\mathbf{a}\,|_{P/O} = \mathbf{a}\,|_{Q/O} + \frac{d\boldsymbol{\Omega}}{dt}\times\mathbf{x}\,|_{P/Q} + \boldsymbol{\Omega}\times(\boldsymbol{\Omega}\times\mathbf{x}\,|_{P/Q}) + 2\boldsymbol{\Omega}\times\mathbf{v}\,|_{P/Q} + \mathbf{a}\,|_{P/Q}\,. \tag{B.1.4}$$

This is the general acceleration equation that describes motion in a non-inertial frame of reference (Spiegel, 1967).

B.1.1 Simplifications

Given that the earth rotates about the z-axis, as shown in Figure B.1 and that the earth surface rotates with constant angular velocity. The following simplification may be made, i.e. the constant angular velocity is given as

$$\boldsymbol{\Omega} = \Omega\boldsymbol{k}, \tag{B.1.5}$$

where Ω is the magnitude of the angular velocity of the earth given by

$$\Omega = \frac{2\pi}{24\times 3600} = 7.27\times 10^{-5}\ \text{rad/s}. \tag{B.1.6}$$

Since Ω is a constant and the direction of the z-axis is fixed, it follows from equation (B.1.5) that

$$\frac{d\boldsymbol{\Omega}}{dt} = \mathbf{0}. \tag{B.1.7}$$

Consider the reference frame at Q to be fixed to the earth and therefore rotates with the earth and does not have any translation. The first term on the right hand side of equation (B.1.4) may be expressed as

$$\mathbf{a}\,|_{Q/O} = \boldsymbol{\Omega}\times(\boldsymbol{\Omega}\times\mathbf{X}\,|_{Q/O}), \tag{B.1.8}$$

to describe the motion of origin Q relative to origin O in Figure B.1. According to Pond & Pickard (1978), equation (B.1.8) is the centripetal acceleration

Stellenbosch University https://scholar.sun.ac.za

required for a fluid element on the earth surface to rotate about the earth axis.

Furthermore, the gravitational pull of the earth on point P yields gravitational acceleration, which expressed in terms of Newton's law of gravitation, may be written as,

$$\mathbf{a}\,|_{P/O} = \frac{\mathbf{F}_{gra}}{m} \;=\; -\frac{GM}{|\,\boldsymbol{\chi}|_{P/O}\,|^3}\,\boldsymbol{\chi}|_{P/O}\,, \tag{B.1.9}$$

where $|\,\boldsymbol{\chi}|_{P/O}\,|$ is the magnitude of the position of point P relative to O, $M \approx 5.972 \times 10^{24}$ kg represents the mass of the earth and $G \approx 6.672 \times 10^{-11}$ N.m^2/kg^2 represents the Universal Gravitational Constant. By using equations (B.1.7) to (B.1.9), it is evident that equation (B.1.4) may be written as

$$-\frac{GM}{|\,\boldsymbol{\chi}|_{P/O}\,|^3}\,\boldsymbol{\chi}|_{P/O} = \boldsymbol{\Omega}\times(\boldsymbol{\Omega}\times\mathbf{X}\,|_{Q/O}) + \mathbf{0} + \boldsymbol{\Omega}\times(\boldsymbol{\Omega}\times\mathbf{x}\,|_{P/Q}) \\ +2\boldsymbol{\Omega}\times\mathbf{v}\,|_{P/Q} + \mathbf{a}\,|_{P/Q}\,, \tag{B.1.10}$$

where the term on the left hand side of equation (B.1.10) is given by equation (B.1.9) and on the right hand side the first term is given by equation (B.1.8) and the second term is given by equation (B.1.7). Equation (B.1.10) when rearranged, may be written as

$$\mathbf{a}\,|_{P/Q} \;=\; -\frac{GM}{|\,\boldsymbol{\chi}|_{P/O}\,|^3}\,\boldsymbol{\chi}|_{P/O} - \boldsymbol{\Omega}\times(\boldsymbol{\Omega}\times\mathbf{X}\,|_{Q/O}) - \boldsymbol{\Omega}\times(\boldsymbol{\Omega}\times\mathbf{x}\,|_{P/Q}) \\ -2\boldsymbol{\Omega}\times\mathbf{v}\,|_{P/Q}\,. \tag{B.1.11}$$

As shown in Figure B.1, a fluid element at the distance $|\,\boldsymbol{\chi}|_{P/O}\,|$ from the center of the earth, will have the gravitation force along the line $\boldsymbol{\chi}$ and the centripetal acceleration towards the axis of rotation. Pond & Pickard (1978) have considered the centripetal acceleration to be much smaller, i.e. 0.3 % of the acceleration due to gravity. This implies that $\boldsymbol{\Omega}\times(\boldsymbol{\Omega}\times\mathbf{x}_{Q/O})$ is approximately 0.3 % of g.

According to Spiegel (1967), the third term on the right hand side of equation (B.1.11) may be neglected near the earth's surface since $\mathbf{x}\,|_{P/Q}$ is much smaller than $\boldsymbol{\chi}|_{P/O}$. Therefore, equation (B.1.11) becomes

$$\mathbf{a}\,|_{P/Q} \;=\; -\frac{GM}{|\,\boldsymbol{\chi}|_{P/O}\,|^3}\,\boldsymbol{\chi}|_{P/O} - \boldsymbol{\Omega}\times(\boldsymbol{\Omega}\times\mathbf{X}\,|_{Q/O}) - 2\boldsymbol{\Omega}\times\mathbf{v}\,|_{P/Q}\,, \tag{B.1.12}$$

which represents the acceleration of the fluid element near the earth's surface in a reference frame fixed to the earth's surface. For use in a non-inertial frame

Stellenbosch University https://scholar.sun.ac.za

of reference it is required that the acceleration due to gravity be expressed as gravitational acceleration (Pond & Pickard, 1978; Pedlosky, 1987) given by

$$\mathbf{g} = -\frac{GM}{|\boldsymbol{\chi}|_{P/O}|^3}\boldsymbol{\chi}|_{P/O} - \boldsymbol{\Omega}\times(\boldsymbol{\Omega}\times\mathbf{X}\,|_{Q/O}). \tag{B.1.13}$$

The next section presents the equations of motion based on equation (B.1.12) given the acceleration due to gravity is given by equation (B.1.13).

B.2 Equations of motion

The reference frame at Q attached to the earth surface is defined such that the z-axis points radially outwards from the center of earth and the x- and y-axis lie in the horizontal plane tangent to the earth. As shown in Figure B.1, for the plane attached to the earth surface and rotation about the earth axis in terms of the colatitude implies that $\boldsymbol{\Omega} = \Omega(\cos\phi\mathbf{j} + \sin\phi\mathbf{k})$ since $\boldsymbol{\Omega}\cdot\mathbf{i} = 0$ because $\mathbf{i}$ is exactly aligned with the direction of the earth's rotation. From equation (B.1.12) the acceleration of a fluid element near the earth surface may be expressed as

$$\left.\begin{aligned}\frac{du}{dt} &= 2\Omega\sin\phi v - 2\Omega\cos\phi w + F_x\\ \frac{dv}{dt} &= -2\Omega\sin\phi u + F_y\\ \frac{dw}{dt} &= -g + 2\Omega\cos\phi u + F_z\end{aligned}\right\} \tag{B.2.1}$$

where $\mathbf{F}/m = (F_x, F_y, F_z)$ and $\mathbf{v}\,|_{P/Q} = u\mathbf{i} + v\mathbf{j} + w\mathbf{k}$.

Under certain assumptions, these equations may be simplified into beta-plane equations, f-plane equations and the shallow water equations. In Chapters 2 and 3, these are explored.

Stellenbosch University https://scholar.sun.ac.za

Appendix C

Time- and depth-averaged equations

The averaging process presented in this Appendix aims to eliminate the dependence of variables on short time and space scales. In which case, no effort is made in resolving process at these scales. In doing so large scale flow is intended and only the motion due to currents is the focus.

It is common practise for most engineering or computational fluid dynamics (CFD) purposes to investigate mean flow, where flow variables are averaged over time and/or space. The usual procedure followed to derive and understand the governing equations is to decompose all the state variables into contributions due to averaged and fluctuating quantities.

The time- and/or space-averaging is used to isolate the desired phenomenon. For the purpose of this appendix, time-averaging is used to determine the Reynolds averaged Navier-Stokes equations (RANS) by removing the fluctuating quantities. The depth (or space)-averaging is used to determine the depth-averaged two-dimensional flow equations or the two-dimensional shallow water equations by removing the vertical variations.

C.1 Reynolds averaged Navier-Stokes equations for rotating fluid

Time averaging is used to isolate the desired current flows. Based on Reynolds decomposition, a velocity field may be written as

$$\mathbf{v} = \overline{\mathbf{v}} + \mathbf{v}', \tag{C.1.1}$$

where the overbar represent time-averaged quantities, given by

$$\overline{\mathbf{v}} = \frac{1}{\Delta t}\int_{t}^{t+\Delta t} \mathbf{v} dt, \tag{C.1.2}$$

Stellenbosch University https://scholar.sun.ac.za

and $\mathbf{v}^{'}$ represents variations due to waves and turbulence (Mei, 1983; Versteeg & Malalasekera, 2007; Bedford *et al.*, 1987). Similarly, all other variables may be decomposed accordingly, i.e.:

$$p = \overline{p} + p^{'}, \rho = \overline{\rho} + \rho^{'}. \tag{C.1.3}$$

By definition, time averaging of any fluctuating part is zero

$$\overline{p^{'}} = \overline{\rho^{'}} = \overline{\mathbf{v}^{'}} = 0. \tag{C.1.4}$$

Moreover, a continual use or reference to common rules of time-averaging (Bedford *et al.*, 1987) will be made without mentioning them.

C.1.1 Time-averaged continuity equation

A substitution of equation (C.1.1) into the continuity equation (2.2.16) yields

$$\nabla \cdot (\overline{\mathbf{v}} + \mathbf{v}^{'}) = 0. \tag{C.1.5}$$

The time averaging of this equation becomes

$$\overline{\nabla \cdot (\overline{\mathbf{v}} + \mathbf{v}^{'})} = 0, \tag{C.1.6}$$

and with the time averaging rules applied, reduces into

$$\nabla \cdot \overline{\mathbf{v}} = 0. \tag{C.1.7}$$

Note that, when equation (C.1.7) is subtracted from (C.1.5) the velocity divergence of the fluctuating velocity is obtained, i.e.:

$$\nabla \cdot \mathbf{v}^{'} = 0. \tag{C.1.8}$$

By equations (C.1.7) and (C.1.8) it is meant that $\overline{\mathbf{v}}$ and $\mathbf{v}^{'}$ satisfy continuity independently.

C.1.2 Time-averaged Navier-Stokes equation

Prior to averaging the Navier-Stokes equations over time, consider the first term on the left hand side of equation (2.3.31), i.e.:

$$\frac{D\mathbf{v}}{Dt} = \underbrace{\frac{\partial \mathbf{v}}{\partial t}}_{local\ acceleration} + \underbrace{\mathbf{v} \cdot \nabla \mathbf{v}}_{advective\ acceleration} \tag{C.1.9}$$

The advection term may be transformed with the help of the continuity equation as

$$\begin{aligned} \mathbf{v} \cdot \nabla \mathbf{v} &= \nabla \cdot (\mathbf{v}\mathbf{v}) - \mathbf{v}\nabla \cdot \mathbf{v} \\ &= \nabla \cdot (\mathbf{v}\mathbf{v}), \end{aligned} \tag{C.1.10}$$

Stellenbosch University https://scholar.sun.ac.za

since $\nabla \cdot \mathbf{v} = 0$ from the continuity equation. Therefore, equation (C.1.9) may be written as

$$\frac{D\mathbf{v}}{Dt} = \frac{\partial \mathbf{v}}{\partial t} + \nabla \cdot (\mathbf{v}\mathbf{v}). \tag{C.1.11}$$

Equation (2.3.31) substituted with equation (C.1.11) becomes

$$\frac{\partial \mathbf{v}}{\partial t} + \nabla \cdot (\mathbf{v}\mathbf{v}) + 2\boldsymbol{\Omega} \times \mathbf{v} = -\frac{1}{\rho}\nabla p + \nu \nabla^2 \mathbf{v} - \mathbf{g}. \tag{C.1.12}$$

and when time-averaged becomes

$$\overline{\frac{\partial(\overline{\mathbf{v}} + \mathbf{v}')}{\partial t} + \nabla \cdot (\overline{\mathbf{v}} + \mathbf{v}')(\overline{\mathbf{v}} + \mathbf{v}') + 2\boldsymbol{\Omega} \times (\overline{\mathbf{v}} + \mathbf{v}') = \overline{-\frac{1}{(\overline{\rho} + \rho')}\nabla(\overline{p} + p') + \nu\nabla^2(\overline{\mathbf{v}} + \mathbf{v}') - \mathbf{g}}}. \tag{C.1.13}$$

When the time averaging rules are applied, this equation reduces into the time-averaged Navier-Stokes equations

$$\frac{\partial \overline{\mathbf{v}}}{\partial t} + \nabla \cdot \overline{(\mathbf{v}\mathbf{v})} + \nabla \cdot \overline{(\mathbf{v}'\mathbf{v}')} + 2\boldsymbol{\Omega} \times \overline{\mathbf{v}} = -\frac{1}{\overline{\rho}}\nabla \overline{p} + \nu \nabla^2 \overline{\mathbf{v}} - \mathbf{g}$$

$$\frac{\partial \overline{\mathbf{v}}}{\partial t} + \nabla \cdot \overline{(\mathbf{v}\mathbf{v})} + 2\boldsymbol{\Omega} \times \overline{\mathbf{v}} = -\frac{1}{\overline{\rho}}\nabla \overline{p} + \nabla \cdot \left(\nu \nabla \overline{\mathbf{v}} - \overline{(\mathbf{v}'\mathbf{v}')}\right) - \mathbf{g}. \tag{C.1.14}$$

This equation is formally known as the Reynolds-averaged Navier-Stokes equations (RANS). The addition term in equation (C.1.14) represent Reynolds turbulent stresses due to time-averaging, i.e. $-\overline{(\mathbf{v}'\mathbf{v}')}$. This additional Reynolds turbulent stresses may only be predicted when necessary turbulent models are developed. Versteeg & Malalasekera (2007) in their page 67 have presented various turbulent models, in which the Reynolds turbulent stresses may be predicted. The discussion about turbulence models is not the aim of this study. Based on the eddy viscosity principle after Boussinesq 1877, the Reynolds turbulent stresses may be linked with the mean velocity gradient (analogy to the viscous stress) through turbulent eddy viscosity ν_t (Pond & Pickard, 1978; LeBlond & Mysak, 1978; Gill, 1982), i.e.:

$$\nabla \cdot (-\overline{(\mathbf{v}'\mathbf{v}')}) \approx \nabla \cdot (\nu_t \nabla \overline{\mathbf{v}}), \tag{C.1.15}$$

and if it is assumed that the turbulent eddy viscosity ν_t is either constant or varying slowly, then

$$\nabla \cdot (-\overline{(\mathbf{v}'\mathbf{v}')}) \approx \nu_t \nabla^2 \overline{\mathbf{v}}. \tag{C.1.16}$$

Stellenbosch University https://scholar.sun.ac.za

According to LeBlond & Mysak (1978), other forms of parameterization of the Reynolds stress are discussed by Pope (1975) and Hinze (1975). The final Reynolds-averaged Navier-Stokes equations read

$$\frac{\partial \overline{\mathbf{v}}}{\partial t} + \nabla \cdot \overline{(\mathbf{vv})} + 2\boldsymbol{\Omega} \times \overline{\mathbf{v}} = -\frac{1}{\overline{\rho}} \nabla \overline{p} + \nu_t \nabla^2 \overline{\mathbf{v}} - \mathbf{g}. \tag{C.1.17}$$

In which case, equations (C.1.7) and (C.1.17) may be written as

$$\left.\begin{aligned} \nabla \cdot \overline{\mathbf{v}} &= 0 \\ \frac{\partial \overline{\mathbf{v}}}{\partial t} + \nabla \cdot \overline{(\mathbf{vv})} + 2\boldsymbol{\Omega} \times \overline{\mathbf{v}} &= -\frac{1}{\overline{\rho}} \nabla \overline{p} + \nu_t \nabla^2 \overline{\mathbf{v}} - \mathbf{g} \end{aligned}\right\}, \tag{C.1.18}$$

and for the sake of completeness the time-averaged equation for varying density may be written as

$$\frac{D\overline{\rho}}{Dt} = 0. \tag{C.1.19}$$

These equations consistute the three-dimensional governing equations.

C.2 Depth-averaged equations

C.2.1 Depth-averaged continuity equation

The continuity equation (3.4.15) integrated over depth may be written as

$$\int_{-h}^{\eta} \left(\frac{\partial u}{\partial x} + \frac{\partial v}{\partial y} \right) dz + \int_{-h}^{\eta} \frac{\partial w}{\partial z} dz = 0. \tag{C.2.1}$$

When the integration theorem (A.3.1) is applied, this equation becomes

$$\int_{-h}^{\eta} \left(\frac{\partial u}{\partial x} + \frac{\partial v}{\partial y} \right) dz + w\,|_{\eta} - w\,|_{-h} = 0. \tag{C.2.2}$$

Applying Leibniz theorem (A.2.1) and rearranging each term, this equation becomes

$$\frac{\partial}{\partial x} \int_{-h}^{\eta} u dz + \frac{\partial}{\partial y} \int_{-h}^{\eta} v dz + \left(-u\,|_{\eta} \frac{\partial \eta}{\partial x} - v\,|_{\eta} \frac{\partial \eta}{\partial y} + w\,|_{\eta} \right) + \left(u\,|_{-h} \frac{\partial (-h)}{\partial x} + v\,|_{-h} \frac{\partial (-h)}{\partial y} - w\,|_{-h} \right) = 0. \tag{C.2.3}$$

The first term in brackets may be reduced into the kinematic boundary condition at the free suraface, i.e.

$$\frac{\partial \eta}{\partial t} = -u\,|_{\eta} \frac{\partial \eta}{\partial x} - v\,|_{\eta} \frac{\partial \eta}{\partial y} + w\,|_{\eta}. \tag{C.2.4}$$

Stellenbosch University https://scholar.sun.ac.za

For a rigid sea bottom, the velocities at the bottom are zero and it follows that

$$-u\mid_{-h}\frac{\partial h}{\partial x}-v\mid_{-h}\frac{\partial h}{\partial y}-w\mid_{-h}=0. \tag{C.2.5}$$

Therefore, the continuity equation may be written as

$$\frac{\partial \eta}{\partial t}+\frac{\partial}{\partial x}\int_{-h}^{\eta}udz+\frac{\partial}{\partial y}\int_{-h}^{\eta}vdz \;=\; 0. \tag{C.2.6}$$

By definition, the integral of the flow velocity over the depth, is the fluid discharge i.e.:

$$q_x=\int_{-h}^{\eta}udz=\widehat{u}H \quad \text{and} \quad q_y=\int_{-h}^{\eta}vdz=\widehat{v}H \tag{C.2.7}$$

where $H=h+\eta$ represents the instantaneous water depth (Figure D.3), and $(\widehat{u},\widehat{v})$ are the depth-averaged velocities. The final depth-averaged (vertically homogenous) continuity equation may be written as

$$\frac{\partial \eta}{\partial t}+\frac{\partial(\widehat{u}H)}{\partial x}+\frac{\partial(\widehat{v}H)}{\partial y} \;=\; 0. \tag{C.2.8}$$

By this equation it is implied that the difference between in-flow and the out-flow of a volume of water, leads to a change in water level.

C.2.2 Depth-averaged momentum equations

The derivations for depth-averaged equations in the present section follows from the expositions by Mei (1983) and Dingemans (1997a).

Consider the momentum equation (3.4.16) in the x-direction which will then be integrated and averaged over the instantaneous water depth $(h+\eta)$, i.e:

$$\underbrace{\int_{-h}^{\eta}\left(\frac{\partial u}{\partial t}+\frac{\partial(uu)}{\partial x}+\frac{\partial(uv)}{\partial y}+\frac{\partial(uw)}{\partial z}\right)dz}_{1}-\underbrace{\int_{-h}^{\eta}fvdz}_{2}=-\underbrace{\int_{-h}^{\eta}\frac{1}{\rho}\frac{\partial p}{\partial x}dz}_{3}+\underbrace{\int_{-h}^{\eta}\nu_t\left(\frac{\partial^2 u}{\partial x^2}+\frac{\partial^2 u}{\partial y^2}+\frac{\partial^2 u}{\partial z^2}\right)dz}_{4} \tag{C.2.9}$$

where the numbers under the braces denote the distinct terms 1 to 4. Each term is expanded by applying Leibniz theorem (A.2.1) and/or the integration theorem (A.3.1). The components of term 1 become

$$\int_{-h}^{\eta}\frac{\partial u}{\partial t}dz \;=\; \frac{\partial}{\partial t}\int_{-h}^{\eta}udz-u\mid_{\eta}\frac{\partial \eta}{\partial t}+u\mid_{-h}\frac{\partial(-h)}{\partial t},$$

Stellenbosch University https://scholar.sun.ac.za

$$\int_{-h}^{\eta} \frac{\partial(uu)}{\partial x} dz = \frac{\partial}{\partial x}\int_{-h}^{\eta}(uu)dz - (uu)\mid_{\eta} \frac{\partial \eta}{\partial x} + (uu)\mid_{-h} \frac{\partial(-h)}{\partial x},$$

$$\int_{-h}^{\eta} \frac{\partial(uv)}{\partial y} dz = \frac{\partial}{\partial y}\int_{-h}^{\eta}(uv)dz - (uv)\mid_{\eta} \frac{\partial \eta}{\partial y} + (uv)\mid_{-h} \frac{\partial(-h)}{\partial y},$$

$$\int_{-h}^{\eta} \frac{\partial(uw)}{\partial z} dz = (uw)\mid_{\eta} - (uw)\mid_{-h}.$$

The sum of the components of term 1 with the kinematic boundary conditions applied (Dingemans, 1997a), yield the following

$$\begin{aligned}
Term\ 1 &= \frac{\partial}{\partial t}\int_{-h}^{\eta} u dz + \frac{\partial}{\partial x}\int_{-h}^{\eta}(uu)dz + \frac{\partial}{\partial y}\int_{-h}^{\eta}(uv)dz - \\
&\quad u\mid_{\eta}\left(\frac{\partial \eta}{\partial t} + \underbrace{u\mid_{\eta}\frac{\partial \eta}{\partial x} + v\mid_{\eta}\frac{\partial \eta}{\partial y} - w\mid_{\eta}}_{=-\frac{\partial \eta}{\partial t}}\right) + \\
&\quad u\mid_{-h}\left(\underbrace{\frac{\partial(-h)}{\partial t}}_{=0} + \underbrace{u\mid_{-h}}_{=0}\frac{\partial(-h)}{\partial x} + \underbrace{v\mid_{-h}}_{=0}\frac{\partial(-h)}{\partial y} - \underbrace{w\mid_{-h}}_{=0}\right) \\
&= \frac{\partial}{\partial t}\int_{-h}^{\eta} u dz + \frac{\partial}{\partial x}\int_{-h}^{\eta}(uu)dz + \frac{\partial}{\partial y}\int_{-h}^{\eta}(uv)dz \\
&= \frac{\partial(\widehat{u}H)}{\partial t} + \frac{\partial(\widehat{u}\widehat{u}H)}{\partial x} + \frac{\partial(\widehat{u}\widehat{v}H)}{\partial y}. \qquad \text{(C.2.10)}
\end{aligned}$$

The Coriolis term (term 2) averaged over depth, yields

$$\int_{-h}^{\eta} f v dz = Hf\widehat{v}. \qquad \text{(C.2.11)}$$

Term 3 when averaged over depth yields

$$\int_{-h}^{\eta} \frac{1}{\rho}\frac{\partial p}{\partial x} dz = \frac{1}{\rho}\left(\frac{\partial}{\partial x}\int_{-h}^{\eta} p dz + p\mid_{\eta}\frac{\partial \eta}{\partial x} - p\mid_{-h}\frac{\partial h}{\partial x}\right). \qquad \text{(C.2.12)}$$

Based on equation (3.5.1) the atmospheric pressure may be set to zero, i.e. $p\mid_{\eta} = p_a = 0$. Therefore, equation (C.2.12) may be simplified to give

$$\int_{-h}^{\eta} \frac{1}{\rho}\frac{\partial p}{\partial x} dz = \frac{1}{\rho}\left(\frac{\partial}{\partial x}\int_{-h}^{\eta} p dz - p\mid_{-h}\frac{\partial h}{\partial x}\right). \qquad \text{(C.2.13)}$$

Stellenbosch University https://scholar.sun.ac.za

Following Mei (1983) the mean dynamic pressure at the bottom may be defined as

$$p = p\,|_{-h} - \rho g(\eta + h), \tag{C.2.14}$$

which implies that the time averaged pressure at the bottom may be written as

$$\begin{aligned} p\,|_{-h}\frac{\partial(-h)}{\partial x} &= p\frac{\partial(-h)}{\partial x} - \rho g(\eta+h)\frac{\partial(-h)}{\partial x} \\ &= p\frac{\partial(-h)}{\partial x} + \frac{\partial}{\partial x}\left(\frac{1}{2}\rho g(\eta+h)^2\right) - \rho g(\eta+h)\frac{\partial \eta}{\partial x}. \end{aligned} \tag{C.2.15}$$

Therefore, equation (C.2.15) substituted into equation (C.2.13) yields

$$\begin{aligned} \int_{-h}^{\eta}\frac{1}{\rho}\frac{\partial p}{\partial x}dz = \frac{1}{\rho}\left(\frac{\partial}{\partial x}\int_{-h}^{\eta} p dz - \left[p\frac{\partial(-h)}{\partial x} + \frac{\partial}{\partial x}\left(\frac{1}{2}\rho g(\eta+h)^2\right)\right.\right. \\ \left.\left. -\rho g(\eta+h)\frac{\partial \eta}{\partial x}\right]\right). \end{aligned} \tag{C.2.16}$$

Depth averaging of term 4 results into

$$\int_{-h}^{\eta}\nu_t\frac{\partial^2 u}{\partial x^2}dz = \frac{\partial}{\partial x}\int_{-h}^{\eta}\left(\nu_t\frac{\partial u}{\partial x}\right)dz - \left(\nu_t\frac{\partial u}{\partial x}\right)\Big|_{\eta}\frac{\partial \eta}{\partial x} + \left(\nu_t\frac{\partial u}{\partial x}\right)\Big|_{-h}\frac{\partial(-h)}{\partial x},$$

$$\int_{-h}^{\eta}\nu_t\frac{\partial^2 u}{\partial y^2}dz = \frac{\partial}{\partial y}\int_{-h}^{\eta}\left(\nu_t\frac{\partial u}{\partial y}\right)dz - \left(\nu_t\frac{\partial u}{\partial y}\right)\Big|_{\eta}\frac{\partial \eta}{\partial y} + \left(\nu_t\frac{\partial u}{\partial y}\right)\Big|_{-h}\frac{\partial(-h)}{\partial y},$$

$$\int_{-h}^{\eta}\nu_t\frac{\partial^2 u}{\partial z^2}dz = \left(\nu_t\frac{\partial u}{\partial z}\right)\Big|_{\eta} - \left(\nu_t\frac{\partial u}{\partial z}\right)\Big|_{-h}.$$

These terms comdined yields the shear stress acting on the fluid. In which case, the terms evaluated at the sea surface characterize the wind shear stress, whereas those evaluated at the sea bottom chraracterize the bottom shear

Stellenbosch University https://scholar.sun.ac.za

stress. The components of term 4 combined yields

$$\begin{aligned} Sum &= \underbrace{-\left(\nu_t\frac{\partial u}{\partial x}\right)\Big|_\eta \frac{\partial \eta}{\partial x} - \left(\nu_t\frac{\partial u}{\partial y}\right)\Big|_\eta \frac{\partial \eta}{\partial y} + \left(\nu_t\frac{\partial u}{\partial z}\right)\Big|_\eta}_{\text{wind stress}} \\ &\quad \underbrace{+\left(\nu_t\frac{\partial u}{\partial x}\right)\Big|_{-h} \frac{\partial (-h)}{\partial x} + \left(\nu_t\frac{\partial u}{\partial y}\right)\Big|_{-h} \frac{\partial (-h)}{\partial y} - \left(\nu_t\frac{\partial u}{\partial z}\right)\Big|_{-h}}_{\text{bottom friction}} \\ &\quad + \frac{\partial}{\partial x}\int_{-h}^{\eta}\left(\nu_t\frac{\partial u}{\partial x}\right)dz + \frac{\partial}{\partial y}\int_{-h}^{\eta}\left(\nu_t\frac{\partial u}{\partial y}\right)dz \\ &= \frac{\tau_{xw}}{\rho} - \frac{\tau_{xb}}{\rho} + \frac{\partial}{\partial x}\int_{-h}^{\eta}\left(\nu_t\frac{\partial u}{\partial x}\right)dz + \frac{\partial}{\partial y}\int_{-h}^{\eta}\left(\nu_t\frac{\partial u}{\partial y}\right)dz, \quad \text{(C.2.17)} \end{aligned}$$

where τ_{xw} and τ_{xb} represents the wind and bottom shear stress in the x-direction, respectively. By comparing equations (C.2.10) to (C.2.17), the final equation with all terms substituted reads

$$\begin{aligned} \frac{\partial(\widehat{u}H)}{\partial t} + \frac{\partial(\widehat{u}\widehat{u}H)}{\partial x} + \frac{\partial(\widehat{u}\widehat{v}H)}{\partial y} - f\widehat{v}H = &-\frac{1}{\rho}\frac{\partial}{\partial x}\int_{-h}^{\eta} p dz + p\frac{1}{\rho}\frac{\partial(-h)}{\partial x} - \\ &\frac{1}{\rho}\frac{\partial}{\partial x}\left(\frac{1}{2}\rho g(\eta+h)^2\right) + g(\eta+h)\frac{\partial \eta}{\partial x} + \frac{\tau_{xw}}{\rho} - \frac{\tau_{xb}}{\rho} + \\ &\frac{\partial}{\partial x}\int_{-h}^{\eta}\left(\nu_t\frac{\partial u}{\partial x}\right)dz + \frac{\partial}{\partial y}\int_{-h}^{\eta}\left(\nu_t\frac{\partial u}{\partial y}\right)dz. \quad \text{(C.2.18)} \end{aligned}$$

This equation may be simplified under the following assumptions, i.e.:

$$p\frac{1}{\rho}\frac{\partial(-h)}{\partial x} = 0, \quad \text{(C.2.19)}$$

if the dynamic pressure at the bottom is zero or when the sloping bottom is set to zero. The expression for the excess momentum fluxes is set to zero, i.e.:

$$\begin{aligned} R_x = -\frac{1}{\rho}\frac{\partial}{\partial x}\int_{-h}^{\eta} p dz - \frac{1}{\rho}\frac{\partial}{\partial x}\left(\frac{1}{2}\rho g(\eta+h)^2\right) + \frac{\partial}{\partial x}\int_{-h}^{\eta}\left(\nu_t\frac{\partial u}{\partial x}\right)dz \\ + \frac{\partial}{\partial y}\int_{-h}^{\eta}\left(\nu_t\frac{\partial u}{\partial y}\right)dz = 0. \quad \text{(C.2.20)} \end{aligned}$$

Therefore, the final 2D depth-averaged momentum equation in the x-direction reads

$$\frac{\partial \widehat{u}}{\partial t} + \frac{\partial \widehat{u}\widehat{u}}{\partial x} + \frac{\partial \widehat{u}\widehat{v}}{\partial y} - f\widehat{v} = -g\frac{\partial \eta}{\partial x} + \frac{\tau_{xw} - \tau_{xb}}{\rho H}. \quad \text{(C.2.21)}$$

Stellenbosch University https://scholar.sun.ac.za

Similarly, depth-averaging of the y-direction momentum equation (3.4.17) yields

$$\frac{\partial \widehat{v}}{\partial t} + \frac{\partial \widehat{v}\widehat{u}}{\partial x} + \frac{\partial \widehat{v}\widehat{v}}{\partial y} + f\widehat{u} = -g\frac{\partial \eta}{\partial y} + \frac{\tau_{yw} - \tau_{yb}}{\rho H}. \tag{C.2.22}$$

These equations are similar to the shallow water equations applicable in coastal modelling studied by (Navon, 2014).

Stellenbosch University https://scholar.sun.ac.za

Appendix D

Modelling dynamics discussed in this study

D.1 Forcing mechanism

The role of primary forces (e.g. gravitation, pressure differences and viscous forces) is to cause the motion. The wind forcing causes various effects, such as wave generation, wave breaking due to wave momentum passed onto the drift current, wave field reaction to determine the effective roughness of the sea surface, etc. (LeBlond & Mysak, 1978; Dingemans, 1997a; Bowden, 1983). The shear stress exerted by the blowing wind is communicated to the fluid below the surface, into the water column and the fluid as a whole as shown in Figure D.1, which represents the Ekman's layers dynamics. Basically, the sea surface moves with each successive layer below it in the water column. Each layer moves with a reduced speed compared to the sea surface. This movement is caused by the friction (i.e. due to coupling of wind and the sea surface) between the layers, determined by the force due to viscous stress. In which case, the eddy viscosity ν_t measures the fluid's resistance in each layer. Given that the force due to viscous stress is linked to the turbulent stress, i.e.:

$$-\overline{(\mathbf{v}'\mathbf{v}')} = \nu_t \nabla \overline{\mathbf{v}}, \tag{D.1.1}$$

formally introduced in Appendix C. According to Gill (1982) the principal driving mechanism and most general dominant forcing of the ocean is wind, this notion is justified by comparing wind effects with other effect in an ocean of constant depth. The wind stress only enters the fluid at $O(0.1)$ (Vallis, 2006). This may produce changes in water level of order $O(0.1$ m) and currents of order $O(0.1$ m/s) (Gill & Schumann, 1974; Gill, 1982; LeBlond & Mysak, 1978; Pedlosky, 1987; Pond & Pickard, 1978). Gill & Schumann (1974) suggested that, at typical scales of about five days, coastal and shelf waves will be generated by cyclones or anticyclones passed over the coastal and shelf regions, particularly in the mid-latitudes. The wind stress on the sea surface is approximately proportional to the wind speed squared (Pond & Pickard, 1978).

Stellenbosch University https://scholar.sun.ac.za

The dragging and drifting by the wind stress to the currents communicated through the water column, as a result penetrates down to the sea-sediment interface.

These dynamics represented in Ekman's spiral in Figure D.1. The reaction

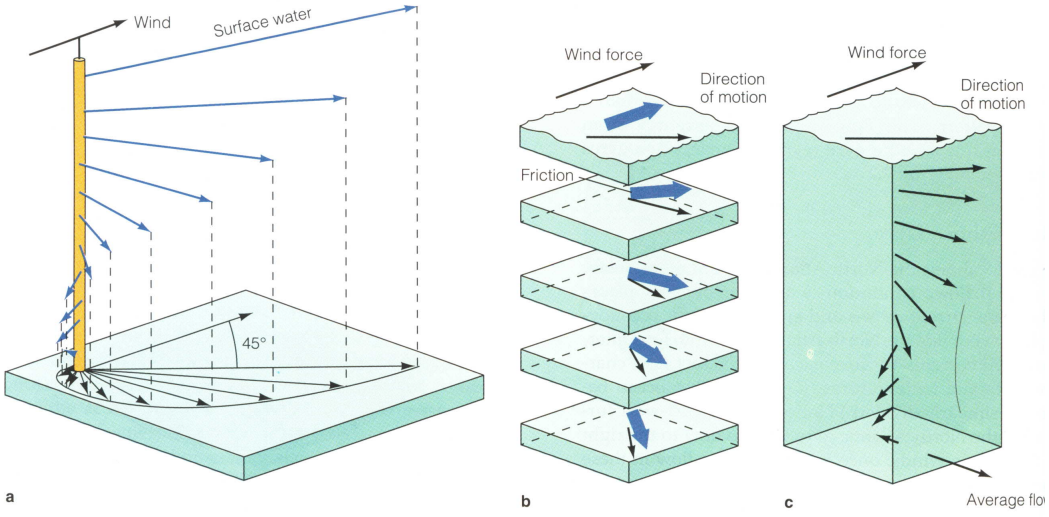

Figure D.1: Forcing mechanism due to wind stress and wind generated set-up, flow set-up and motion (Garrison, 1993; Figure 9.5) as in Oceanography (2014).

to wind also, cause water to pile up against the pressure gradient in the direction the wind is blowing. In which case, the force due to gravity tends to pull the water down and the pressure gradient may become proportional to the water level gradient. As a response to the flow, secondary forces, e.g. Coriolis force cause deflection of the current. As a result water tends to pile up toward the coast or offshore, depending on the direction the wind is blowing. The importance of the Coriolis forcing is determined by the Rossby number Ro, introduced later in Appendix E.

Note that this appendix does not attempt to describe how the forces balance in the fluid, rather what the force does to the fluid. Both wind driving and the effects due to density changes are important for the overall flow. For the purpose of this study only wind-driven flow shall be discussed without differential density driving. The main focus is water level set-up, under the flow dynamics summarised in Figure D.2, particularly on the boundaries.

Stellenbosch University https://scholar.sun.ac.za

D.2 Water level set-up

The motion of sea water is driven by different forces which are dependent on a number of environmental factors. For example, a passage of weather systems over coastal and shelf seas induce changes in currents and water level set-up, both by variation in surface pressure and the action of associated wind stress (Gill & Schumann, 1974). The movement of sea water leads to numerous discrepancies, e.g. density differences in the ocean, sea level rise, etc. The dynamics due to wind shear stress give rise to currents. Currents may be referred to according to their forcing mechanism, i.e. thermohaline (driven by salinity and temperature) or wind-driven. Understanding the dynamics and the fluid flow is key to modelling the discrepancies in the ocean. Figure D.2 summarizes the flow dynamics of wind set-up. In which case, the Ekman depth is much larger than the water balancing the free surface set-up in the direction of the wind against the bottom roughness thus generating a bottom return flow.

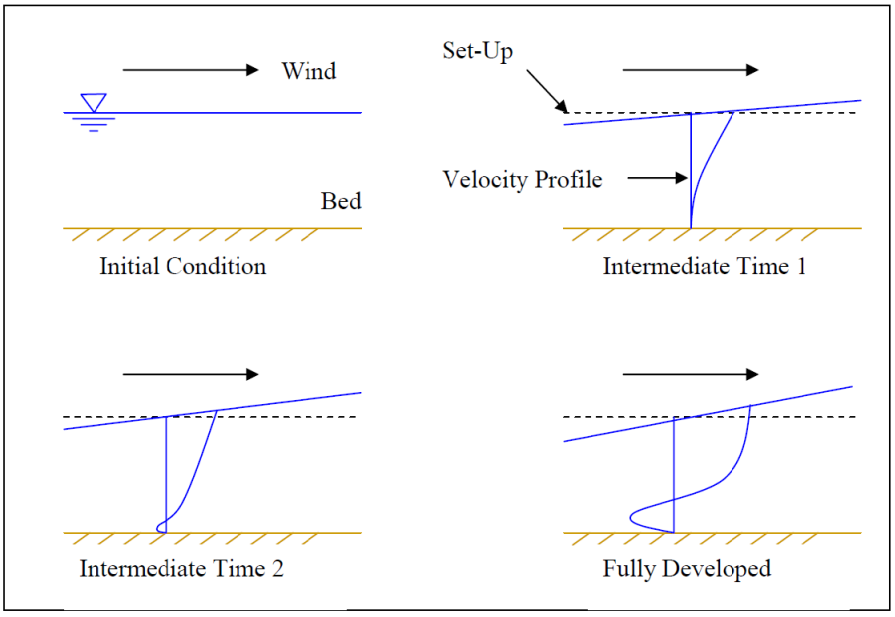

Figure D.2: Developing flow dynamics and set-up.

Stellenbosch University https://scholar.sun.ac.za

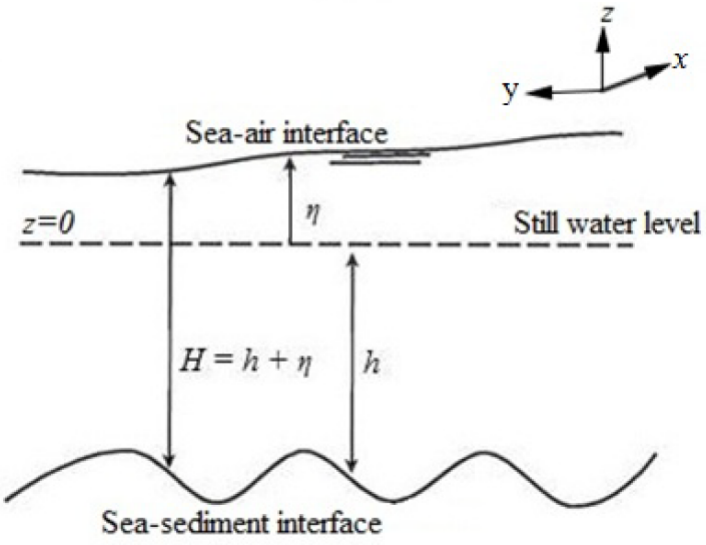

Figure D.3: Mean water level, bottom depth, set-up and the reference frame.

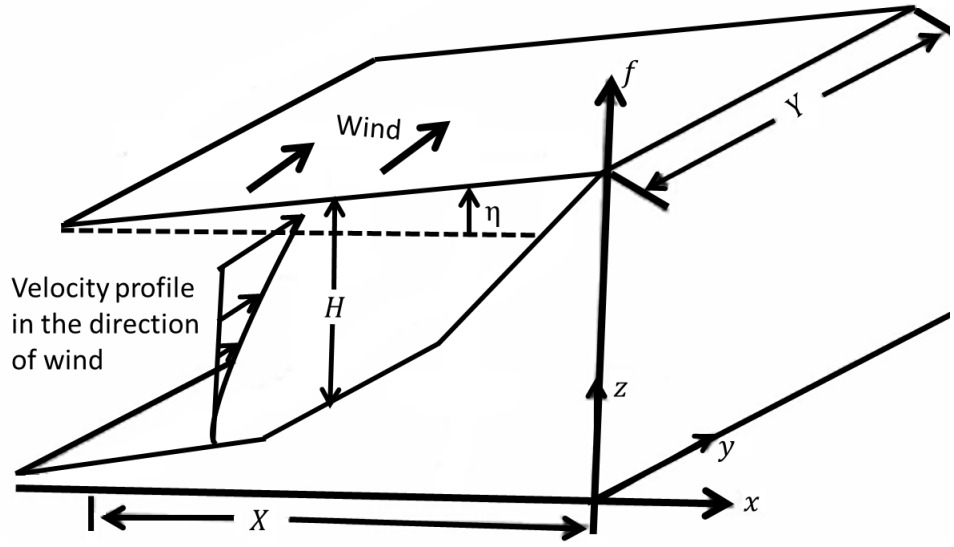

Figure D.4: Mean water level, bottom depth, set-up and the reference frame of the 2-dimensional geostrophic balanced flow.

The details are shown in Figure D.3. Figure D.3 represents a typical ocean model which constitutes the free surface, the bottom topography and the interior ocean water. The information in Figure D.3 is described based on the primary and secondary forces described in Chapter 2.

Stellenbosch University https://scholar.sun.ac.za

An effective tangential stress exerted on the sea surface (as in Figure D.4) causes wind set-up and the sea surface layer to move. As the wind blows on the surface, it pushes the water and Coriolis arising from these currents tilts the sea surface. Surface tilt means a change in water level and leads to sea level elevation (Figures D.3 and D.4), a change from still water depth.

Stellenbosch University https://scholar.sun.ac.za

D.3 Model geometry

In shallow water a destabilization problem may occur as $H \to 0$ towards the coast (Stelling, 1983). The source being the bottom friction term, defined as

$$\boldsymbol{\tau}_b = (\tau_{xb}, \tau_{yb}). \tag{D.3.1}$$

Basically, when $H \to 0$ the boundary condition applied at the coast is simply that there is no cross-shelf volume transport at the coast, i.e.:

$$H(0)u = 0, \tag{D.3.2}$$

where u is the cross-shore velocity and $H(0)$ is the depth at the coast. To

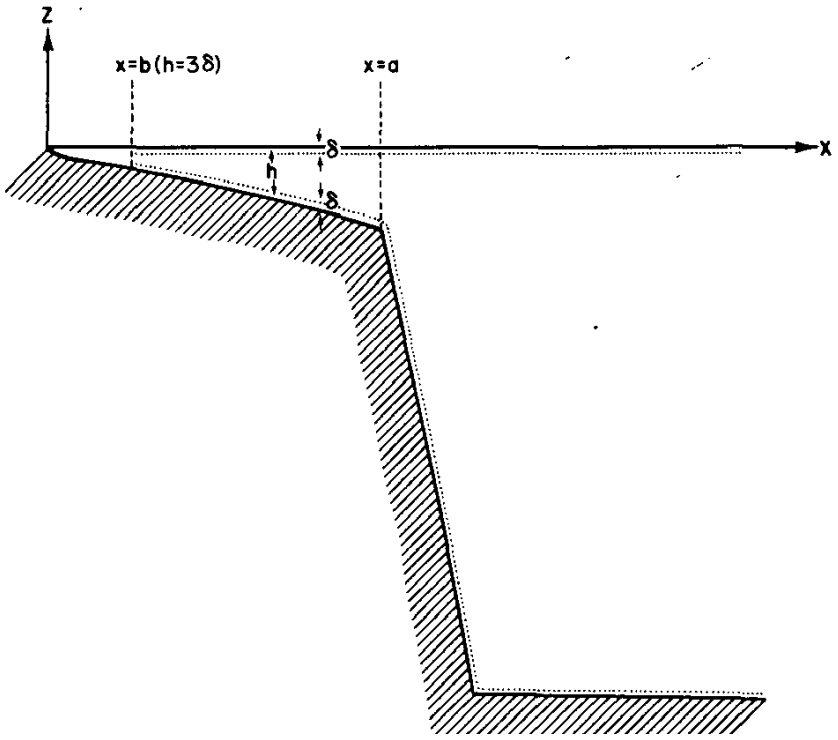

Figure D.5: Cross-section of the model geometry as in Clarke & Brink (1985), showing the location of the axes and the meaning of various quantities in the text. In the figure δ represents the scale thickness of the surface (top and bottom) Ekman layers.

overcome this problem, Clarke & Brink (1985) designed the model domain such that the coastal boundary may be located at a small distance b offshore, i.e.:

$$H(b)u = 0. \tag{D.3.3}$$

Stellenbosch University https://scholar.sun.ac.za

Figure D.5 represents the model domain designed such that problems due to $H \to 0$ may be ommitted. A coastal wall is essentially assumed at $H(b)$ to be three times the scale thickness δ of the turbulent (Ekman's) boundary layer (Clarke & Brink, 1985; Van Ballegooyen, 1995). This will allow an exclusion of the highly turbulent inner shelf (Van Ballegooyen, 1995).

Stellenbosch University https://scholar.sun.ac.za

Appendix E

Scaling of the 2D shallow water equations

Firstly, the scales that are used for scaling and non-dimensionalization of the equations are introduced. Table E.1 is a summary of the scales that are used in this appendix. The 2D shallow water equations can be non-dimensionalised as follows

$$\frac{\partial \eta^*}{\partial t^*}\left[\frac{\eta'}{t_\tau}\right] + \frac{\partial (H^* u^*)}{\partial x^*}\left[\frac{H_z U}{X}\right] + \frac{\partial (H^* v^*)}{\partial y^*}\left[\frac{H_z V}{Y}\right] = 0 \tag{E.0.1}$$

$$\begin{aligned}\frac{\partial u^*}{\partial t^*}\left[\frac{U}{t_\tau}\right] + \frac{\partial (u^* u^*)}{\partial x^*}\left[\frac{UU}{X}\right] + \frac{\partial (v^* u^*)}{\partial y^*}\left[\frac{UV}{Y}\right] - v^*\left[fV\right] = \\ -\frac{\partial \eta^*}{\partial x^*}\left[g\frac{\eta'}{X}\right] + \frac{\tau^*_{wx}}{H^*}\left[\frac{\tau'_{xw}}{H_z}\right] - \frac{\tau^*_{bx}}{H^*}\left[\frac{\tau'_{xb}}{H_z}\right]\end{aligned} \tag{E.0.2}$$

$$\begin{aligned}\frac{\partial v^*}{\partial t^*}\left[\frac{V}{t_\tau}\right] + \frac{\partial (v^* u^*)}{\partial x^*}\left[\frac{UV}{X}\right] + \frac{\partial (v^* v^*)}{\partial y^*}\left[\frac{VV}{Y}\right] + u^*\left[fU\right] = \\ -\frac{\partial \eta^*}{\partial y^*}\left[g\frac{\eta'}{Y}\right] + \frac{\tau^*_{wy}}{H^*}\left[\frac{\tau'_{yw}}{H_z}\right] - \frac{\tau^*_{by}}{H^*}\left[\frac{\tau'_{yb}}{H_z}\right].\end{aligned} \tag{E.0.3}$$

In the next section, these equations are simplified based on scaling.

E.1 Some scaling assumptions

Following Pedlosky (1987), the scale for water level change from still water depth may be determined from the geostrophic balance. According to LeBlond

Stellenbosch University https://scholar.sun.ac.za

Table E.1: Basic scales and dimensionless variables related to those defined in Table 5.1.

Scale	Dimensionless variables	Dimensions
Water level scale η'	$\eta^* = \frac{\eta}{\eta'}$	$\eta' \approx 10^{-1}$ to 1 m
Length scales cross-shore, alongshore and vertical (X, Y, H_z)	$x^* = \frac{x}{X}, y^* = \frac{y}{Y}, z^* = \frac{z}{H_z}$	$X \approx 10$ to 10^2 m, $Y \approx 10^2$ to 10^3 m, $H_z \approx 10$ to 10^4 m
Velocity scales cross-shore, alongshore and vertical (U, V, W)	$u^* = \frac{u}{U}, v^* = \frac{v}{V}, w^* = \frac{w}{W}$	$U \approx 10^{-2}$ to 10^{-1} m/s, $V \approx 10^{-1}$ to 1 m/s, $W \approx 10^{-4}$ m/s
Variations in bottom topography scales cross-shore and alongshore (X_h, Y_h)	$x^* = \frac{x}{X_h}, y^* = \frac{y}{Y_h}$	$X_h \approx \lvert X_h \rvert$ m, $Y_h \approx \lvert Y_h \rvert$ m
Time scales (t_τ, f)	$t^* = \frac{t}{(1/f)}, t^* = \frac{t}{t_\tau}$	10^0 to 10^6 s
Wind stress scales cross-shore and alongshore (τ'_{xw}, τ'_{yw})	$\tau^*_{xw} = \frac{\tau_{xw}}{\tau'_{xw}}, \tau^*_{yw} = \frac{\tau_{yw}}{\tau'_{yw}}$	
Bottom friction scales cross-shore and alongshore (τ'_{xb}, τ'_{yb})	$\tau^*_{xb} = \frac{\tau_{xb}}{\tau'_{xb}}, \tau^*_{yb} = \frac{\tau_{yb}}{\tau'_{yb}}$	

Stellenbosch University https://scholar.sun.ac.za

& Mysak (1978), geostrophic balance may be obtained at very low-frequency. Written in a scaled form the geostrophic balance read

$$-v^* \left[fV\right] = -\frac{\partial \eta^*}{\partial x^*} \left[g\frac{\eta'}{X}\right], \tag{E.1.1}$$

$$u^* \left[fU\right] = -\frac{\partial \eta^*}{\partial y^*} \left[g\frac{\eta'}{Y}\right], \tag{E.1.2}$$

and when rearranged to give

$$-v^* = -\frac{\partial \eta^*}{\partial x^*} \quad ; \quad \eta' = \left[\frac{fVX}{g}\right], \tag{E.1.3}$$

$$u^* = -\frac{\partial \eta^*}{\partial y^*} \quad ; \quad \eta' = \left[\frac{fVY}{g}\right], \tag{E.1.4}$$

the terms of order one and the scales for water level change alongshore and cross-shore. According to Pedlosky (1987), the geostrophic balance is necessary for the cross-shore and alongshore velocities to be different from zero. This assumption have been made in the study by Van Ballegooyen (1995), whereby only the cross-shore water level scale have been used and was not mentioned explicitly.

For the purpose of this study the scales for the wind and bottom shear stress assume the generic dynamic patterns presented in Figure E.1. According to the patterns, (a.) represents the case where alongshore scale is much greater than the cross-shore scale, (b.) represents same alongshore and cross-shore scale and (c.) represents the alongshore scale much smaller than the cross-shore scale, for the wind and bottom shear stress. Pattern (a.) may be considered a primary response, whereas patterns (b.) and (c.) is aimed for violations of the dynamics. Corresponding to the patterns is the conversion of the variables in Table E.2. Table E.2 is only limited to changes due to wind and bottom shear stress, because flow patterns may be difficult to understand particularly when $U = V$ for the flow cross-shore and alongshore dynamics and cannot be distinguished.

Following the work done by Van Ballegooyen (1995), for simplicity a small parameter $\zeta \approx 10^{-1}$ is introduced such that, any combination of scales can be written as

$$ft_\tau \approx \zeta^{-1}; \; \frac{X}{Y} \approx \zeta \; ; \; \frac{U}{V} \approx \zeta \quad \text{and} \quad \frac{U}{fX} \approx \frac{V}{fX} \approx \zeta^2. \tag{E.1.5}$$

For the purpose of this study a limitation on the wind and bottom shear stress relationship requires that the relative friction factor to be approximated to unit, in order to allow strong relationship in the shear stresses. In which case the relationship is forced to have both wind and bottom stress to be the same for the particular direction (i.e. alongshore or cross-shore).

Stellenbosch University https://scholar.sun.ac.za

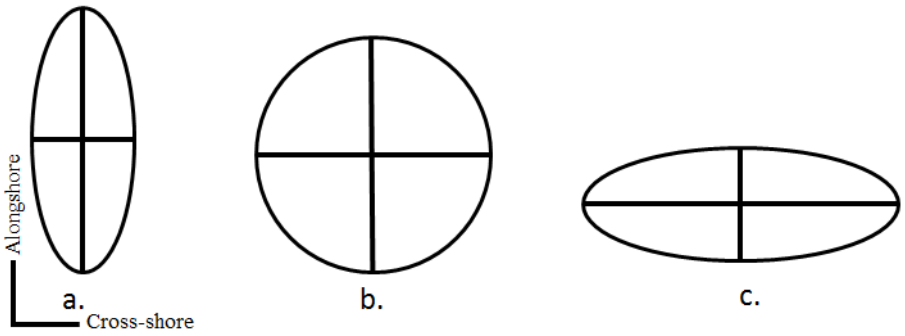

Figure E.1: Generic patterns of flow and for changes in wind and bottom shear stress.

Table E.2: Conversion associated with Figure E.1 for wind and bottom stress patterns only.

Pattern a.	Pattern b.	Pattern c.
$(\tau'_{xw}, \tau'_{xb}) \ll (\tau'_{yw}, \tau'_{yb})$ and allow for the flow $U = \frac{X}{Y}V$	$(\tau'_{xw}, \tau'_{xb}) \sim (\tau'_{yw}, \tau'_{yb})$ and allow for the shear stresses $U = V$	$(\tau'_{xw}, \tau'_{xb}) \gg (\tau'_{yw}, \tau'_{yb})$ and allow for the flow $U = \frac{1}{\left(\frac{X}{Y}\right)}V$

E.2 Scaling based on pattern (a.) of Figure E.1

Scaling of the cross-shore equation

The cross-shore **i**-direction scaled momentum equation with the water level scale substituted, read

$$\frac{\partial u^*}{\partial t^*}\left[\frac{U}{t_\tau}\right] + \frac{\partial (u^*u^*)}{\partial x^*}\left[\frac{UU}{X}\right] + \frac{\partial (v^*u^*)}{\partial y^*}\left[\frac{UV}{Y}\right] - v^*\left[fV\right] = -\frac{\partial \eta^*}{\partial x^*}\left[fV\right] + \frac{\tau^*_{wx}}{H^*}\left[\frac{\tau'_{xw}}{H_z}\right] - \frac{\tau^*_{bx}}{H^*}\left[\frac{\tau'_{xb}}{H_z}\right]. \quad \text{(E.2.1)}$$

Stellenbosch University https://scholar.sun.ac.za

The wind and bottom shear stress scales defined according to pattern (a.) in Figure E.1 may be written as

$$\tau'_{xw} = fH_zU \quad \text{and} \quad \tau'_{xb} = fH_zU. \tag{E.2.2}$$

In which case, the scaled cross-shore equation becomes

$$\frac{\partial u^*}{\partial t^*}\left[\frac{U}{t_\tau}\right] + \frac{\partial (u^*u^*)}{\partial x^*}\left[\frac{UU}{X}\right] + \frac{\partial (v^*u^*)}{\partial y^*}\left[\frac{UV}{Y}\right] - v^*\left[fV\right] = -\frac{\partial \eta^*}{\partial x^*}\left[fV\right] + \frac{\tau^*_{wx}}{H^*}\left[fU\right] - \frac{\tau^*_{bx}}{H^*}\left[fU\right]. \tag{E.2.3}$$

Applying the velocity conversion in Table E.2, i.e. $U = \frac{X}{Y}V$, yields

$$\frac{\partial u^*}{\partial t^*}\left[\frac{\frac{X}{Y}V}{t_\tau}\right] + \frac{\partial (u^*u^*)}{\partial x^*}\left[\frac{\left(\frac{X}{Y}V\right)^2}{X}\right] + \frac{\partial (v^*u^*)}{\partial y^*}\left[\frac{\frac{X}{Y}VV}{Y}\right] - v^*\left[fV\right] = -\frac{\partial \eta^*}{\partial x^*}\left[fV\right] + \frac{\tau^*_{wx}}{H^*}\left[f\frac{X}{Y}V\right] - \frac{\tau^*_{bx}}{H^*}\left[f\frac{X}{Y}V\right], \tag{E.2.4}$$

and when the scales are rearranged this equation may be written as

$$\frac{\partial u^*}{\partial t^*}\left[\frac{1}{ft_\tau}\frac{X}{Y}\right] + \frac{\partial (u^*u^*)}{\partial x^*}\left[\frac{V}{fX}\left(\frac{X}{Y}\right)^2\right] + \frac{\partial (v^*u^*)}{\partial y^*}\left[\frac{V}{fX}\left(\frac{X}{Y}\right)^2\right] - v^*\left[1\right] = -\frac{\partial \eta^*}{\partial x^*}\left[1\right] + \frac{\tau^*_{wx}}{H^*}\left[\frac{X}{Y}\right] - \frac{\tau^*_{bx}}{H^*}\left[\frac{X}{Y}\right] \tag{E.2.5}$$

The simplifications in equation (E.1.5) applied leads to a balanced reduced equation, i.e.:

$$-v^*\left[1\right] = -\frac{\partial \eta^*}{\partial x^*}\left[1\right], \tag{E.2.6}$$

the cross-shore geostrophic balance. This is the reduced form of the cross-shore equation, which represents the first order response.

Scaling of the alongshore equation

Similarly, the alongshore **j**-direction scaled momentum equation may be reduced. Without repeating the simplifications already presented, applying the alongshore water level scale (i.e. equation E.1.4), the wind and bottom shear stress scales defined as follows

$$\tau'_{yw} = fH_zV \quad \text{and} \quad \tau'_{yb} = fH_zV, \tag{E.2.7}$$

Stellenbosch University https://scholar.sun.ac.za

and the velocity conversion in Table E.2, i.e. $U = \frac{X}{Y}V$, yields

$$\frac{\partial v^*}{\partial t^*}\left[\frac{1}{ft_\tau}\frac{1}{\left(\frac{X}{Y}\right)}\right] + \frac{\partial (v^*u^*)}{\partial x^*}\left[\frac{V}{fX}\right] + \frac{\partial (v^*v^*)}{\partial y^*}\left[\frac{V}{fX}\right] + u^*\left[1\right] = -\frac{\partial \eta^*}{\partial y^*}\left[1\right] + \frac{\tau^*_{wy}}{H^*}\left[\frac{1}{\left(\frac{X}{Y}\right)}\right] - \frac{\tau^*_{by}}{H^*}\left[\frac{1}{\left(\frac{X}{Y}\right)}\right]. \quad \text{(E.2.8)}$$

Therefore, applying the scaling parameters in equation (E.1.5) leads to a balanced first order response reduced equation, i.e.:

$$\frac{\partial v^*}{\partial t^*}\left[1\right] + u^*\left[1\right] = -\frac{\partial \eta^*}{\partial y^*}\left[1\right]. \quad \text{(E.2.9)}$$

The scaling based on pattern (a.) resulted in equations (E.2.6) and (E.2.9) as the reduced hydrodynamic equations.

E.3 Scaling based on pattern (b.) of Figure E.1

For pattern (b.) the wind and the bottom shear stress may be defined as

$$\tau'_{xw} = \tau'_{yw} = \tau'_{xb} = \tau'_{yb} = fH_zU \quad \text{or} \quad = fH_zV. \quad \text{(E.3.1)}$$

Note that a choice of fH_zV may lead to additional friction terms cross-shore, whereas alongshore friction terms may be negligible, and vice versa for a choice of fH_zU. This only hold when $U \neq V$ for the flow, assuming the flow dynamics may be complicated when $U = V$.

Scaling of the cross-shore equation

For wind and bottom stress scales defined as fH_zU the scaled cross-shore equation may be written as

$$\frac{\partial u^*}{\partial t^*}\left[\frac{U}{t_\tau}\right] + \frac{\partial (u^*u^*)}{\partial x^*}\left[\frac{UU}{X}\right] + \frac{\partial (v^*u^*)}{\partial y^*}\left[\frac{UV}{Y}\right] - v^*\left[fV\right] = -\frac{\partial \eta^*}{\partial x^*}\left[fV\right] + \frac{\tau^*_{wx}}{H^*}\left[fU\right] - \frac{\tau^*_{bx}}{H^*}\left[fU\right], \quad \text{(E.3.2)}$$

and simplified to give

$$\frac{\partial u^*}{\partial t^*}\left[\frac{1}{ft_\tau}\frac{U}{V}\right] + \frac{\partial (u^*u^*)}{\partial x^*}\left[\frac{U}{fX}\frac{U}{V}\right] + \frac{\partial (v^*u^*)}{\partial y^*}\left[\frac{U}{fX}\frac{X}{Y}\right] - v^*\left[1\right] = -\frac{\partial \eta^*}{\partial x^*}\left[1\right] + \frac{\tau^*_{wx}}{H^*}\left[\frac{U}{V}\right] - \frac{\tau^*_{bx}}{H^*}\left[\frac{U}{V}\right]. \quad \text{(E.3.3)}$$

Stellenbosch University https://scholar.sun.ac.za

In which case, the scaling parameters in equation (E.1.5) leads to a reduced hydrodynamic cross-shore equation expressed as

$$-v^*\left[1\right] = -\frac{\partial \eta^*}{\partial x^*}\left[1\right]. \tag{E.3.4}$$

Alternatively, for wind and bottom stress scales defined as fH_zV the scaled cross-shore equation may be written as

$$\frac{\partial u^*}{\partial t^*}\left[\frac{U}{t_\tau}\right] + \frac{\partial (u^*u^*)}{\partial x^*}\left[\frac{UU}{X}\right] + \frac{\partial (v^*u^*)}{\partial y^*}\left[\frac{UV}{Y}\right] - v^*\left[fV\right] = -\frac{\partial \eta^*}{\partial x^*}\left[fV\right] + \frac{\tau^*_{wx}}{H^*}\left[fV\right] - \frac{\tau^*_{bx}}{H^*}\left[fV\right], \tag{E.3.5}$$

and simplified to give

$$\frac{\partial u^*}{\partial t^*}\left[\frac{1}{ft_\tau}\frac{U}{V}\right] + \frac{\partial (u^*u^*)}{\partial x^*}\left[\frac{U}{fX}\frac{U}{V}\right] + \frac{\partial (v^*u^*)}{\partial y^*}\left[\frac{U}{fX}\frac{X}{Y}\right] - v^*\left[1\right] = -\frac{\partial \eta^*}{\partial x^*}\left[1\right] + \frac{\tau^*_{wx}}{H^*}\left[1\right] - \frac{\tau^*_{bx}}{H^*}\left[1\right],$$

hence with the scaling parameters in equation (E.1.5) applied yields

$$-v^*\left[1\right] = -\frac{\partial \eta^*}{\partial x^*}\left[1\right] + \frac{\tau^*_{wx}}{H^*}\left[1\right] - \frac{\tau^*_{bx}}{H^*}\left[1\right]. \tag{E.3.6}$$

The additional shear stress terms in this equation allows this equation to differ from equation (E.3.4). In which case, the cross-shore dynamics depart from geostrophic balance if the wind and bottom stress scales are defined as fH_zV.

Scaling of the alongshore equation

Again, for wind and bottom stress scales defined as fH_zU the alongshore equation may be written in simplified form as

$$\frac{\partial v^*}{\partial t^*}\left[\frac{1}{ft_\tau}\frac{1}{\left(\frac{U}{V}\right)}\right] + \frac{\partial (v^*u^*)}{\partial x^*}\left[\frac{V}{fX}\right] + \frac{\partial (v^*v^*)}{\partial y^*}\left[\frac{V}{fX}\frac{1}{\left(\frac{U}{V}\right)}\frac{X}{Y}\right] + u^*\left[1\right] = -\frac{\partial \eta^*}{\partial y^*}\left[1\right] + \frac{\tau^*_{wy}}{H^*}\left[1\right] - \frac{\tau^*_{by}}{H^*}\left[1\right]. \tag{E.3.7}$$

Therefore, applying the scaling parameters in equation (E.1.5) leads to a balanced first order response reduced equation, i.e.:

$$\frac{\partial v^*}{\partial t^*}\left[1\right] + u^*\left[1\right] = -\frac{\partial \eta^*}{\partial y^*}\left[1\right] + \frac{\tau^*_{wy}}{H^*}\left[1\right] - \frac{\tau^*_{by}}{H^*}\left[1\right]. \tag{E.3.8}$$

Stellenbosch University https://scholar.sun.ac.za

Similarly, if wind and bottom stress scales is defined as fH_zV the alongshore equation may be written in simplified form as

$$\frac{\partial v^*}{\partial t^*}\left[\frac{1}{ft_\tau}\frac{1}{\left(\frac{U}{V}\right)}\right]+\frac{\partial(v^*u^*)}{\partial x^*}\left[\frac{V}{fX}\right]+\frac{\partial(v^*v^*)}{\partial y^*}\left[\frac{V}{fX}\frac{1}{\left(\frac{U}{V}\right)}\frac{X}{Y}\right]+$$
$$u^*\left[1\right]=-\frac{\partial\eta^*}{\partial y^*}\left[1\right]+\frac{\tau^*_{wy}}{H^*}\left[\frac{1}{\left(\frac{U}{V}\right)}\right]-\frac{\tau^*_{by}}{H^*}\left[\frac{1}{\left(\frac{U}{V}\right)}\right], \qquad \text{(E.3.9)}$$

and when the scaling parameters in equation (E.1.5) is applied, a first order response reduced equation is obtained, i.e.:

$$\frac{\partial v^*}{\partial t^*}\left[1\right]+u^*\left[1\right]=-\frac{\partial\eta^*}{\partial y^*}\left[1\right]. \qquad \text{(E.3.10)}$$

In conclusion the scaling based on pattern (b.) is that, the first order response reduced hydrodynamic equations are represented by equations (E.3.4) and (E.3.8) if the scales for shear stresses is fH_zU and for the scale of fH_zV the reduced hydrodynamic equations are represented by equations (E.3.6) and (E.3.10). The equations that describe *Tilt* can only partially be justified when the scale for wind or bottom shear stress is fH_zV for cross-shore and fH_zU for alongshore. This may result to equations (E.3.6) and (E.3.8), and this equations are partially similar to *Tilt* equations. Based on pattern (a.) similar equations may be obtained when the scale for wind or bottom shear stress is fH_zV for cross-shore and fH_zU for alongshore. For the purpose of presenting *Tilt* cross-shore equation the role of the relative friction factor must be taken in to account and may not be equal to one, as the wind and bottom stresses are different.

E.4 Scaling based on pattern (c.) of Figure E.1

Pattern (c.) of Figure E.1 represents the dynamics where cross-shore wind and bottom stress scales defined as fH_zU are much larger compared to the alongshore wind and bottom stress scales defined as fH_zV. In which case, the conversion of the flow velocity in Table E.2 may be applied.

Stellenbosch University https://scholar.sun.ac.za

Scaling of the cross-shore equation

Scaling the cross-shore equation and applying the conversion of the flow velocity, the equation can be simplified to give

$$\frac{\partial u^*}{\partial t^*}\left[\frac{1}{ft_\tau}\frac{1}{\left(\frac{X}{Y}\right)}\right]+\frac{\partial(u^*u^*)}{\partial x^*}\left[\frac{V}{fX}\frac{1}{\left(\frac{X}{Y}\right)^2}\right]+\frac{\partial(u^*v^*)}{\partial y^*}\left[\frac{V}{fX}\right]-v^*\left[1\right]= -\frac{\partial \eta^*}{\partial x^*}\left[1\right]+\frac{\tau^*_{wx}}{H^*}\left[\frac{1}{\left(\frac{X}{Y}\right)}\right]-\frac{\tau^*_{bx}}{H^*}\left[\frac{1}{\left(\frac{X}{Y}\right)}\right].$$

Applying the scaling parameters in equation (E.1.5) leads to a reduced hydrodynamic equation, i.e.:

$$\frac{\partial u^*}{\partial t^*}\left[1\right]+\frac{\partial(u^*u^*)}{\partial x^*}\left[1\right]-v^*\left[1\right]=-\frac{\partial \eta^*}{\partial x^*}\left[1\right], \tag{E.4.1}$$

a first order response.

Scaling of the alongshore equation

Similarly, scaling the alongshore equation and applying the conversion of the flow velocity, the equation can be simplified to give

$$\frac{\partial v^*}{\partial t^*}\left[\frac{1}{ft_\tau}\frac{X}{Y}\right]+\frac{\partial(v^*u^*)}{\partial x^*}\left[\frac{V}{fX}\frac{X}{Y}\right]+\frac{\partial(v^*v^*)}{\partial y^*}\left[\frac{V}{fX}\left(\frac{X}{Y}\right)^2\right]+u^*\left[1\right]= -\frac{\partial \eta^*}{\partial y^*}\left[1\right]+\frac{\tau^*_{wy}}{H^*}\left[\frac{X}{Y}\right]-\frac{\tau^*_{by}}{H^*}\left[\frac{X}{Y}\right].$$

Therefore, applying the scaling parameters in equation (E.1.5) this equation reduces to a first order response equation, i.e.:

$$u^*\left[1\right]=-\frac{\partial \eta^*}{\partial y^*}\left[1\right], \tag{E.4.2}$$

the geostrophic balance alongshore.

E.5 Scaling of the continuity equation

One of the major aim for this study is to investigate a change in sea level due to wind set-up and the sea surface layer movement. In particular, water level set-up or tilt is investigated. Upon scaling the continuity equation a divergence parameter may be defined as

$$\begin{aligned}\epsilon^2 &= \frac{f^2X^2}{gH_z}\\ &= \frac{X^2/(1/f)^2}{gH_z}\end{aligned} \tag{E.5.1}$$

Stellenbosch University https://scholar.sun.ac.za

where $X^2/(1/f)^2$ (i.e. typical horizontal current speed) and gH_z is the scale for wave speed (LeBlond & Mysak, 1978; Gill, 1982; Van Ballegooyen, 1995). This parameter measures the changes in sea level from the still water depth.

According to LeBlond & Mysak (1978), mostly in shallow water and/or for long waves or coastal trapped wave motion the divergence parameter is much smaller to the order of $O(10^{-3})$ to $O(1)$. For the purpose of this study it may be difficult to quantify the value of the divergence parameter. Based on *Tilt* equations the continuity equation is not solved, rather a change in water level is considered as a consequence of flow. The latter requires a balanced inflow and outflow. In the work done by Van Ballegooyen (1995), the divergence parameter have been neglected by assuming a rigid lid condition, basically no change in water level at the free surface. The scaling of the continuity equation is done for both without topographic control and with topographic control.

Scaling without topographic control

To express the scaled continuity equation (E.0.1) in terms of the divergence parameter, particularly the first term of equation (E.0.1). The cross-shore scale for water level (i.e. equation (E.1.3)) and a unity multipler, an expression of the water depth scale is used. In which case, equation (E.0.1) can be expressed as

$$\frac{\partial \eta^*}{\partial t^*}\left[\frac{fVXH_z}{gt_\tau H_z}\right] + \frac{\partial (H^* u^*)}{\partial x^*}\left[\frac{H_z U}{X}\right] + \frac{\partial (H^* v^*)}{\partial y^*}\left[\frac{H_z V}{Y}\right] = 0. \tag{E.5.2}$$

Note that the scaling of the first term can be expressed as

$$\left[\frac{fVXH_z}{gt_\tau H_z}\right] = \left[\frac{(fX)^2}{gH_z}\frac{1}{ft_\tau}\frac{VH_z}{X}\right] \tag{E.5.3}$$

and when substituted to equation (E.0.1) and rearranged to give

$$\frac{\partial \eta^*}{\partial t^*}\left[\frac{(fX)^2}{gH_z}\right] + \frac{\partial (H^* u^*)}{\partial x^*}\left[ft_\tau \frac{U}{V}\right] + \frac{\partial (H^* v^*)}{\partial y^*}\left[ft_\tau \frac{X}{Y}\right] = 0. \tag{E.5.4}$$

It is discussed that topographic effects are important, then the next section presents the scaling of the continuity equation with topographic effects.

Scaling with topographic control

The scales for the continuity equation may be expanded to include spatial scale of variations in topography, i.e.:

$$\frac{\partial \eta^*}{\partial t^*}\left[\frac{\eta'}{t_\tau}\right] + H^* \frac{\partial u^*}{\partial x^*}\left[H_z \frac{U}{X}\right] + u^* \frac{\partial H^*}{\partial x_h^*}\left[U \frac{H_z}{X_h}\right] + H^* \frac{\partial v^*}{\partial y^*}\left[H_z \frac{V}{Y}\right] + v^* \frac{\partial H^*}{\partial y_h^*}\left[V \frac{H_z}{Y_h}\right] = 0. \tag{E.5.5}$$

Stellenbosch University https://scholar.sun.ac.za

Therefore, applying the water level scale in equation (E.5.3) and rearranging this equation yields

$$\frac{\partial \eta^*}{\partial t^*}\left[\frac{(fX)^2}{gH_z}\right] + H^*\frac{\partial u^*}{\partial x^*}\left[ft_\tau\frac{U}{V}\right] + u^*\frac{\partial H^*}{\partial x_h^*}\left[ft_\tau\frac{U}{V}\frac{X}{X_h}\right] + H^*\frac{\partial v^*}{\partial y^*}\left[ft_\tau\frac{X}{Y}\right] + v^*\frac{\partial H^*}{\partial y_h^*}\left[ft_\tau\frac{X}{X_h}\frac{X_h}{Y_h}\right] = 0, \tag{E.5.6}$$

According to Van Ballegooyen (1995), the flow may respond to topographic effects as follows:

1. Strong response due to strong alongshore topographic control

$$X_h \ll Y_h \quad ; \quad \frac{X_h}{Y_h} \approx \zeta, \tag{E.5.7}$$

   where X_h is the cross-shore topographic scale and Y_h is the alongshore topographic scale and $\zeta \approx 10^{-1}$ is the small parameter of magnitude introduced early in this appendix.

2. Strong response due to weak alongshore topographic control

$$X_h \ll Y_h \quad ; \quad \frac{X_h}{Y_h} \approx \zeta^2. \tag{E.5.8}$$

For important alongshore effects in particular for coastal trapped waves, it may be assumed that $X \approx X_h$ and as a result equation (E.5.6) can be simplified.

Stellenbosch University https://scholar.sun.ac.za

List of References

Aldrighetti, E. 2007. *Computational hydraulic techniques for the Saint Venant Equations in arbitrarily shaped geometry.* PhD Thesis, Universita degli Studi di Trento.

Batchelor, G K. 1967. *An introduction to Fliud Dynamics.* Cambridge University Press.

Bedford, K. W., Dingman, J. S., & Yeo, W. K. 1987. Preparation of estuary and marine model equations by generalized filtering methods, In: Three-Dimensional models of marine and estuarine dynamics, Edited by J. C. J. Nihoul, and B. M. Jamart. *Elsevier*, 113–125.

Bennett, A F., & McIntosh, P C. 1982. Open Ocean Modeling as an Inverse Problem: Tidal Theory. *J. Phys. Oceanogr*, 12(1), 1004–1018.

Bird, R. B., Stewart, W. E., & Lightfoot, E. N. 2007. Transport phenomena. *Wiley.*

Blayo, & Debreu. 2004. Revisiting open boundary conditions from the point of view of characteristic variables. *Elsevier*, 9(1), 231–252.

Blumberg, A F., & Khanta, L H. 1985. Open boundary conditions for circulation models. *J. Hydraul. Engng*, 11(1), 237–255.

Bowden, K F. 1983. *Physical oceanography of coastal waters.* Ellis Horwood Ltd.

Brink, K. H. 1991. Coastal-trapped waves and wind-driven currents over the continental shelf. *Annu. Rev. Fluid Mech.*, 23(1), 389–412.

Camerlengo, A. L., & O'Brien, J. J. 1980. Open boundary condition in rotating fluid. *J. Comput. Phys.*

CEM. 2002. Coastal Engineering Manual (CEM).

Chapman, D C. 1985. Numerical treatment of cross-shelf open boundaries in a barotropic coastal ocean model. *J. Phys. Oceanogr.*, 15(1), 1060–1075.

Clarke, A J., & Brink, K H. 1985. The response of stratified frictional flow of shelf and slope waters to fluctuating, large-scale low-frequency wind forcing. *J. Phys. Oceanogr.*, 15(1), 439–453.

Dellar, P. J. 2010. Variations on a beta-plane: derivation of non-trational beta-plane equations from Hamilton's principle on a sphere. *J. Fluid Mech*, 1–16.

Stellenbosch University https://scholar.sun.ac.za

Deltares. 2011. Simulation of multi-dimensional hydrodynamic flows and transport phenomena, including sediments.

Deltares. 2015. *Delft3D Open Source Community.* `http://oss.deltares.nl/web/delft3d`.

Dingemans, M W. 1997a. *Water wave propagation over uneven bottoms: Part 1 - Linear Wave Propagation, Advanced Series on Ocean Engineering.* Vol. 13. World Scientific Publishers.

Dingemans, M W. 1997b. *Water wave propagation over uneven bottoms: Part 2 - Non-linear Wave Propagation, Advanced Series on Ocean Engineering.* Vol. 13. World Scientific Publishers.

Engedahl, H. 1995. Use of the flow relaxation scheme in a three-dimensional baroclinic ocean model with realistic topography. *Tellus 47A*, 365–382.

Flather, R. A. 1976. A tidal model of the northwest European continental shelf. *Mem. Soc. R. Sci. Liege, Ser. 6(10)*, 141–164.

Gill, A E. 1982. *Atmosphere-Ocean Dynamics.* Academic Press.

Gill, A E., & Schumann, E H. 1974. The generation of long-shelf waves by the wind. *J. Phys. Oceanogr.*, 4(1), 83–90.

Herzfeld, M., Schmidt, M., Griffies, S M., & Liang, Z. 2011. Realistic test cases for limited area ocean modelling. *Ocean Modelling*, 37(1), 1–34.

Hinze, J. O. 1975. Turbulence. *McGraw-Hill, New York, 2nd edit., 790 pp.*

Kay, M. 2008. *Practical hydraulics.* Tylor Francis Group.

Kee, R. J., Coltrin, M. E., & Glarborg, P. 2003. *Chemically Reaction Flow: Theory Practice.* John Wiley Sons, Inc.

Landau, L D., & Lifshitz, E M. 1959. *Fluid Mechanics.* Pergamon Press.

LeBlond, P H., & Mysak, L A. 1978. *Waves in the Ocean.* Elsevier.

Leendertse, J J., & Liu, S. 1975. A three-dimensional model for estuaries and coastal seas: Aspects of computation. *Report of the office of water research and technology, department of interior, June*, 2.

Leendertse, J J., Alexander, R C., & Liu, S. 1973. A three-dimensional model for estuaries and coastal seas: Principles of computation. *Report of the office of water research and technology, department of interior, December*, 1.

Martinsen, E. A., & Engedahl, H. 1987. Implementation and testing of a lateral boundary scheme as an open boundary condition in a barotropic ocean model. *Coastal Eng.*, 11(1), 603–627.

Stellenbosch University https://scholar.sun.ac.za

Mei, C C. 1983. *The Applied Dynamics of the Ocean Surface Waves.* New York: A Wiley-Interscience Publication, John Wiley and Sons.

Miller, M. J., & Thorpe, A. J. 1981. Radiation conditions for the lateral boundaries of limited-area numerical models. *Quart J. R. Met. Soc.*, 615–628.

Moran, J M., & Shapiro, H N. 2006. *Fundamentals of Engineering Thermodynamics.* 5th edition edn. John Wiley and Sons, Inc.

Navon, I M. 2014. A review of finite-element methods for solving the shallow-water equations.

Oceanography. 2014. *The Basic Concepts of Physical Oceanography.* `https://www.eeb.ucla.edu/test/faculty/nezlin/PhysicalOceanography.htm`.

Oddo, P., & Pinardi, N. 2007. Lateral open boundary conditions for nested limited area models: A scale selective approach. *Elsevier*, 20(1), 134–156.

Orlanski, I. 1976. A simple boundary condition for unbounded hyperbolic flows. *Academic Press Inc.*

Palma, E D., & Matano, R P. 1998. On the implementation of passive open boundary conditions for a general circulation model: The barotropic mode. *J. of Geophysical research*, 103(1), 1319–1341.

Palma, E D., & Matano, R P. 2001. Dynamical impacts associated with radiation boundary conditions. *J. of Sea Research*, 46(1), 117–132.

Pedlosky, J. 1987. *Geophysical Fluid Dynamics.* Springer.

Philips, O M. 1980. *The dynamics of the Upper Oceans.* Cambridge University Press, London.

Pond, S., & Pickard, G L. 1978. *Introductory dynamic oceanography.* Oxford: Pergamon Press.

Pope, S. B. 1975. A more general effective-viscosity hypothesis. *J. Fluid Mech.*, 331–340.

Roed, L. P., & Cooper, C. K. 1987. A study of various open boundary conditions for wind-forced barotropic numerical ocean models, In: Three-Dimensional models of marine and estuarine dynamics, Edited by J. C. J. Nihoul, and B. M. Jamart. *Elsevier*, 305–335.

Roelvink, J A., & Walstra, D J R. 2004. Keeping it simple by using complex models. *Int. Conf. on Hydroscience and Engineering (ICHE-2004), Brisbane, Australia.*

Sommerfeld, A. 1949. Partial differential equations. Lectures in Theorectical Physics 6. *Academic Press, New York.*

Spiegel, M R. 1967. *Theory and problems of Theoretical Mechanics.* McGraw-Hill, Inc.

Stellenbosch University https://scholar.sun.ac.za

Stelling, G S. 1983. *On the construction of computational methods for shallow water flow problems.* PhD. Thesis, Technische Hogeschool Delft.

Tang, Y., & Grimshaw, R. 1996. Radiation boundary conditions in barotropic coastal ocean numerical models. *J. Comput. Phys.*, 96–110.

Vallis, G K. 2006. *Atmospheric and Oceanic Fluid Dynamics Fundamentals and Large scale circulation.* Cambridge University Press.

Van Ballegooyen, R C. 1995. *Forced synoptic coastal-trapped waves along the Southern Africa coastline.* MSc. Thesis, University of Cape Town.

Verboom, G. K., Stelling, G. S., & Officier, M. J. 1981. Non-reflective boundary conditions in horizontal flow models. *Proceedings Int. Conf. Numerical Methods for Coupled Problems, Swansea.*

Verboom, G. K., Stelling, G. S., & Officier, M. J. 1982. Boundary conditions for shallow water equations. *In Engineering Applications for Computational Hydraulics, Volume 1, (M. B. Abbott and J. A. Cunge ed.) Pitman Publishing.*

Versteeg, H K., & Malalasekera, W. 2007. *An Introductory to Computational Fluid Dynamics.* Pearson Prentice Hall.